Doctoral Dissertation
博士論文

Dynamics and Thermodynamics of Coupled Quantum Oscillators
(結合量子振動子系の動力学と熱力学)

A Dissertation Submitted for the Degree of Doctor of Philosophy
December 2021
令和３年１２月博士（理学）申請

Department of Physics, Graduate School of Science,
The University of Tokyo
東京大学大学院理学系研究科物理学専攻

Takaaki Aoki
青木　隆明

Abstract

In this thesis, we investigate two quantum models. The first model is a Kerr-nonlinear parametric oscillator (KPO) coupled to a bath of harmonic oscillators. We assume that the detuning is zero, then the Hamiltonian of the KPO has two degenerate ground states. We also assume that the parametric pump is much stronger than the Kerr-nonlinearity. In this case, the approximate forms of the first two excited states are known. Using these four states, we derive the Gorini-Kossakowski-Sudarshan-Lindblad (GKSL)-type Markovian master equation for a KPO from the microscopic Hamiltonian. We compare our GKSL equation with the GKSL equation in the literature. We show that a KPO under our GKSL equation is more robust to excitation errors than that under the GKSL equation in the literature. In particular, we show that in the low-temperature limit of the bath, the state of a KPO under our GKSL equation is mostly confined to the subspace spanned by KPO's two degenerate ground states.

The second model consists of coupled harmonic oscillators in a star configuration, where the central harmonic oscillator (system) is coupled to a finite number of surrounding harmonic oscillators (bath). We define and investigate the nonequilibrium thermodynamic entropy of the total system. In this model, when the initial state of the total system is given by the tensor product of the Gibbs states of the system and the bath, every harmonic oscillator is always in a Gibbs state with a time-dependent temperature. This enables us to define time-dependent thermodynamic entropy for each harmonic oscillator, and thereby define the total nonequilibrium thermodynamic entropy as their summation. We analytically confirm that our total thermodynamic entropy satisfies the third law of thermodynamics. Our numerical solutions show that, though the finite-time dynamics of the system is well approximated by the GKSL equation, the total thermodynamic entropy production rate can be negative, while the total thermodynamic entropy satisfies the second law of thermodynamics.

A part of this thesis has been published in the following journal article:

- Takaaki Aoki, Yuichiro Matsuzaki, and Hideaki Hakoshima, "Possibility of the total thermodynamic entropy production rate of a finite-sized isolated quantum system to be negative for the Gorini-Kossakowski-Sudarshan-Lindblad-type markovian dynamics of its subsystem," Phys. Rev. A **103**, 052208 (2021).

Acknowledgment

I am really indebted to Prof. Naomichi Hatano for teaching me how to conduct research: boldly tackling new frontiers; persistently addressing a problem; believing in myself even if I am confronted with difficulty and for giving me a lot of keen comments and valuable advice. I am deeply obliged to Dr. Yuichiro Matsuzaki for dedicated assistance and firm guidance; in particular, research in Finland with him and Akseli Mäkinen was a precious experience. I sincerely appreciate collaboration with Dr. Yuichiro Matsuzaki, Dr. Hideaki Hakoshima, and Akseli Mäkinen. I am most grateful to all the members of the Hatano group in the University of Tokyo and of the Kawabata group in National Institute of Advanced Industrial Science and Technology for useful discussions, kind support, and enjoyable time. I am very thankful to Prof. Hosho Katsura, Prof. Yuto Ashida, Prof. Sosuke Ito, Prof. Mio Murao, and Prof. Miho Yanagisawa for helpful comments on this thesis.

Contents

Chapter 1

Introduction

In general, it is difficult to isolate a quantum system; the system always interacts with its environment, which causes decoherence and dissipation of the system [1, 2]. Such a system is called an open quantum system [3–5]. The total system, which consists of the system of interest and the environment, may be isolated and its dynamics can be unitary. As the degrees of freedom of the environment is huge, however, pursuing the total dynamics is generally beyond our computational ability. Besides, the dynamics of the environment itself is typically of little interest. Thus, we usually focus on the dynamics of the open system by taking the partial trace over the degrees of freedom of the environment.

In the theory of open quantum systems, it is often assumed that the environment is in a thermal equilibrium (Gibbs) state at the initial time. We call such an environment a bath. Because of the interaction with the bath, the dynamics of the system is not unitary; it is not described by the Schrödinger equation nor by the von Neumann equation. We do not have a simple form of the time-evolution equation for the system for a general coupling. Nontheless, when the coupling is weak enough for the time scale of the bath to be much shorter than that of the system, the dynamics of the system is called Markovian; under several approximations its dynamics can be described by a simple form of the time-evolution equation called the Gorini-Kossakowski-Sudarshan-Lindblad (GKSL)-type Markovian master equation [3, 4, 6–8]. This equation comprises two parts; one is related to the dynamics induced by the Hamiltonian of the system and the other is related to the decoherence which comes from the interaction with the bath.

There is a procedure to derive the GKSL equation from the microscopic Hamiltonian of the system, the bath, and their interaction; we will explain this procedure in Chapter 2. In the derivation, we need the complete set of the eigenstates of the Hamiltonian of the system. When the system is simple like a two-level system and a harmonic oscillator, we know the eigenstates and can derive the explicit form of the GKSL equation [3, 4, 9]. On the other hand, when the system is complicated like a Kerr-nonlinear parametric oscillator (KPO) [10], which we study in Chapter 4, only several eigenstates of the Hamiltonian are known, and hence it is difficult to derive its GKSL equation. Instead in the literature, as a decoherence part of the GKSL equation for a KPO, the decoherence part of the GKSL equation for a harmonic oscillator is often used [11–13]. As this decoherence part is not derived from the microscopic Hamiltonian of the total system which consists of a KPO and its environment, it is doubtful whether this decoherence part accurately describes the decoherence of the KPO. Indeed, we derive the GKSL equation for a KPO starting from the microscopic Hamiltonian of the total system comprised of the KPO and a bath of harmonic oscillators, finding a different form of the decoherence term. Studying the decoherence of a KPO is practically important because the KPO is expected to

be utilized as a qubit for a quantum computer [11, 14, 15]; it is necessary to reduce noise from the environment as much as possible for precise quantum computation.

On the other hand, we study in Chapter 5 a total system made up of coupled harmonic oscillators in a star configuration, in which the central harmonic oscillator (system of interest) is coupled to a finite number of surrounding harmonic oscillators (bath). When the initial state of the total system is a Gaussian state [16–20], not only the dynamics of the system of interest but also the dynamics of the total system including the bath can be pursued [6]. Even when the size of the bath is finite, we can set the parameters so that the finite-time dynamics of the system of interest may be well approximated by the GKSL equation [6].

An open quantum system and a bath is one of the typical setups in the research field of quantum thermodynamics [21–23], which explains microscopic thermodynamic changes of microscopic quantum systems coupled with macroscopic ones. One of the most fundamental problems in quantum thermodynamics is how to define thermodynamic quantities such as the thermodynamic entropy, the temperature, heat, and work. Of particular importance is the thermodynamic entropy because it characterizes the irreversibility of thermodynamics. This is why researchers have suggested several definitions of thermodynamic entropy [24–26] and various ones of entropy production and of its rate; see Ref. [27] and references therein. Nevertheless, there is no consensus for now.

There is active research [28–33] into the relation between non-Markovianity [34] of the dynamics of an open quantum system and a negative entropy production rate of the total system. However, there is no agreement about this relation mainly because there is no unified definition of the entropy production rate or of non-Markovianity. On the other hand, when an open quantum system is under the GKSL-type Markovian dynamics, it is widely believed that the entropy production rate of the total system is non-negative [28–33], and researchers often use the von Neumann entropy production rate [35], which is the negated time-derivative of the von Neumann relative entropy [36, Sec. 11.8] between the reduced state of the system and the reference stationary state of the GKSL equation. As we will see in Chapter 5, there is an implicit assumption in the form of the von Neumann entropy production rate that the size of a bath is so macroscopically large that its temperature does not change during the dynamics. Although the temperature of the whole bath does not change macroscopically, the temperature of a part of the bath can change microscopically; see Chapter 5. The von Neumann entropy production rate cannot take this microscopic temperature change into account. In Chapter 5, we consider the quantum model of coupled harmonic oscillators in a star configuration, pursuing the time evolution of the temperature of each harmonic oscillator. We thereby define the nonequilibrium thermodynamic entropy of the total system which incorporates the microscopic temperature change of the bath. As a result, our total thermodynamic entropy production rate can be negative though the finite-time dynamics of the central harmonic oscillator is well approximated by the GKSL equation.

1.1 Purpose

In summary, our purpose in this thesis is to study dynamics and thermodynamics of coupled quantum oscillators, based on the Hamiltonian of the total system which consists of a system of interest and a bath. First, we want to clarify the relationship between the dynamics of a KPO (the system of interest) and the Hamiltonian of the total system. Thus, we derive the GKSL equation for a KPO starting from the total Hamiltonian. A KPO is a promising candidate for a qubit in a quantum computer. Hence, the study of the decoherence of a KPO is of practical importance. Second, we want to elucidate the relationship between the dynamics and

thermodynamics of the quantum model of coupled harmonic oscillators. By considering this model, we can pursue the dynamics of the total system microscopically. We analyze the effects of the microscopic temperature changes of the subsystems on the nonequilibrium thermodynamic entropy that we define for the total system. We believe that this study sheds a new light on the connection between quantum mechanics and thermodynamics.

1.2 Organization of this thesis

Let us explain the organization of this thesis. In Chapter 2, we review a Gorini-Kossakowski-Sudarshan-Lindblad (GKSL)-type Markovian master equation [7, 8]. Starting from the general Hamiltonian of the total system consisting of a system of interest and a bath, we derive the GKSL equation, Eq. (2.40) with Eq. (2.45), by performing the Born-Markov and the secular (rotating-wave) approximations [3]. We also talk about a stationary state of the GKSL equation. As an example, we derive the GKSL equation (2.99) for a damped harmonic oscillator [4, 6]. The decoherence part of this GKSL equation appears in the GKSL equation for a KPO (4.57) in the literature, which we treat in Chapter 4. The GKSL equation of the damped harmonic oscillator is also used in Chapter 5.

In Chapter 3, we review a Kerr-nonlinear parametric oscillator (KPO) [10]. We can construct a KPO using a quantum circuit. We begin with an LC circuit, which is equivalent to a harmonic oscillator [37]. Replacing the inductance L by a Josephson junction, we obtain a transmon [37], which has nonlinearlity. If we use a loop with two parallel Josephson junctions threaded by a magnetic flux, instead of using a single Josephson junction, we would have a SQUID transmon, where SQUID is the abbreviation for a superconducting quantum interference device [37]. Then, after some approximations and moving to a rotating frame, we arrive at the Hamiltonian (3.38) of the KPO. We explain KPO's two degenerate exact ground states and approximate excited states. We can use the two degenerate exact ground states as the logical states of a qubit for a quantum computer [11, 14, 15].

In Chapter 4, we tackle the decoherence of a KPO. After referring to the GKSL equation (4.2) for a KPO in the literature, we derive our GKSL equation (4.56) for a KPO; starting from the total Hamiltonian (4.8) of the KPO, the bath, and their interaction, we follow the procedure explained in Chapter 2. Then, we compare our GKSL equation and the GKSL equation in the literature. We show that a KPO under our GKSL equation is more robust to excitation errors than that under the GKSL equation in the literature. In particular, in the low-temperature limit of the bath, the state of a KPO under our GKSL equation is mostly confined to the subspace spanned by KPO's two degenerate ground states.

In Chapter 5, we define and investigate a total nonequilibrium thermodynamic entropy (5.51) of the quantum model of coupled harmonic oscillators in a star configuration, introduced in Chapter 2. In particular, we show that our total thermodynamic entropy production rate (5.56) can be negative, though the finite-time dynamics of the system is well approximated by the GKSL equation. This comes from the temperature change of each harmonic oscillator, which is incorporated in our nonequilibrium thermodynamic entropy. This Chapter is based on the following journal article:

- Takaaki Aoki, Yuichiro Matsuzaki, and Hideaki Hakoshima, "Possibility of the total thermodynamic entropy production rate of a finite-sized isolated quantum system to be negative for the Gorini-Kossakowski-Sudarshan-Lindblad-type markovian dynamics of its subsystem," Phys. Rev. A **103**, 052208 (2021).

In Chapter 6, we conclude this thesis with future prospects.

Chapter 2

Open quantum systems

In this Chapter, we review the Gorini-Kossakowski-Sudarshan-Lindblad (GKSL)-type Markovian master equation [7, 8]. We assume that the environment is large and in a thermal equilibrium state at the initial time. We refer to such an environment as a bath. We also consider the weak coupling limit.

Let us call the open quantum system [3, 4] A and the bath B. The total Hilbert space is $\mathcal{H}_A \otimes \mathcal{H}_B$. The total Hamiltonian is given by

$$\hat{H} = \hat{H}_A + \hat{H}_B + \hat{H}_I, \tag{2.1}$$

where $\hat{H}_A$ and $\hat{H}_B$ are the Hamiltonians of the system and the bath, respectively, while $\hat{H}_I$ is the interaction Hamiltonian. The dynamics of the total system in the Schrödinger picture is governed by the von Neumann equation:

$$\frac{\mathrm{d}\hat{\rho}(t)}{\mathrm{d}t} = -\frac{\mathrm{i}}{\hbar}[\hat{H}_A + \hat{H}_B + \hat{H}_I, \hat{\rho}(t)], \tag{2.2}$$

where $\hat{\rho}(t)$ is the density operator of the total system.

As we consider the weak coupling limit, we will treat the interaction Hamiltonian in a perturbative manner. Thus, it is more convenient to transfer to the interaction picture, in which the density operator $\hat{\rho}^I(t)$ and the observable operator $\hat{O}^I(t)$ are given by

$$\hat{\rho}^I(t) = \mathrm{e}^{\frac{\mathrm{i}}{\hbar}(\hat{H}_A+\hat{H}_B)t}\hat{\rho}(t)\mathrm{e}^{-\frac{\mathrm{i}}{\hbar}(\hat{H}_A+\hat{H}_B)t}, \tag{2.3}$$

$$\hat{O}^I(t) = \mathrm{e}^{\frac{\mathrm{i}}{\hbar}(\hat{H}_A+\hat{H}_B)t}\hat{O}(t)\mathrm{e}^{-\frac{\mathrm{i}}{\hbar}(\hat{H}_A+\hat{H}_B)t}. \tag{2.4}$$

Here, $\hat{O}(t)$ is the observable operator in the Schrödinger picture. Then, the von Neumann equation in the interaction picture is written as

$$\frac{\mathrm{d}\hat{\rho}^I(t)}{\mathrm{d}t} = -\frac{\mathrm{i}}{\hbar}[\hat{H}_I^I(t), \hat{\rho}^I(t)], \tag{2.5}$$

whose integral expression is

$$\hat{\rho}^I(t) = \hat{\rho}^I(0) - \frac{\mathrm{i}}{\hbar}\int_0^t \mathrm{d}s\,[\hat{H}_I^I(s), \hat{\rho}^I(s)]. \tag{2.6}$$

By substituting Eq. (2.6) into Eq. (2.5), we obtain

$$\frac{\mathrm{d}\hat{\rho}^I(t)}{\mathrm{d}t} = -\frac{\mathrm{i}}{\hbar}[\hat{H}_I^I(t), \hat{\rho}^I(0)] - \frac{1}{\hbar^2}\int_0^t \mathrm{d}s\,[\hat{H}_I^I(t), [\hat{H}_I^I(s), \hat{\rho}^I(s)]]. \tag{2.7}$$

What we want is a closed equation on the dynamics of the system. For this purpose, let us trace out the degrees of freedom of the bath:

$$\frac{\mathrm{d}\hat{\rho}_A^I(t)}{\mathrm{d}t} = -\frac{\mathrm{i}}{\hbar}\mathrm{Tr}_B[\hat{H}_I^I(t), \hat{\rho}^I(0)] - \frac{1}{\hbar^2}\int_0^t \mathrm{d}s\, \mathrm{Tr}_B[\hat{H}_I^I(t), [\hat{H}_I^I(s), \hat{\rho}^I(s)]], \tag{2.8}$$

where

$$\begin{aligned}
\hat{\rho}_A^I(t) &= \mathrm{Tr}_B[\hat{\rho}^I(t)] \\
&= \mathrm{Tr}_B[\mathrm{e}^{\frac{\mathrm{i}}{\hbar}(\hat{H}_A+\hat{H}_B)t}\hat{\rho}(t)\mathrm{e}^{-\frac{\mathrm{i}}{\hbar}(\hat{H}_A+\hat{H}_B)t}] \\
&= \mathrm{e}^{\frac{\mathrm{i}}{\hbar}\hat{H}_A t}\mathrm{Tr}_B[\mathrm{e}^{\frac{\mathrm{i}}{\hbar}\hat{H}_B t}\hat{\rho}(t)\mathrm{e}^{-\frac{\mathrm{i}}{\hbar}\hat{H}_B t}]\mathrm{e}^{-\frac{\mathrm{i}}{\hbar}\hat{H}_A t} \\
&= \mathrm{e}^{\frac{\mathrm{i}}{\hbar}\hat{H}_A t}\mathrm{Tr}_B[\hat{\rho}(t)]\mathrm{e}^{-\frac{\mathrm{i}}{\hbar}\hat{H}_A t} \\
&=: \mathrm{e}^{\frac{\mathrm{i}}{\hbar}\hat{H}_A t}\hat{\rho}_A(t)\mathrm{e}^{-\frac{\mathrm{i}}{\hbar}\hat{H}_A t}
\end{aligned} \tag{2.9}$$

is the density operator of the system in the interaction picture with $\hat{\rho}_A(t)$ being the the density operator of the system in the Schrödinger picture.

We prepare the following initial state:

$$\hat{\rho}^I(0) = \hat{\rho}(0) = \hat{\rho}_A(0) \otimes \hat{\rho}_B^{\mathrm{th}} := \hat{\rho}_A(0) \otimes \frac{\mathrm{e}^{-\beta_B^0 \hat{H}_B}}{\mathrm{Tr}\left[\mathrm{e}^{-\beta_B^0 \hat{H}_B}\right]}, \tag{2.10}$$

where we set the initial state of the bath to the Gibbs state with inverse temperature β_B^0. There is no correlation between the system and the bath initially. The most general interaction Hamiltonian in the Schrödinger picture is [38] (see also Sec. 3.3.1 in Ref. [3] and Sec. II.A in Ref. [34])

$$\hat{H}_I = \hbar \sum_\alpha \hat{A}_\alpha \otimes \hat{B}_\alpha, \tag{2.11}$$

where $\hat{A}_\alpha^\dagger = \hat{A}_\alpha$ and $\hat{B}_\alpha^\dagger = \hat{B}_\alpha$. In the interaction picture, we have

$$\hat{H}_I^I(t) = \hbar \sum_\alpha \hat{A}_\alpha^I(t) \otimes \hat{B}_\alpha^I(t), \tag{2.12}$$

where $\hat{A}_\alpha^I(t) = \mathrm{e}^{\frac{\mathrm{i}}{\hbar}\hat{H}_A t}\hat{A}_\alpha \mathrm{e}^{-\frac{\mathrm{i}}{\hbar}\hat{H}_A t}$ and $\hat{B}_\alpha^I(t) = \mathrm{e}^{\frac{\mathrm{i}}{\hbar}\hat{H}_B t}\hat{B}_\alpha \mathrm{e}^{-\frac{\mathrm{i}}{\hbar}\hat{H}_B t}$. We assume that the first term in Eq. (2.8) is zero [3, Sec. 3.3.1], so that we obtain

$$\frac{\mathrm{d}\hat{\rho}_A^I(t)}{\mathrm{d}t} = -\frac{1}{\hbar^2}\int_0^t \mathrm{d}s\, \mathrm{Tr}_B[\hat{H}_I^I(t), [\hat{H}_I^I(s), \hat{\rho}^I(s)]]. \tag{2.13}$$

We note that the assumption $\mathrm{Tr}_B[\hat{H}_I^I(t), \hat{\rho}^I(0)] = 0$ is satisfied by $\hat{H}_I^I(t)$ in Eq. (2.70) and $\hat{\rho}^I(0) = \hat{\rho}_A(0) \otimes \mathrm{e}^{-\beta_B^0 \hat{H}_B}/\mathrm{Tr}\left[\mathrm{e}^{-\beta_B^0 \hat{H}_B}\right]$ with $\hat{H}_B$ in Eq. (2.61); see Sec. 2.5. We also note that the assumption $\mathrm{Tr}_B[\hat{H}_I^{\mathrm{R},I}(t), \hat{\rho}^{\mathrm{R},I}(0)] = \mathrm{Tr}_B[\hat{H}_I^{\mathrm{R},I}(t), \hat{\rho}^{\mathrm{R}}(0)] = 0$ is satisfied by $\hat{H}_I^{\mathrm{R},I}(t)$ in Eq. (4.30) and $\hat{\rho}^{\mathrm{R}}(0)$ in Eq. (4.13); see Sec. 4.2.

2.1 The Born-Markov approximation

We here apply the Born approximation [3, Sec. 3.3.1], which states that because of weak coupling, there occurs few correlations between the system and the bath, and the state of the bath hardly changes in the time evolution:

$$\hat{\rho}(t) \approx \hat{\rho}_A(t) \otimes \hat{\rho}_B^{\mathrm{th}}. \tag{2.14}$$

The total density operator in the interaction picture has a similar form:

$$\hat{\rho}^I(t) \approx \hat{\rho}_A^I(t) \otimes \hat{\rho}_B^{\mathrm{th}}. \tag{2.15}$$

Substitution of Eq. (2.15) into Eq. (2.13) yields

$$\frac{\mathrm{d}\hat{\rho}_A^I(t)}{\mathrm{d}t} = -\frac{1}{\hbar^2}\int_0^t \mathrm{d}s\, \mathrm{Tr}_B[\hat{H}_I^I(t), [\hat{H}_I^I(s), \hat{\rho}_A^I(s) \otimes \hat{\rho}_B^{\mathrm{th}}]]. \tag{2.16}$$

We note that the Born approximation (2.14) is not a necessary condition for the dynamics of the system to obey the GKSL equation. In some cases, the dynamics of the system is well approximated by the GKSL equation while the state of the total system $\hat{\rho}(t)$ is far from the tensor product state [6, Sec. 2.3.3].

Looking at Eq. (2.16), we see that the time derivative of the state of the system $\hat{\rho}_A^I(t)$ depends on the state of the system $\hat{\rho}_A^I(s)$ in the past ($0 \leq s \leq t$). In order to get rid of this memory effect, we here perform the Markov approximation.

First, we replace the integral variable in Eq. (2.16) from s to $t - s$:

$$\frac{\mathrm{d}\hat{\rho}_A^I(t)}{\mathrm{d}t} = -\frac{1}{\hbar^2}\int_0^t \mathrm{d}s\, \mathrm{Tr}_B[\hat{H}_I^I(t), [\hat{H}_I^I(t-s), \hat{\rho}_A^I(t-s) \otimes \hat{\rho}_B^{\mathrm{th}}]]. \tag{2.17}$$

Let τ_B denote the correlation time of the bath, which is a characteristic time scale in which the integrand in the right-hand side of Eq. (2.17) decays. Roughly speaking, the integrand is nonzero for $0 \leq s \lesssim \tau_B$. We assume that the relaxation time of the system τ_R is much larger than τ_B, and thereby replace $\hat{\rho}_A^I(t-s)$ by $\hat{\rho}_A^I(t)$. This is sometimes called the first Markov approximation [34, Sec. IV.B.1], which results in:

$$\frac{\mathrm{d}\hat{\rho}_A^I(t)}{\mathrm{d}t} = -\frac{1}{\hbar^2}\int_0^t \mathrm{d}s\, \mathrm{Tr}_B[\hat{H}_I^I(t), [\hat{H}_I^I(t-s), \hat{\rho}_A^I(t) \otimes \hat{\rho}_B^{\mathrm{th}}]]. \tag{2.18}$$

Note that this equation is local in time.

As the integrand rapidly goes to zero for $s \gg \tau_B$, we extend the upper limit of the integral to ∞, which is known as the second Markov approximation [34, Sec. IV.B.1]:

$$\frac{\mathrm{d}\hat{\rho}_A^I(t)}{\mathrm{d}t} = -\frac{1}{\hbar^2}\int_0^\infty \mathrm{d}s\, \mathrm{Tr}_B[\hat{H}_I^I(t), [\hat{H}_I^I(t-s), \hat{\rho}_A^I(t) \otimes \hat{\rho}_B^{\mathrm{th}}]]. \tag{2.19}$$

2.2 The Redfield equation

This is called the Redfield equation [39, 40]. We give two words of caution. First, the Redfield equation is not guaranteed to be completely positive [41]. Hence, a system under the Redfield equation may have negative populations, which is unphysical [1]. In order to achieve the complete positivity, we need to perform the secular (rotating-wave) approximation, which we will explain in Sec. 2.3. Second, in some literature, Eq. (2.18) instead of Eq. (2.19) is called the Redfield equation (for example, Eq. (3.117) in Ref. [3] and Eq. (5.135) in Ref. [42]). However, as pointed out at footnote 12 in Ref. [1], Redfield did extend the upper limit of the integral to ∞ in his original paper; see Eq. (2.14) in Ref. [39].

We now transform the Redfield equation (2.19) using the interaction Hamiltonian (2.12). Let ϵ_j and $|\psi_j\rangle$ denote the jth eigenvalue and eigenstate of the Hamiltonian of the system:

$$\hat{H}_A = \sum_j \epsilon_j |\psi_j\rangle\langle\psi_j|. \tag{2.20}$$

We assume that the eigenstates $\{|\psi_j\rangle\}$ have no degeneracy. As $\{|\psi_j\rangle\}$ is a complete orthonormal set in $\mathcal{H}_A$, we can rewrite $A^I_\alpha(t)$ as

$$\begin{aligned}\hat{A}^I_\alpha(t) &= \mathrm{e}^{\frac{\mathrm{i}}{\hbar}\hat{H}_A t}\hat{A}_\alpha \mathrm{e}^{-\frac{\mathrm{i}}{\hbar}\hat{H}_A t} \\ &= \sum_{j,k} \mathrm{e}^{\frac{\mathrm{i}}{\hbar}\hat{H}_A t}|\psi_j\rangle\langle\psi_j|\hat{A}_\alpha|\psi_k\rangle\langle\psi_k|\mathrm{e}^{-\frac{\mathrm{i}}{\hbar}\hat{H}_A t} \\ &= \sum_{j,k} \mathrm{e}^{-\frac{\mathrm{i}}{\hbar}(\epsilon_k-\epsilon_j)t}|\psi_j\rangle\langle\psi_j|\hat{A}_\alpha|\psi_k\rangle\langle\psi_k| \\ &= \sum_{\omega_A} \mathrm{e}^{-\mathrm{i}\omega_A t}\hat{A}_\alpha(\omega_A), \end{aligned} \tag{2.21}$$

where in the summation in the last line, ω_A is taken from $\{\epsilon_k - \epsilon_j | j,k = 1,2\dots\}$ except for duplication. Here, we have defined $\hat{A}_\alpha(\omega_A)$ as

$$\hat{A}_\alpha(\omega_A) = \sum_{\substack{j,k \\ \epsilon_k-\epsilon_j=\hbar\omega_A}} |\psi_j\rangle\langle\psi_j|\hat{A}_\alpha|\psi_k\rangle\langle\psi_k|. \tag{2.22}$$

Note that the following relations are satisfied:

$$\hat{A}^\dagger_\alpha(\omega_A) = \hat{A}_\alpha(-\omega_A), \tag{2.23}$$

$$[\hat{H}_A, \hat{A}_\alpha(\omega_A)] = -\hbar\omega_A\hat{A}_\alpha(\omega_A), \tag{2.24}$$

$$[\hat{H}_A, \hat{A}^\dagger_\alpha(\omega_A)] = \hbar\omega_A\hat{A}^\dagger_\alpha(\omega_A), \tag{2.25}$$

$$[\hat{H}_A, \hat{A}^\dagger_\alpha(\omega_A)\hat{A}_\beta(\omega_A)] = 0, \tag{2.26}$$

$$\sum_{\omega_A}\hat{A}_\alpha(\omega_A) = \sum_{\omega_A}\hat{A}^\dagger_\alpha(\omega_A) = \hat{A}_\alpha. \tag{2.27}$$

Inserting Eq. (2.21) into Eq. (2.12), we obtain

$$\hat{H}^I_I(t) = \hbar\sum_{\alpha,\omega_A}\mathrm{e}^{-\mathrm{i}\omega_A t}\hat{A}_\alpha(\omega_A)\otimes\hat{B}^I_\alpha(t) = \hbar\sum_{\alpha,\omega_A}\mathrm{e}^{\mathrm{i}\omega_A t}\hat{A}^\dagger_\alpha(\omega_A)\otimes\hat{B}^I_\alpha(t), \tag{2.28}$$

where the last equality follows from the Hermiticity of $\hat{H}^I_I(t)$ and $\hat{B}^I_\alpha(t)$.

We obtain another form of the Redfield equation by combining (2.19) and Eq. (2.28):

$$\begin{aligned}\frac{\mathrm{d}\hat{\rho}^I_A(t)}{\mathrm{d}t} &= -\frac{1}{\hbar^2}\int_0^\infty \mathrm{d}s\,\mathrm{Tr}_B[\hat{H}^I_I(t),\hat{H}^I_I(t-s)\hat{\rho}^I_A(t)\otimes\hat{\rho}^{\mathrm{th}}_B - \hat{\rho}^I_A(t)\otimes\hat{\rho}^{\mathrm{th}}_B\hat{H}^I_I(t-s)] \\ &= -\frac{1}{\hbar^2}\int_0^\infty \mathrm{d}s\,\mathrm{Tr}_B[\hat{H}^I_I(t)\hat{H}^I_I(t-s)\hat{\rho}^I_A(t)\otimes\hat{\rho}^{\mathrm{th}}_B - \hat{H}^I_I(t)\hat{\rho}^I_A(t)\otimes\hat{\rho}^{\mathrm{th}}_B\hat{H}^I_I(t-s) \\ &\quad - \hat{H}^I_I(t-s)\hat{\rho}^I_A(t)\otimes\hat{\rho}^{\mathrm{th}}_B\hat{H}^I_I(t) + \hat{\rho}^I_A(t)\otimes\hat{\rho}^{\mathrm{th}}_B\hat{H}^I_I(t-s)\hat{H}^I_I(t)] \\ &= \frac{1}{\hbar^2}\int_0^\infty \mathrm{d}s\,\mathrm{Tr}_B[\hat{H}^I_I(t-s)\hat{\rho}^I_A(t)\otimes\hat{\rho}^{\mathrm{th}}_B\hat{H}^I_I(t) - \hat{H}^I_I(t)\hat{H}^I_I(t-s)\hat{\rho}^I_A(t)\otimes\hat{\rho}^{\mathrm{th}}_B] + \mathrm{h.c.} \\ &= \int_0^\infty \mathrm{d}s\,\mathrm{Tr}_B\left[\sum_{\beta,\omega_A}\mathrm{e}^{-\mathrm{i}\omega_A(t-s)}\hat{A}_\beta(\omega_A)\otimes\hat{B}^I_\beta(t-s)\hat{\rho}^I_A(t)\otimes\hat{\rho}^{\mathrm{th}}_B\sum_{\alpha,\omega'_A}\mathrm{e}^{\mathrm{i}\omega'_A t}\hat{A}^\dagger_\alpha(\omega'_A)\otimes\hat{B}^I_\alpha(t)\right. \\ &\quad \left. - \sum_{\alpha,\omega'_A}\mathrm{e}^{\mathrm{i}\omega'_A t}\hat{A}^\dagger_\alpha(\omega'_A)\otimes\hat{B}^I_\alpha(t)\sum_{\beta,\omega_A}\mathrm{e}^{-\mathrm{i}\omega_A(t-s)}\hat{A}_\beta(\omega_A)\otimes\hat{B}^I_\beta(t-s)\hat{\rho}^I_A(t)\otimes\hat{\rho}^{\mathrm{th}}_B\right] + \mathrm{h.c.} \\ &= \sum_{\omega_A,\omega'_A}\sum_{\alpha,\beta}\mathrm{e}^{\mathrm{i}(\omega'_A-\omega_A)t}\int_0^\infty \mathrm{d}s\,\mathrm{e}^{\mathrm{i}\omega_A s}\left\{\mathrm{Tr}_B[\hat{B}^I_\beta(t-s)\hat{\rho}^{\mathrm{th}}_B\hat{B}^I_\alpha(t)]\hat{A}_\beta(\omega_A)\hat{\rho}^I_A(t)\hat{A}^\dagger_\alpha(\omega'_A)\right. \end{aligned}$$

$$
\begin{aligned}
&\quad - \mathrm{Tr}_B[\hat{B}^I_\alpha(t)\hat{B}^I_\beta(t-s)\hat{\rho}^{\mathrm{th}}_B]\hat{A}^\dagger_\alpha(\omega'_A)\hat{A}_\beta(\omega_A)\hat{\rho}^I_A(t)\Big\} + \mathrm{h.c.} \\
&= \sum_{\omega_A,\omega'_A}\sum_{\alpha,\beta} \mathrm{e}^{\mathrm{i}(\omega'_A-\omega_A)t}\Gamma_{\alpha,\beta}(\omega_A)[\hat{A}_\beta(\omega_A)\hat{\rho}^I_A(t)\hat{A}^\dagger_\alpha(\omega'_A) - \hat{A}^\dagger_\alpha(\omega'_A)\hat{A}_\beta(\omega_A)\hat{\rho}^I_A(t)] + \mathrm{h.c.},
\end{aligned}
\tag{2.29}
$$

where h.c. means the Hermitian conjugate and

$$
\Gamma_{\alpha,\beta}(\omega_A) = \int_0^\infty \mathrm{d}s\, \mathrm{e}^{\mathrm{i}\omega_A s}\mathrm{Tr}_B[\hat{B}^I_\alpha(s)\hat{B}_\beta\hat{\rho}^{\mathrm{th}}_B] \tag{2.30}
$$

is a one-sided Fourier transform of the correlation function of the bath.

2.3 The secular (rotating wave) approximation and the GKSL equation

In Eq. (2.29), if $|\omega'_A - \omega_A|^{-1}$ ($\omega'_A \neq \omega_A$) is much smaller than the relaxation time of the system τ_R, the terms with $\omega'_A \neq \omega_A$ rapidly oscillate. Neglecting these terms, called the secular (rotating-wave) approximation [3, Sec. 3.3.1], results in

$$
\frac{\mathrm{d}\hat{\rho}^I_A(t)}{\mathrm{d}t} = \sum_{\omega_A}\sum_{\alpha,\beta}\Gamma_{\alpha,\beta}(\omega_A)[\hat{A}_\beta(\omega_A)\hat{\rho}^I_A(t)\hat{A}^\dagger_\alpha(\omega_A) - \hat{A}^\dagger_\alpha(\omega_A)\hat{A}_\beta(\omega_A)\hat{\rho}^I_A(t)] + \mathrm{h.c.} \tag{2.31}
$$

In order to divide the above equation into the Lamb-shift part and the decoherence part, we decompose $\Gamma_{\alpha,\beta}(\omega_A)$ as

$$
\Gamma_{\alpha,\beta}(\omega_A) = \frac{1}{2}\gamma_{\alpha,\beta}(\omega_A) + \mathrm{i}S_{\alpha,\beta}(\omega_A), \tag{2.32}
$$

where the elements

$$
S_{\alpha,\beta}(\omega_A) = \frac{1}{2\mathrm{i}}[\Gamma_{\alpha,\beta}(\omega_A) - \Gamma^*_{\beta,\alpha}(\omega_A)] \tag{2.33}
$$

form a Hermitian matrix and the elements

$$
\begin{aligned}
\gamma_{\alpha,\beta}(\omega_A) &= \Gamma_{\alpha,\beta}(\omega_A) + \Gamma^*_{\beta,\alpha}(\omega_A) \\
&= \int_0^\infty \mathrm{d}s\, \mathrm{e}^{\mathrm{i}\omega_A s}\mathrm{Tr}_B[\hat{B}^I_\alpha(s)\hat{B}_\beta\hat{\rho}^{\mathrm{th}}_B] + \int_0^\infty \mathrm{d}s\, \mathrm{e}^{-\mathrm{i}\omega_A s}\mathrm{Tr}_B[\hat{\rho}^{\mathrm{th}}_B\hat{B}_\alpha\hat{B}^I_\beta(s)] \\
&= \int_0^\infty \mathrm{d}s\, \mathrm{e}^{\mathrm{i}\omega_A s}\mathrm{Tr}_B[\hat{B}^I_\alpha(s)\hat{B}_\beta\hat{\rho}^{\mathrm{th}}_B] + \int_0^\infty \mathrm{d}s\, \mathrm{e}^{-\mathrm{i}\omega_A s}\mathrm{Tr}_B[\hat{B}^I_\alpha(-s)\hat{B}_\beta\hat{\rho}^{\mathrm{th}}_B] \\
&= \int_{-\infty}^\infty \mathrm{d}s\, \mathrm{e}^{\mathrm{i}\omega_A s}\mathrm{Tr}_B[\hat{B}^I_\alpha(s)\hat{B}_\beta\hat{\rho}^{\mathrm{th}}_B]
\end{aligned}
\tag{2.34}
$$

form a positive semidefinite matrix [4, Sec. 6.2.2]. We then arrive at

$$
\begin{aligned}
\frac{\mathrm{d}\hat{\rho}^I_A(t)}{\mathrm{d}t} &= \sum_{\omega_A}\sum_{\alpha,\beta}\Gamma_{\alpha,\beta}(\omega_A)[\hat{A}_\beta(\omega_A)\hat{\rho}^I_A(t)\hat{A}^\dagger_\alpha(\omega_A) - \hat{A}^\dagger_\alpha(\omega_A)\hat{A}_\beta(\omega_A)\hat{\rho}^I_A(t)] \\
&\quad + \sum_{\omega_A}\sum_{\alpha,\beta}\Gamma^*_{\alpha,\beta}(\omega_A)[\hat{A}_\alpha(\omega_A)\hat{\rho}^I_A(t)\hat{A}^\dagger_\beta(\omega_A) - \hat{\rho}^I_A(t)\hat{A}^\dagger_\beta(\omega_A)\hat{A}_\alpha(\omega_A)] \\
&= \sum_{\omega_A}\sum_{\alpha,\beta}\Gamma_{\alpha,\beta}(\omega_A)[\hat{A}_\beta(\omega_A)\hat{\rho}^I_A(t)\hat{A}^\dagger_\alpha(\omega_A) - \hat{A}^\dagger_\alpha(\omega_A)\hat{A}_\beta(\omega_A)\hat{\rho}^I_A(t)]
\end{aligned}
$$

$$
\begin{aligned}
&+\sum_{\omega_A}\sum_{\alpha,\beta}\Gamma^*_{\beta,\alpha}(\omega_A)[\hat{A}_\beta(\omega_A)\hat{\rho}_A^I(t)\hat{A}^\dagger_\alpha(\omega_A)-\hat{\rho}_A^I(t)\hat{A}^\dagger_\alpha(\omega_A)\hat{A}_\beta(\omega_A)]\\
&=\sum_{\omega_A}\sum_{\alpha,\beta}[\Gamma_{\alpha,\beta}(\omega_A)+\Gamma^*_{\beta,\alpha}(\omega_A)]\hat{A}_\beta(\omega_A)\hat{\rho}_A^I(t)\hat{A}^\dagger_\alpha(\omega_A)\\
&\quad-\sum_{\omega_A}\sum_{\alpha,\beta}[\Gamma_{\alpha,\beta}(\omega_A)\hat{A}^\dagger_\alpha(\omega_A)\hat{A}_\beta(\omega_A)\hat{\rho}_A^I(t)+\Gamma^*_{\beta,\alpha}(\omega_A)\hat{\rho}_A^I(t)\hat{A}^\dagger_\alpha(\omega_A)\hat{A}_\beta(\omega_A)]\\
&=\sum_{\omega_A}\sum_{\alpha,\beta}\gamma_{\alpha,\beta}(\omega_A)\hat{A}_\beta(\omega_A)\hat{\rho}_A^I(t)\hat{A}^\dagger_\alpha(\omega_A)\\
&\quad-\sum_{\omega_A}\sum_{\alpha,\beta}\left[\frac{1}{2}\gamma_{\alpha,\beta}(\omega_A)+\mathrm{i}S_{\alpha,\beta}(\omega_A)\right]\hat{A}^\dagger_\alpha(\omega_A)\hat{A}_\beta(\omega_A)\hat{\rho}_A^I(t)\\
&\quad-\sum_{\omega_A}\sum_{\alpha,\beta}\left[\frac{1}{2}\gamma_{\alpha,\beta}(\omega_A)-\mathrm{i}S_{\alpha,\beta}(\omega_A)\right]\hat{\rho}_A^I(t)\hat{A}^\dagger_\alpha(\omega_A)\hat{A}_\beta(\omega_A)\\
&=-\frac{\mathrm{i}}{\hbar}[\hat{H}_{\mathrm{LS}},\hat{\rho}_A^I(t)]+\mathcal{D}[\hat{\rho}_A^I(t)],
\end{aligned}
\tag{2.35}
$$

where

$$
\hat{H}_{\mathrm{LS}}=\sum_{\omega_A}\sum_{\alpha,\beta}\hbar S_{\alpha,\beta}(\omega_A)\hat{A}^\dagger_\alpha(\omega_A)\hat{A}_\beta(\omega_A)
\tag{2.36}
$$

is called the Lamb-shift Hamiltonian [3, Sec. 3.3.1] and

$$
\mathcal{D}[\hat{\rho}_A^I(t)]=\sum_{\omega_A}\sum_{\alpha,\beta}\gamma_{\alpha,\beta}(\omega_A)\left(\hat{A}_\beta(\omega_A)\hat{\rho}_A^I(t)\hat{A}^\dagger_\alpha(\omega_A)-\frac{1}{2}\{\hat{A}^\dagger_\alpha(\omega_A)\hat{A}_\beta(\omega_A),\hat{\rho}_A^I(t)\}\right)
\tag{2.37}
$$

is the decoherence part. Here, the curly parentheses $\{\bullet,\bullet\}$ denote the anticommutator. From Eq. (2.26), we find that the system Hamiltonian and the Lamb-shift Hamiltonian commute:

$$
[\hat{H}_A,\hat{H}_{\mathrm{LS}}]=0.
\tag{2.38}
$$

Let us transform Eq. (2.35) into the Schrödinger-picture version. From Eq. (2.9) we obtain

$$
\hat{\rho}_A(t)=\mathrm{e}^{-\frac{\mathrm{i}}{\hbar}\hat{H}_At}\hat{\rho}_A^I(t)\mathrm{e}^{\frac{\mathrm{i}}{\hbar}\hat{H}_At},
\tag{2.39}
$$

whose time-derivative is calculated as in

$$
\begin{aligned}
\frac{\mathrm{d}\hat{\rho}_A(t)}{\mathrm{d}t}&=-\frac{\mathrm{i}}{\hbar}[\hat{H}_A,\hat{\rho}_A(t)]+\mathrm{e}^{-\frac{\mathrm{i}}{\hbar}\hat{H}_At}\frac{\mathrm{d}\hat{\rho}_A^I(t)}{\mathrm{d}t}\mathrm{e}^{\frac{\mathrm{i}}{\hbar}\hat{H}_At}\\
&=-\frac{\mathrm{i}}{\hbar}[\hat{H}_A,\hat{\rho}_A(t)]+\mathrm{e}^{-\frac{\mathrm{i}}{\hbar}\hat{H}_At}\left(-\frac{\mathrm{i}}{\hbar}[\hat{H}_{\mathrm{LS}},\hat{\rho}_A^I(t)]+\mathcal{D}[\hat{\rho}_A^I(t)]\right)\mathrm{e}^{\frac{\mathrm{i}}{\hbar}\hat{H}_At}\\
&=-\frac{\mathrm{i}}{\hbar}[\hat{H}_A+\hat{H}_{\mathrm{LS}},\hat{\rho}_A(t)]+\mathcal{D}[\hat{\rho}_A(t)],
\end{aligned}
\tag{2.40}
$$

where

$$
\mathcal{D}[\hat{\rho}_A(t)]=\sum_{\omega_A}\sum_{\alpha,\beta}\gamma_{\alpha,\beta}(\omega_A)\left(\hat{A}_\beta(\omega_A)\hat{\rho}_A(t)\hat{A}^\dagger_\alpha(\omega_A)-\frac{1}{2}\{\hat{A}^\dagger_\alpha(\omega_A)\hat{A}_\beta(\omega_A),\hat{\rho}_A(t)\}\right).
\tag{2.41}
$$

Here, we have used Eq. (2.38) and

$$
\mathrm{e}^{-\frac{\mathrm{i}}{\hbar}\hat{H}_At}\hat{A}_\beta(\omega_A)\mathrm{e}^{\frac{\mathrm{i}}{\hbar}\hat{H}_At}=\mathrm{e}^{\mathrm{i}\omega_At}\hat{A}_\beta(\omega_A),
\tag{2.42}
$$

$$
\mathrm{e}^{-\frac{\mathrm{i}}{\hbar}\hat{H}_At}\hat{A}^\dagger_\alpha(\omega_A)\mathrm{e}^{\frac{\mathrm{i}}{\hbar}\hat{H}_At}=\mathrm{e}^{-\mathrm{i}\omega_At}\hat{A}^\dagger_\alpha(\omega_A),
\tag{2.43}
$$

which come from Eqs. (2.24) and (2.25).

Let us transform Eq. (2.41) into the GKSL form [3, Sec. 3.2.2]. Since the matrix $\gamma(\omega_A) = (\gamma_{\alpha,\beta}(\omega_A))$ is positive semidefinite, it can be diagonalized using the unitary matrix $u(\omega_A)$ as $u(\omega_A)\gamma(\omega_A)u^\dagger(\omega_A) = \tilde{\gamma}(\omega_A)$, where $\tilde{\gamma}(\omega_A)$ is the diagonal matrix whose diagonal element $\tilde{\gamma}_\alpha(\omega_A) = \tilde{\gamma}_{\alpha,\alpha}(\omega_A)$ is non-negative. Defining new operators $\{\hat{C}_\alpha(\omega_A)\}$ as

$$\hat{C}_\alpha(\omega_A) = \sum_\beta u_{\alpha,\beta}(\omega_A)\hat{A}_\beta(\omega_A), \tag{2.44}$$

the decoherence part (2.41) is diagonalized:

$$\mathcal{D}[\hat{\rho}_A(t)] = \sum_{\omega_A}\sum_\alpha \tilde{\gamma}_\alpha(\omega_A)\left(\hat{C}_\alpha(\omega_A)\hat{\rho}_A(t)\hat{C}_\alpha^\dagger(\omega_A) - \frac{1}{2}\{\hat{C}_\alpha^\dagger(\omega_A)\hat{C}_\alpha(\omega_A), \hat{\rho}_A(t)\}\right). \tag{2.45}$$

We have finally obtained the GKSL master equation: Eq. (2.40) with Eq. (2.45).

Let us give explicit forms of $\gamma_{\alpha,\beta}(\omega_A)$ and $S_{\alpha,\beta}(\omega_A)$. In a similar way with Eq. (2.21), we rewrite $\hat{B}_\alpha^I(s)$ as

$$\hat{B}_\alpha^I(s) = \sum_{\omega_B} \mathrm{e}^{-\mathrm{i}\omega_B s}\hat{B}_\alpha(\omega_B) \tag{2.46}$$

with

$$\hat{B}_\alpha(\omega_B) = \sum_{\substack{j,k \\ \epsilon_k^B - \epsilon_j^B = \hbar\omega_B}} \left|\psi_j^B\right\rangle\!\left\langle\psi_j^B\right| \hat{B}_\alpha \left|\psi_k^B\right\rangle\!\left\langle\psi_k^B\right|, \tag{2.47}$$

where ϵ_j^B and $\left|\psi_j^B\right\rangle$ denote the jth eigenvalue and eigenstate of the Hamiltonian of the bath:

$$\hat{H}_B = \sum_j \epsilon_j^B \left|\psi_j^B\right\rangle\!\left\langle\psi_j^B\right|. \tag{2.48}$$

Substituting this into Eq. (2.30), we obtain

$$\begin{aligned}\Gamma_{\alpha,\beta}(\omega_A) &= \sum_{\omega_B}\int_0^\infty \mathrm{d}s\, \mathrm{e}^{\mathrm{i}(\omega_A-\omega_B)s}\mathrm{Tr}_B[\hat{B}_\alpha(\omega_B)\hat{B}_\beta\hat{\rho}_B^{\mathrm{th}}] \\ &= \sum_{\omega_B}\left[\pi\delta(\omega_A-\omega_B) + \mathrm{i}\,\mathrm{P.V.}\left(\frac{1}{\omega_A-\omega_B}\right)\right]\mathrm{Tr}_B[\hat{B}_\alpha(\omega_B)\hat{B}_\beta\hat{\rho}_B^{\mathrm{th}}],\end{aligned} \tag{2.49}$$

where P.V. means the the Cauchy principal value. From Eq. (2.34), we similarly have

$$\begin{aligned}\gamma_{\alpha,\beta}(\omega_A) &= \sum_{\omega_B}\int_{-\infty}^\infty \mathrm{d}s\, \mathrm{e}^{\mathrm{i}(\omega_A-\omega_B)s}\mathrm{Tr}_B[\hat{B}_\alpha(\omega_B)\hat{B}_\beta\hat{\rho}_B^{\mathrm{th}}] \\ &= \sum_{\omega_B} 2\pi\delta(\omega_A-\omega_B)\mathrm{Tr}_B[\hat{B}_\alpha(\omega_B)\hat{B}_\beta\hat{\rho}_B^{\mathrm{th}}].\end{aligned} \tag{2.50}$$

Combining Eqs. (2.32), (2.49), and (2.50) yields

$$\begin{aligned}S_{\alpha,\beta}(\omega_A) &= -\mathrm{i}\Gamma_{\alpha,\beta}(\omega_A) + \frac{\mathrm{i}}{2}\gamma_{\alpha,\beta}(\omega_A) \\ &= \sum_{\omega_B}\mathrm{P.V.}\left(\frac{\mathrm{Tr}_B[\hat{B}_\alpha(\omega_B)\hat{B}_\beta\hat{\rho}_B^{\mathrm{th}}]}{\omega_A-\omega_B}\right).\end{aligned} \tag{2.51}$$

2.4 A stationary state

In this subsection, we show that the Gibbs state of the system at inverse temperature β_B^0,

$$\hat{\rho}_A^{\rm th} := \frac{{\rm e}^{-\beta_B^0 \hat{H}_A}}{{\rm Tr}\left[{\rm e}^{-\beta_B^0 \hat{H}_A}\right]} \tag{2.52}$$

is a stationary solution [4, Sec. 6.2.8] of the Markovian master equation (2.40). Note that the first term in Eq. (2.40) vanishes for $\hat{\rho}_A(t) = \hat{\rho}_A^{\rm th}$ because of Eq. (2.38). Since the decoherence part (2.41) depends on $\gamma_{\alpha,\beta}(\omega_A)$, we derive the relation about $\gamma_{\alpha,\beta}(\omega_A)$. Note that the correlation function of the bath satisfies the following relation:

$$\begin{aligned}
\langle \hat{B}_\alpha^I(s)\hat{B}_\beta\rangle &:= {\rm Tr}_B[\hat{B}_\alpha^I(s)\hat{B}_\beta\hat{\rho}_B^{\rm th}] \\
&= \frac{{\rm Tr}_B[{\rm e}^{\frac{\rm i}{\hbar}\hat{H}_B s}\hat{B}_\alpha {\rm e}^{-\frac{\rm i}{\hbar}\hat{H}_B s}\hat{B}_\beta {\rm e}^{-\beta_B^0\hat{H}_B}]}{{\rm Tr}_B\left[{\rm e}^{-\beta_B^0\hat{H}_B}\right]} \\
&= \frac{{\rm Tr}_B[\hat{B}_\beta {\rm e}^{\frac{\rm i}{\hbar}\hat{H}_B(s+{\rm i}\hbar\beta_B^0)}\hat{B}_\alpha {\rm e}^{-\frac{\rm i}{\hbar}\hat{H}_B s}]}{{\rm Tr}_B\left[{\rm e}^{-\beta_B^0\hat{H}_B}\right]} \\
&= \frac{{\rm Tr}_B[\hat{B}_\beta {\rm e}^{\frac{\rm i}{\hbar}\hat{H}_B(s+{\rm i}\hbar\beta_B^0)}\hat{B}_\alpha {\rm e}^{-\frac{\rm i}{\hbar}\hat{H}_B(s+{\rm i}\hbar\beta_B^0)}{\rm e}^{-\beta_B^0\hat{H}_B}]}{{\rm Tr}_B\left[{\rm e}^{-\beta_B^0\hat{H}_B}\right]} \\
&= {\rm Tr}_B[\hat{B}_\beta\hat{B}_\alpha^I(s+{\rm i}\hbar\beta_B^0)\hat{\rho}_B^{\rm th}] \\
&= \langle \hat{B}_\beta\hat{B}_\alpha^I(s+{\rm i}\hbar\beta_B^0)\rangle,
\end{aligned} \tag{2.53}$$

which is called the Kubo-Martin-Schwinger (KMS) condition [43, 44]. Then, we obtain

$$\begin{aligned}
\gamma_{\alpha,\beta}(\omega_A) &= \int_{-\infty}^{\infty} {\rm d}s\, {\rm e}^{{\rm i}\omega_A s}{\rm Tr}_B[\hat{B}_\alpha^I(s)\hat{B}_\beta\hat{\rho}_B^{\rm th}] \\
&= \int_{-\infty}^{\infty} {\rm d}s\, {\rm e}^{{\rm i}\omega_A s}{\rm Tr}_B[\hat{B}_\beta\hat{B}_\alpha^I(s+{\rm i}\hbar\beta_B^0)\hat{\rho}_B^{\rm th}] \\
&= \sum_{\omega_B} {\rm e}^{\hbar\beta_B^0\omega_B}\int_{-\infty}^{\infty} {\rm d}s\, {\rm e}^{{\rm i}(\omega_A-\omega_B)s}{\rm Tr}_B[\hat{B}_\beta\hat{B}_\alpha(\omega_B)\hat{\rho}_B^{\rm th}] \\
&= \sum_{\omega_B} {\rm e}^{\hbar\beta_B^0\omega_B} 2\pi\delta(\omega_A-\omega_B){\rm Tr}_B[\hat{B}_\beta\hat{B}_\alpha(\omega_B)\hat{\rho}_B^{\rm th}] \\
&= {\rm e}^{\hbar\beta_B^0\omega_A}\sum_{\omega_B} 2\pi\delta(\omega_A-\omega_B){\rm Tr}_B[\hat{B}_\alpha^\dagger(\omega_B)\hat{B}_\beta\hat{\rho}_B^{\rm th}]^* \\
&= {\rm e}^{\hbar\beta_B^0\omega_A}\sum_{\omega_B} 2\pi\delta(\omega_A-\omega_B){\rm Tr}_B[\hat{B}_\alpha(-\omega_B)\hat{B}_\beta\hat{\rho}_B^{\rm th}]^* \\
&= {\rm e}^{\hbar\beta_B^0\omega_A}\gamma_{\alpha,\beta}^*(-\omega_A) \\
&= {\rm e}^{\hbar\beta_B^0\omega_A}\gamma_{\beta,\alpha}(-\omega_A).
\end{aligned} \tag{2.54}$$

Moreover, using the relations (2.24), (2.25), and (2.26), we find

$$\hat{\rho}_A^{\rm th}\hat{A}_\alpha(\omega_A) = {\rm e}^{\hbar\beta_B^0\omega_A}\hat{A}_\alpha(\omega_A)\hat{\rho}_A^{\rm th}, \tag{2.55}$$

$$\hat{\rho}_A^{\rm th}\hat{A}_\alpha^\dagger(\omega_A) = {\rm e}^{-\hbar\beta_B^0\omega_A}\hat{A}_\alpha^\dagger(\omega_A)\hat{\rho}_A^{\rm th}, \tag{2.56}$$

$$\hat{\rho}_A^{\rm th}\hat{A}_\alpha^\dagger(\omega_A)\hat{A}_\beta(\omega_A) = \hat{A}_\alpha^\dagger(\omega_A)\hat{A}_\beta(\omega_A)\hat{\rho}_A^{\rm th}. \tag{2.57}$$

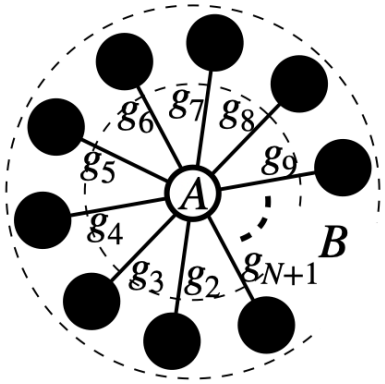

Figure 2.1: A quantum model of coupled harmonic oscillators in a star configuration.

Using Eqs. (2.23), (2.54), (2.55), (2.56), and (2.57), we finally find that $\hat{\rho}_A^{\rm th}$ is a stationary state:

$$\begin{aligned}
\frac{\mathrm{d}\hat{\rho}_A^{\rm th}}{\mathrm{d}t} &= \mathcal{D}[\hat{\rho}_A^{\rm th}] \\
&= \sum_{\omega_A}\sum_{\alpha,\beta}\gamma_{\alpha,\beta}(\omega_A)\left(\hat{A}_\beta(\omega_A)\hat{\rho}_A^{\rm th}\hat{A}_\alpha^\dagger(\omega_A) - \frac{1}{2}\{\hat{A}_\alpha^\dagger(\omega_A)\hat{A}_\beta(\omega_A),\hat{\rho}_A^{\rm th}\}\right) \\
&= \sum_{\omega_A}\sum_{\alpha,\beta}\gamma_{\alpha,\beta}(\omega_A)\left(\mathrm{e}^{-\hbar\beta_B^0\omega_A}\hat{A}_\beta(\omega_A)\hat{A}_\alpha^\dagger(\omega_A)\hat{\rho}_A^{\rm th} - \hat{A}_\alpha^\dagger(\omega_A)\hat{A}_\beta(\omega_A)\hat{\rho}_A^{\rm th}\right) \\
&= \sum_{\omega_A}\sum_{\alpha,\beta}\left(\gamma_{\beta,\alpha}(-\omega_A)\hat{A}_\beta^\dagger(-\omega_A)\hat{A}_\alpha(-\omega_A)\hat{\rho}_A^{\rm th} - \gamma_{\alpha,\beta}(\omega_A)\hat{A}_\alpha^\dagger(\omega_A)\hat{A}_\beta(\omega_A)\hat{\rho}_A^{\rm th}\right) \\
&= \sum_{\omega_A}\sum_{\alpha,\beta}\left(\gamma_{\alpha,\beta}(-\omega_A)\hat{A}_\alpha^\dagger(-\omega_A)\hat{A}_\beta(-\omega_A)\hat{\rho}_A^{\rm th} - \gamma_{\alpha,\beta}(\omega_A)\hat{A}_\alpha^\dagger(\omega_A)\hat{A}_\beta(\omega_A)\hat{\rho}_A^{\rm th}\right) \\
&= 0.
\end{aligned} \tag{2.58}$$

2.5 A damped harmonic oscillator

As an example, let us consider a quantum model of coupled harmonic oscillators in a star configuration [45, Sec. III.A]; see Fig. 2.1. It consists of the central harmonic oscillator $j = 1$, which we refer to as the system A, and N surrounding harmonic oscillators $j = 2, \ldots, N+1$, which we refer to as the bath B. The system A and each harmonic oscillator j in B interact with each other with the coupling constant g_j. The total system is isolated, and hence its Hamiltonian is time-independent as in

$$\hat{H} = \hat{H}_A + \hat{H}_B + \hat{H}_I, \tag{2.59}$$

where

$$\hat{H}_A = \hbar\omega_1\left(\hat{a}_1^\dagger\hat{a}_1 + \frac{1}{2}\right), \tag{2.60}$$

$$\hat{H}_B = \sum_{j=2}^{N+1}\hat{H}_j, \quad \hat{H}_j = \hbar\omega_j\left(\hat{a}_j^\dagger\hat{a}_j + \frac{1}{2}\right), \tag{2.61}$$

$$\hat{H}_I = \sum_{j=2}^{N+1}\hbar g_j\left(\hat{a}_1^\dagger\hat{a}_j + \hat{a}_1\hat{a}_j^\dagger\right), \tag{2.62}$$

with $\hat{a}_j$ and $\hat{a}_j^\dagger$ denoting the annihilation and creation operators of the jth harmonic oscillator, which satisfies the following commutation relations:

$$\left[\hat{a}_j, \hat{a}_k^\dagger\right] = \delta_{j,k}, \tag{2.63}$$

$$[\hat{a}_j, \hat{a}_k] = \left[\hat{a}_j^\dagger, \hat{a}_k^\dagger\right] = 0 \quad \text{for} \quad j,k = 1,\dots,N+1. \tag{2.64}$$

This total Hamiltonian is a type of Fano-Anderson Hamiltonian in condensed matter physics and of Lee-Friedrichs Hamiltonian in atomic physics [46–51]. When the counter-rotating terms $\sum_{j=2}^{N+1} \hbar g_j(\hat{a}_1^\dagger \hat{a}_j^\dagger + \hat{a}_1 \hat{a}_j)$ are added to the interaction Hamiltonian in Eq. (2.62), the total Hamiltonian becomes the Caldeira-Leggett Hamiltonian [51,52]. When N is large enough, the system is damped by the bath, and hence is called a damped harmonic oscillator [4, 6]. If the couplings $\{g_j\}$ of the harmonic oscillators are sufficiently weak, the dynamics of the system is well approximated by the GKSL master equation [3, 4, 6–8], which we derive in this subsection.

Let us rewrite the interaction Hamiltonian (2.62) in the form of Eq. (2.11):

$$\hat{H}_I = \hbar \sum_{\alpha=1}^{2} \hat{A}_\alpha \otimes \hat{B}_\alpha, \tag{2.65}$$

$$\hat{A}_1 = \hat{a}_1^\dagger + \hat{a}_1, \tag{2.66}$$

$$\hat{A}_2 = \mathrm{i}(\hat{a}_1^\dagger - \hat{a}_1), \tag{2.67}$$

$$\hat{B}_1 = \sum_{j=2}^{N+1} \frac{g_j}{2}(\hat{a}_j^\dagger + \hat{a}_j), \tag{2.68}$$

$$\hat{B}_2 = \sum_{j=2}^{N+1} \frac{\mathrm{i}g_j}{2}(\hat{a}_j^\dagger - \hat{a}_j). \tag{2.69}$$

In the interaction picture, we have

$$\hat{H}_I^I(t) = \hbar \sum_{\alpha=1}^{2} \hat{A}_\alpha^I(t) \otimes \hat{B}_\alpha^I(t), \tag{2.70}$$

$$\hat{A}_1^I(t) = \mathrm{e}^{-\mathrm{i}\omega_1 t}\hat{a}_1 + \mathrm{e}^{\mathrm{i}\omega_1 t}\hat{a}_1^\dagger = \sum_{\omega_A = \pm\omega_1} \mathrm{e}^{-\mathrm{i}\omega_A t}\hat{A}_1(\omega_A), \tag{2.71}$$

$$\hat{A}_1(\omega_1) = \hat{a}_1, \quad \hat{A}_1(-\omega_1) = \hat{a}_1^\dagger, \tag{2.72}$$

$$\hat{A}_2^I(t) = -\mathrm{i}\mathrm{e}^{-\mathrm{i}\omega_1 t}\hat{a}_1 + \mathrm{i}\mathrm{e}^{\mathrm{i}\omega_1 t}\hat{a}_1^\dagger = \sum_{\omega_A = \pm\omega_1} \mathrm{e}^{-\mathrm{i}\omega_A t}\hat{A}_2(\omega_A), \tag{2.73}$$

$$\hat{A}_2(\omega_1) = -\mathrm{i}\hat{a}_1, \quad \hat{A}_2(-\omega_1) = \mathrm{i}\hat{a}_1^\dagger, \tag{2.74}$$

$$\hat{B}_1^I(t) = \sum_{j=2}^{N+1} \left(\mathrm{e}^{-\mathrm{i}\omega_j t}\frac{g_j}{2}\hat{a}_j + \mathrm{e}^{\mathrm{i}\omega_j t}\frac{g_j}{2}\hat{a}_j^\dagger\right) = \sum_{\omega_B \in \{\omega_j, -\omega_j | j=2,\dots,N+1\}} \mathrm{e}^{-\mathrm{i}\omega_B t}\hat{B}_1(\omega_B), \tag{2.75}$$

$$\hat{B}_1(\omega_j) = \frac{g_j}{2}\hat{a}_j, \quad \hat{B}_1(-\omega_j) = \frac{g_j}{2}\hat{a}_j^\dagger \tag{2.76}$$

$$\hat{B}_2^I(t) = \sum_{j=2}^{N+1} \left(-\mathrm{i}\mathrm{e}^{-\mathrm{i}\omega_j t}\frac{g_j}{2}\hat{a}_j + \mathrm{i}\mathrm{e}^{\mathrm{i}\omega_j t}\frac{g_j}{2}\hat{a}_j^\dagger\right) = \sum_{\omega_B \in \{\omega_j, -\omega_j | j=2,\dots,N+1\}} \mathrm{e}^{-\mathrm{i}\omega_B t}\hat{B}_2(\omega_B), \tag{2.77}$$

$$\hat{B}_2(\omega_j) = -\mathrm{i}\frac{g_j}{2}\hat{a}_j, \quad \hat{B}_2(-\omega_j) = \mathrm{i}\frac{g_j}{2}\hat{a}_j^\dagger. \tag{2.78}$$

Using them, we calculate $\gamma_{\alpha,\beta}(\omega_A)$ in Eq. (2.50); its (1,1)-component is given by

$$\begin{aligned}
\gamma_{1,1}(\omega_A) &= \sum_{\omega_B} 2\pi\delta(\omega_A-\omega_B)\mathrm{Tr}_B[\hat{B}_1(\omega_B)\hat{B}_1\hat{\rho}_B^{\mathrm{th}}] \\
&= \sum_j \sum_{\omega_B} 2\pi\delta(\omega_A-\omega_B)\mathrm{Tr}_B\left[\hat{B}_1(\omega_B)\frac{g_j}{2}(\hat{a}_j^\dagger+\hat{a}_j)\hat{\rho}_B^{\mathrm{th}}\right] \\
&= \sum_j \sum_{\omega_B=\pm\omega_j} 2\pi\delta(\omega_A-\omega_B)\mathrm{Tr}_j\left[\hat{B}_1(\omega_B)\frac{g_j}{2}(\hat{a}_j^\dagger+\hat{a}_j)\hat{\rho}_j^{\mathrm{th}}\right] \\
&= \sum_j 2\pi\delta(\omega_A-\omega_j)\mathrm{Tr}_j\left[\frac{g_j}{2}\hat{a}_j\frac{g_j}{2}(\hat{a}_j^\dagger+\hat{a}_j)\hat{\rho}_j^{\mathrm{th}}\right] \\
&\quad + \sum_j 2\pi\delta(\omega_A+\omega_j)\mathrm{Tr}_j\left[\frac{g_j}{2}\hat{a}_j^\dagger\frac{g_j}{2}(\hat{a}_j^\dagger+\hat{a}_j)\hat{\rho}_j^{\mathrm{th}}\right] \\
&= \sum_j \frac{\pi g_j^2}{2}\delta(\omega_A-\omega_j)\mathrm{Tr}_j\left[(\hat{a}_j^\dagger\hat{a}_j+1)\hat{\rho}_j^{\mathrm{th}}\right] \\
&\quad + \sum_j \frac{\pi g_j^2}{2}\delta(\omega_A+\omega_j)\mathrm{Tr}_j\left[\hat{a}_j^\dagger\hat{a}_j\hat{\rho}_j^{\mathrm{th}}\right] \\
&= \sum_j \frac{\pi g_j^2}{2}[(\bar{n}(\omega_j)+1)\delta(\omega_A-\omega_j)+\bar{n}(\omega_j)\delta(\omega_A+\omega_j)] \\
&= \sum_j \frac{\pi g_j^2}{2}[(\bar{n}(\omega_A)+1)\delta(\omega_A-\omega_j)+\bar{n}(-\omega_A)\delta(\omega_A+\omega_j)] \\
&= (\bar{n}(\omega_A)+1)\sum_j \frac{\pi g_j^2}{2}[\delta(\omega_A-\omega_j)-\delta(\omega_A+\omega_j)],
\end{aligned} \tag{2.79}$$

where

$$\bar{n}(\omega_j) = \frac{1}{\mathrm{e}^{\beta_B^0\hbar\omega_j}-1} \tag{2.80}$$

is the mean excitation number of a harmonic oscillator at thermal equilibrium with frequency ω_j at inverse temperature β_B^0, and we used

$$\bar{n}(-\omega_j) = -(\bar{n}(\omega_j)+1), \tag{2.81}$$

$$\hat{\rho}_B^{\mathrm{th}} = \frac{\mathrm{e}^{-\beta_B^0\hat{H}_B}}{\mathrm{Tr}\left[\mathrm{e}^{-\beta_B^0\hat{H}_B}\right]} = \bigotimes_{j=2}^{N+1}\frac{\mathrm{e}^{-\beta_B^0\hat{H}_j}}{\mathrm{Tr}\left[\mathrm{e}^{-\beta_B^0\hat{H}_j}\right]} =: \bigotimes_{j=2}^{N+1}\hat{\rho}_j^{\mathrm{th}}. \tag{2.82}$$

Similarly, we have the other components as

$$\gamma_{1,2}(\omega_A) = (\bar{n}(\omega_A)+1)\sum_j \frac{\mathrm{i}\pi g_j^2}{2}[\delta(\omega_A-\omega_j)+\delta(\omega_A+\omega_j)], \tag{2.83}$$

$$\gamma_{2,1}(\omega_A) = \gamma_{1,2}^*(\omega_A) = -\gamma_{1,2}(\omega_A) = -(\bar{n}(\omega_A)+1)\sum_j \frac{\mathrm{i}\pi g_j^2}{2}[\delta(\omega_A-\omega_j)+\delta(\omega_A+\omega_j)], \tag{2.84}$$

$$\gamma_{2,2}(\omega_A) = (\bar{n}(\omega_A)+1)\sum_j \frac{\pi g_j^2}{2}[\delta(\omega_A-\omega_j)-\delta(\omega_A+\omega_j)] = \gamma_{1,1}(\omega_A). \tag{2.85}$$

From Eqs. (2.71) and (2.73), we need to consider two cases: $\omega_A = \pm\omega_1$, so that we have

$$\gamma_{1,1}(\omega_1) = \gamma_{2,2}(\omega_1) = (\bar{n}(\omega_1)+1)\sum_j \frac{\pi g_j^2}{2}\delta(\omega_1-\omega_j) = \frac{\Gamma[\bar{n}(\omega_1)+1]}{2}, \tag{2.86}$$

$$\gamma_{1,2}(\omega_1) = -\gamma_{2,1}(\omega_1) = \frac{\mathrm{i}\Gamma[\bar{n}(\omega_1)+1]}{2}, \tag{2.87}$$

$$\gamma_{1,1}(-\omega_1) = \gamma_{2,2}(-\omega_1) = \frac{\Gamma\bar{n}(\omega_1)}{2}, \tag{2.88}$$

$$\gamma_{1,2}(-\omega_1) = -\gamma_{2,1}(-\omega_1) = -\frac{\mathrm{i}\Gamma\bar{n}(\omega_1)}{2}, \tag{2.89}$$

where

$$\Gamma = \pi J(\omega_1) \tag{2.90}$$

is the relaxation rate of the system with

$$J(\omega) = \sum_{j=2}^{N+1} g_j^2\,\delta(\omega-\omega_j) \tag{2.91}$$

being the spectral density of the bath. Note that this spectral density is a comb of delta peaks [53, Sec. I]. If $\omega_1 \neq \omega_j$ for $j = 2,\ldots,N+1$, we have $\Gamma = \pi J(\omega_1) = 0$. Thus, when we calculate Γ in Eq. (2.90), we need to take the limit of $N\to\infty$ so that the spectral density $J(\omega)$ may become a continuous function. For example, if we consider an Ohmic bath [6, 34], the spectral density is written as $J(\omega) = \eta\omega \mathrm{e}^{-\omega/\omega_c}$, where η is the coupling strength between the system and the bath and ω_c is the cutoff frequency. Having obtained the explicit forms of $\gamma_{\alpha,\beta}(\omega_A)$ in Eqs. (2.86), (2.87), (2.88), and (2.89), and of $\hat{A}_\alpha(\omega_A)$ in Eqs. (2.72) and (2.74), we find the decoherence part (2.41) in the form

$$\begin{aligned}
\mathcal{D}[\hat{\rho}_A(t)] &= \gamma_{1,1}(\omega_1)\left(\hat{A}_1(\omega_1)\hat{\rho}_A(t)\hat{A}_1^\dagger(\omega_1) - \frac{1}{2}\{\hat{A}_1^\dagger(\omega_1)\hat{A}_1(\omega_1),\hat{\rho}_A(t)\}\right)\\
&\quad+\gamma_{1,2}(\omega_1)\left(\hat{A}_2(\omega_1)\hat{\rho}_A(t)\hat{A}_1^\dagger(\omega_1) - \frac{1}{2}\{\hat{A}_1^\dagger(\omega_1)\hat{A}_2(\omega_1),\hat{\rho}_A(t)\}\right)\\
&\quad+\gamma_{2,1}(\omega_1)\left(\hat{A}_1(\omega_1)\hat{\rho}_A(t)\hat{A}_2^\dagger(\omega_1) - \frac{1}{2}\{\hat{A}_2^\dagger(\omega_1)\hat{A}_1(\omega_1),\hat{\rho}_A(t)\}\right)\\
&\quad+\gamma_{2,2}(\omega_1)\left(\hat{A}_2(\omega_1)\hat{\rho}_A(t)\hat{A}_2^\dagger(\omega_1) - \frac{1}{2}\{\hat{A}_2^\dagger(\omega_1)\hat{A}_2(\omega_1),\hat{\rho}_A(t)\}\right)\\
&\quad+\gamma_{1,1}(-\omega_1)\left(\hat{A}_1(-\omega_1)\hat{\rho}_A(t)\hat{A}_1^\dagger(-\omega_1) - \frac{1}{2}\{\hat{A}_1^\dagger(-\omega_1)\hat{A}_1(-\omega_1),\hat{\rho}_A(t)\}\right)\\
&\quad+\gamma_{1,2}(-\omega_1)\left(\hat{A}_2(-\omega_1)\hat{\rho}_A(t)\hat{A}_1^\dagger(-\omega_1) - \frac{1}{2}\{\hat{A}_1^\dagger(-\omega_1)\hat{A}_2(-\omega_1),\hat{\rho}_A(t)\}\right)\\
&\quad+\gamma_{2,1}(-\omega_1)\left(\hat{A}_1(-\omega_1)\hat{\rho}_A(t)\hat{A}_2^\dagger(-\omega_1) - \frac{1}{2}\{\hat{A}_2^\dagger(-\omega_1)\hat{A}_1(-\omega_1),\hat{\rho}_A(t)\}\right)\\
&\quad+\gamma_{2,2}(-\omega_1)\left(\hat{A}_2(-\omega_1)\hat{\rho}_A(t)\hat{A}_2^\dagger(-\omega_1) - \frac{1}{2}\{\hat{A}_2^\dagger(-\omega_1)\hat{A}_2(-\omega_1),\hat{\rho}_A(t)\}\right)\\
&= \Gamma(\bar{n}(\omega_1)+1)\left(2\hat{a}_1\hat{\rho}_A(t)\hat{a}_1^\dagger - \left\{\hat{a}_1^\dagger\hat{a}_1,\hat{\rho}_A(t)\right\}\right)\\
&\quad+\Gamma\bar{n}(\omega_1)\left(2\hat{a}_1^\dagger\hat{\rho}_A(t)\hat{a}_1 - \left\{\hat{a}_1\hat{a}_1^\dagger,\hat{\rho}_A(t)\right\}\right).
\end{aligned} \tag{2.92}$$

Next, in an analogous way with the calculation of $\gamma_{\alpha,\beta}(\omega_A)$, we calculate $S_{\alpha,\beta}(\omega_A)$ (2.51), which appears in the Lamb-shift Hamiltonian (2.36):

$$\begin{aligned}
S_{1,1}(\omega_1) &= \sum_{\omega_B} \mathrm{P.V.} \left(\frac{\mathrm{Tr}_B[\hat{B}_1(\omega_B)\hat{B}_1\hat{\rho}_B^{\mathrm{th}}]}{\omega_1 - \omega_B} \right) \\
&= \mathrm{P.V.} \sum_j \frac{g_j^2}{4} \left(\frac{\bar{n}(\omega_j)+1}{\omega_1 - \omega_j} + \frac{\bar{n}(\omega_j)}{\omega_1 + \omega_j} \right) \\
&= \mathrm{P.V.} \int_0^\infty \mathrm{d}\omega \sum_j \frac{g_j^2}{4} \delta(\omega - \omega_j) \left(\frac{\bar{n}(\omega)+1}{\omega_1 - \omega} + \frac{\bar{n}(\omega)}{\omega_1 + \omega} \right) \\
&= \frac{1}{4} \mathrm{P.V.} \int_0^\infty \mathrm{d}\omega\, J(\omega) \left(\frac{\bar{n}(\omega)+1}{\omega_1 - \omega} + \frac{\bar{n}(\omega)}{\omega_1 + \omega} \right), \qquad (2.93) \\
S_{1,2}(\omega_1) &= S_{2,1}^*(\omega_1) = \frac{\mathrm{i}}{4} \mathrm{P.V.} \int_0^\infty \mathrm{d}\omega\, J(\omega) \left(\frac{\bar{n}(\omega)+1}{\omega_1 - \omega} - \frac{\bar{n}(\omega)}{\omega_1 + \omega} \right), \qquad (2.94) \\
S_{2,2}(\omega_1) &= S_{1,1}(\omega_1), \qquad (2.95) \\
S_{1,1}(-\omega_1) &= S_{2,2}(-\omega_1) = -\frac{1}{4} \mathrm{P.V.} \int_0^\infty \mathrm{d}\omega\, J(\omega) \left(\frac{\bar{n}(\omega)+1}{\omega_1 + \omega} + \frac{\bar{n}(\omega)}{\omega_1 - \omega} \right), \qquad (2.96) \\
S_{1,2}(-\omega_1) &= S_{2,1}^*(-\omega_1) = -\frac{\mathrm{i}}{4} \mathrm{P.V.} \int_0^\infty \mathrm{d}\omega\, J(\omega) \left(\frac{\bar{n}(\omega)+1}{\omega_1 + \omega} - \frac{\bar{n}(\omega)}{\omega_1 - \omega} \right). \qquad (2.97)
\end{aligned}$$

Then, the Lamb-shift Hamiltonian (2.36) is calculated as

$$\begin{aligned}
\frac{\hat{H}_{\mathrm{LS}}}{\hbar} &= S_{1,1}(\omega_1)\hat{A}_1^\dagger(\omega_1)\hat{A}_1(\omega_1) + S_{2,2}(\omega_1)\hat{A}_2^\dagger(\omega_1)\hat{A}_2(\omega_1) \\
&\quad + S_{1,2}(\omega_1)\hat{A}_1^\dagger(\omega_1)\hat{A}_2(\omega_1) + S_{2,1}(\omega_1)\hat{A}_2^\dagger(\omega_1)\hat{A}_1(\omega_1) \\
&\quad + S_{1,1}(-\omega_1)\hat{A}_1^\dagger(-\omega_1)\hat{A}_1(-\omega_1) + S_{2,2}(-\omega_1)\hat{A}_2^\dagger(-\omega_1)\hat{A}_2(-\omega_1) \\
&\quad + S_{1,2}(-\omega_1)\hat{A}_1^\dagger(-\omega_1)\hat{A}_2(-\omega_1) + S_{2,1}(-\omega_1)\hat{A}_2^\dagger(-\omega_1)\hat{A}_1(-\omega_1) \\
&= 2S_{1,1}(\omega_1)\hat{a}_1^\dagger\hat{a}_1 - 2\mathrm{i}S_{1,2}(\omega_1)\hat{a}_1^\dagger\hat{a}_1 + 2S_{1,1}(-\omega_1)\hat{a}_1\hat{a}_1^\dagger + 2\mathrm{i}S_{1,2}(-\omega_1)\hat{a}_1\hat{a}_1^\dagger \\
&= 2[S_{1,1}(\omega_1) - \mathrm{i}S_{1,2}(\omega_1) + S_{1,1}(-\omega_1) + \mathrm{i}S_{1,2}(-\omega_1)]\hat{a}_1^\dagger\hat{a}_1 + \mathrm{const.} \\
&= \mathrm{P.V.} \int_0^\infty \mathrm{d}\omega\, \frac{J(\omega)}{\omega_1 - \omega} \hat{a}_1^\dagger\hat{a}_1 + \mathrm{const.}. \qquad (2.98)
\end{aligned}$$

Therefore, the GKSL equation for the damped harmonic oscillator is given by

$$\begin{aligned}
\frac{\mathrm{d}\hat{\rho}_A(t)}{\mathrm{d}t} &= -\mathrm{i}[(\omega_1 + \Delta)\hat{a}_1^\dagger\hat{a}_1, \hat{\rho}_A(t)] + \Gamma(\bar{n}(\omega_1)+1)\left(2\hat{a}_1\hat{\rho}_A(t)\hat{a}_1^\dagger - \left\{\hat{a}_1^\dagger\hat{a}_1, \hat{\rho}_A(t)\right\}\right) \\
&\quad + \Gamma\bar{n}(\omega_1)\left(2\hat{a}_1^\dagger\hat{\rho}_A(t)\hat{a}_1 - \left\{\hat{a}_1\hat{a}_1^\dagger, \hat{\rho}_A(t)\right\}\right), \qquad (2.99) \\
\Delta &= \mathrm{P.V.} \int_0^\infty \mathrm{d}\omega\, \frac{J(\omega)}{\omega_1 - \omega}. \qquad (2.100)
\end{aligned}$$

Under this GKSL master equation, the system is equilibrated with the bath in the limit $t \to \infty$:

$$\hat{\rho}_A(\infty) = \hat{\rho}_A^{\mathrm{th}} = \frac{\mathrm{e}^{-\beta_B^0 \hat{H}_A}}{\mathrm{Tr}[\mathrm{e}^{-\beta_B^0 \hat{H}_A}]}. \qquad (2.101)$$

This is the stationary state explained in Sec. 2.4.

Chapter 3

Kerr-nonlinear parametric oscillator

A Kerr-nonlinear parametric oscillator (KPO) can be constructed using a quantum circuit. We review the quantum circuit in Sec. 3.1 and the Hamiltonian of a KPO in Sec. 3.2.

3.1 Quantum circuit

3.1.1 An LC circuit

Let us first consider a classical LC oscillator [54, Sec. 2.3], which consists of an inductor L and a capacitor C; see Fig. 3.1. We set the sign of the charge Q on the capacitor and the direction of the current I along the circuit as in Fig. 3.1. Then we have

$$I = -\frac{\mathrm{d}Q}{\mathrm{d}t}. \tag{3.1}$$

Kirchhoff's voltage law dictates

$$\frac{Q}{C} = \frac{\mathrm{d}\Phi}{\mathrm{d}t} = L\frac{\mathrm{d}I}{\mathrm{d}t}, \tag{3.2}$$

where $\Phi = LI$ is a magnetic flux through the inductor. From the above equations, we obtain

$$\frac{\mathrm{d}^2 I}{\mathrm{d}t^2} = -\omega_0^2 I, \quad \omega_0 = \frac{1}{\sqrt{LC}}, \tag{3.3}$$

which shows that the LC oscillator is equivalent to a harmonic oscillator. The magnetic energy stored by the inductor is $\Phi^2/2L$ and the electrical energy stored by the capacitor is $Q^2/2C = C\dot{\Phi}^2/2$, and hence the classical Hamiltonian of the LC oscillator is given by

$$H_{LC} = \frac{C}{2}\dot{\Phi}^2 + \frac{1}{2L}\Phi^2. \tag{3.4}$$

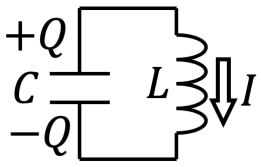

Figure 3.1: An LC oscillator.

Table 3.1: The correspondence between the mechanical oscillator and the LC oscillator.

mechanical oscillator	LC oscillator
m	C
k	$1/L$
x	Φ
$p = m\dot{x}$	$Q = C\dot{\Phi}$

Let us quantize this Hamiltonian by comparing it with that of a mechanical oscillator

$$H_m = \frac{m}{2}\dot{x}^2 + \frac{k}{2}x^2. \tag{3.5}$$

We find the correspondence between the mechanical oscillator and the LC oscillator as in Table 3.1.

The quantum Hamiltonian of the mechanical oscillator is given by

$$\hat{H}_m = \frac{\hat{p}^2}{2m} + \frac{k}{2}\hat{x}^2 \tag{3.6}$$

with the following canonical commutation relation:

$$[\hat{x}, \hat{p}] = \mathrm{i}\hbar. \tag{3.7}$$

Analogously, the quantum Hamiltonian of the LC oscillator is given by

$$\hat{H}_{LC} = \frac{\hat{Q}^2}{2C} + \frac{\hat{\Phi}^2}{2L} \tag{3.8}$$

with the following canonical commutation relation:

$$[\hat{\Phi}, \hat{Q}] = \mathrm{i}\hbar. \tag{3.9}$$

The LC oscillator behaves quantum mechanically if the circuit is constructed of superconducting materials and is held at a sufficiently low temperature [37, Sec. II.A]. It is common to use dimensionless observables $\hat{\varphi}$ and $\hat{n}$ defined by

$$\hat{\varphi} = \frac{\hat{\Phi}}{\Phi_0}, \quad \Phi_0 = \frac{\hbar}{2e}, \tag{3.10}$$

$$\hat{n} = \frac{\hat{Q}}{2e}, \tag{3.11}$$

where Φ_0 is the reduced magnetic flux quantum ($2\pi\Phi_0 = h/2e$ is the magnetic flux quantum), $\hat{\varphi}$ is the phase difference across the inductor [55, Sec. 3.2], and $\hat{n}$ is the number of Cooper pairs [37, Sec. II.A]. Then, the Hamiltonian (3.8) and the commutation relation (3.9) of the quantum LC oscillator are expressed as

$$\hat{H}_{LC} = 4E_C\hat{n}^2 + \frac{E_L}{2}\hat{\varphi}^2, \tag{3.12}$$

$$[\hat{\varphi}, \hat{n}] = \mathrm{i}, \tag{3.13}$$

where $E_C = e^2/2C$ is the charging energy and $E_L = \Phi_0^2/L = \hbar^2/4e^2L$ is the inductive energy [37, Sec. II.A]. Note that the frequency of the LC oscillator can be written as

$$\omega_0 = \frac{1}{\sqrt{LC}} = \frac{2\sqrt{2E_LE_C}}{\hbar}. \tag{3.14}$$

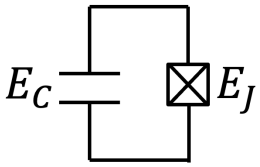

Figure 3.2: A transmon.

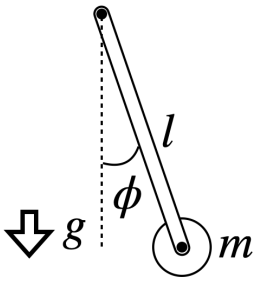

Figure 3.3: A quantum rotor under the force of the gravity.

3.1.2 Transmon

Since the energy levels of the LC oscillator are separated equally, we cannot induce a specific transition; for example, one between the ground and the first excited states. Thus, we cannot use these states as a qubit. In order to encode qubits, we need nonlinearity. As a nonlinear element, we introduce a Josephson junction, whose Hamiltonian is given by

$$\hat{H}_J = -E_J \cos\hat{\varphi}, \tag{3.15}$$

where E_J is the Josephson energy [37, Sec. II.B]. Replacing the inductor in the LC oscillator by the Josephson junction and setting $E_J \gg E_C$, we obtain a transmission-line shunted plasma oscillation qubit, called the transmon, which was introduced in Ref. [56]. Because of the large ratio of E_J/E_C, the transmon is insensitive to the charge noise. Its Hamiltonian is given by [37, Sec. II.C]

$$\hat{H} = 4E_C\hat{n}^2 - E_J \cos\hat{\varphi}. \tag{3.16}$$

The circuit of the transmon is shown in Fig. 3.2

We can grasp the behavior of the transmon by mapping its Hamiltonian on that of a quantum rotor under the force of the gravity [56]; see Fig. 3.3. Let us use cylindrical coordinates (r, ϕ, z). A mass m is attached to one end of a massless rod of length l. The other end of the rod is fixed to the coordinate origin. The rotation axis and the rotation angle are z and $\hat{\phi}$, respectively. Then the Hamiltonian of the rotor is given by

$$\hat{H} = \frac{\hat{L}_z^2}{2ml^2} - mgl\cos\hat{\phi}, \tag{3.17}$$

where $\hat{L}_z = -i\hbar\partial/\partial\phi$ is the angular momentum of the rotor. Comparing Eq. (3.16) with Eq. (3.17), we find the correspondence in Table 3.2. The transmon regime $E_J \gg E_C$ corresponds to a large gravitational force mg and a large moment of inertia ml^2, which restricts the motion of the rotor to $\langle\hat{\phi}^2\rangle \ll 1$. From this correspondence, we find that the Taylor expansion of $\cos\hat{\varphi}$ in Eq. (3.16) to the fourth order, which we will employ in Eq. (3.20), is a good approximation.

Table 3.2: The correspondence between the transmon and the quantum rotor.

transmon	quantum rotor
$\hat{n}$	$\hat{L}_z/\hbar$
$\hat{\varphi}$	$\hat{\phi}$
E_C	$\hbar^2/8ml^2$
E_J	mgl

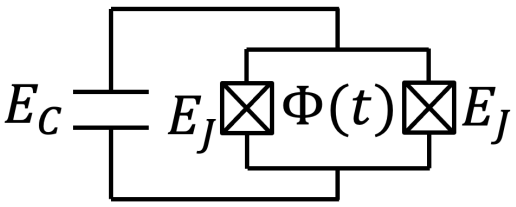

Figure 3.4: A SQUID transmon.

3.1.3 A SQUID transmon

The Josephson energy E_J of the transmon in Fig. 3.2 is a fixed parameter that depends on the design and the fabrication of the Josephson junction. By replacing the single Josephson junction by a loop with two parallel Josephson junctions, we can control the Josephson energy using a magnetic flux threading the loop [37, Sec. II.C]; see Fig. 3.4. A superconducting loop with multiple Josephson junctions is called a superconducting quantum interference device (SQUID) [37, Sec. II.C].

The Hamiltonian of the SQUID transmon in Fig. 3.4 is given by [37, Sec. II.C]

$$\begin{aligned}\hat{H} &= 4E_C\hat{n}^2 - E_J(\cos\hat{\varphi}_1 + \cos\hat{\varphi}_2) \\ &= 4E_C\hat{n}^2 - 2E_J\cos\left(\frac{\hat{\varphi}_1 - \hat{\varphi}_2}{2}\right)\cos\left(\frac{\hat{\varphi}_1 + \hat{\varphi}_2}{2}\right) \\ &= 4E_C\hat{n}^2 - 2E_J\cos\left(\frac{\phi(t)}{2}\right)\cos\hat{\varphi} \\ &= 4E_C\hat{n}^2 - \tilde{E}_J(\phi(t))\cos\hat{\varphi}, \end{aligned} \tag{3.18}$$

where $\hat{\varphi}_1$ and $\hat{\varphi}_2$ are phase differences across each Josephson junction, $\phi(t) := \Phi(t)/\Phi_0$, $\hat{\varphi} := (\hat{\varphi}_1 + \hat{\varphi}_2)/2$, and $\tilde{E}_J(\phi(t)) := 2E_J\cos(\phi(t)/2)$. The second to the last line follows from the following relation [57, Sec. 6.4.1]:

$$\hat{\varphi}_1 - \hat{\varphi}_2 = \phi(t) \mod 2\pi. \tag{3.19}$$

Note that we can tune the Josephson energy $\tilde{E}_J(\phi(t))$ of the SQUID transmon by varying ϕ.

3.2 Hamiltonian of a KPO

3.2.1 KPO with a single SQUID

We here derive the Hamiltonian of a KPO from that of the SQUID transmon in Eq. (3.18). As discussed in Sec. 3.1.2, the average phase difference $\hat{\varphi}$ of the SQUID transmon satisfies $\langle\hat{\varphi}^2\rangle \ll 1$

in the transmon regime $E_J \gg E_C$. Thus, we Taylor-expand $\cos\hat{\varphi}$ to the fourth order:

$$\cos\hat{\varphi} \approx 1 - \frac{1}{2}\hat{\varphi}^2 + \frac{1}{24}\hat{\varphi}^4. \tag{3.20}$$

We define the dc and ac parts of $\phi(t)$ as in [10, Sec. 4.1]

$$\phi(t) = \phi^{\mathrm{dc}} + \phi^{\mathrm{ac}}(t), \quad \phi^{\mathrm{ac}}(t) = 2\pi\delta_p \cos\omega_p t. \tag{3.21}$$

When $\delta_p \ll 1$, we can approximate $\cos(\phi(t)/2)$ as

$$\begin{aligned}\cos\left(\frac{\phi(t)}{2}\right) &= \cos\left(\frac{\phi^{\mathrm{dc}}}{2}\right)\cos\left(\frac{\phi^{\mathrm{ac}}(t)}{2}\right) - \sin\left(\frac{\phi^{\mathrm{dc}}}{2}\right)\sin\left(\frac{\phi^{\mathrm{ac}}(t)}{2}\right) \\ &\approx \cos\left(\frac{\phi^{\mathrm{dc}}}{2}\right) - \pi\delta_p \sin\left(\frac{\phi^{\mathrm{dc}}}{2}\right)\cos\omega_p t.\end{aligned} \tag{3.22}$$

Then we have

$$\tilde{E}_J(\phi(t)) = 2E_J\cos(\phi(t)/2) = \tilde{E}_j^{\mathrm{dc}} + \tilde{E}_j^{\mathrm{ac}}(t), \tag{3.23}$$

$$\tilde{E}_j^{\mathrm{dc}} := 2E_J\cos\left(\frac{\phi^{\mathrm{dc}}}{2}\right), \tag{3.24}$$

$$\tilde{E}_j^{\mathrm{ac}}(t) := -2\pi\delta_p E_J \sin\left(\frac{\phi^{\mathrm{dc}}}{2}\right)\cos\omega_p t. \tag{3.25}$$

From Eqs. (3.18), (3.20), and (3.23), we obtain [10, Sec. 4.1]

$$\hat{H} \approx 4E_C\hat{n}^2 + \frac{\tilde{E}_j^{\mathrm{dc}}}{2}\hat{\varphi}^2 + \frac{\tilde{E}_j^{\mathrm{ac}}(t)}{2}\hat{\varphi}^2 - \frac{\tilde{E}_j^{\mathrm{dc}}}{24}\hat{\varphi}^4, \tag{3.26}$$

where we neglected c-valued terms and the smallest q-valued term $\tilde{E}_j^{\mathrm{ac}}(t)\hat{\varphi}^4/24$. The first and the second terms constitute the Hamiltonian of a harmonic oscillator:

$$\begin{aligned}4E_C\hat{n}^2 + \frac{\tilde{E}_j^{\mathrm{dc}}}{2}\hat{\varphi}^2 &= 2\sqrt{2\tilde{E}_j^{\mathrm{dc}}E_C}\,\frac{1}{2}\left(\frac{1}{2}\sqrt{\frac{\tilde{E}_j^{\mathrm{dc}}}{2E_C}}\hat{\varphi}^2 + 2\sqrt{\frac{2E_C}{\tilde{E}_j^{\mathrm{dc}}}}\hat{n}^2\right) \\ &= \hbar\omega_c^{(0)}\left(\hat{a}^\dagger\hat{a} + \frac{1}{2}\right),\end{aligned} \tag{3.27}$$

where $\omega_c^{(0)} := 2\sqrt{2\tilde{E}_j^{\mathrm{dc}}E_C}/\hbar$ is the Josephson plasma frequency [10, Sec. 4.1] and we have introduced the bosonic creation and annihilation operators $\hat{a}^\dagger$ and $\hat{a}$ as in

$$\hat{\varphi} = \left(\frac{2E_C}{\tilde{E}_j^{\mathrm{dc}}}\right)^{\frac{1}{4}}(\hat{a} + \hat{a}^\dagger), \tag{3.28}$$

$$\hat{n} = -\frac{\mathrm{i}}{2}\left(\frac{\tilde{E}_j^{\mathrm{dc}}}{2E_C}\right)^{\frac{1}{4}}(\hat{a} - \hat{a}^\dagger). \tag{3.29}$$

Then, the Hamiltonian (3.26) is rewritten as

$$\hat{H} = \hbar\omega_c^{(0)}\hat{a}^\dagger\hat{a} - \frac{\hbar K}{12}(\hat{a} + \hat{a}^\dagger)^4 + \hbar p(\hat{a} + \hat{a}^\dagger)^2\cos\omega_p t, \tag{3.30}$$

where

$$K = E_C/\hbar, \tag{3.31}$$

$$p = -\frac{\pi\delta_p E_J}{\hbar}\sqrt{\frac{2E_C}{\tilde{E}_j^{\mathrm{dc}}}}\sin\left(\frac{\phi^{\mathrm{dc}}}{2}\right) = -\frac{\pi\delta_p\omega_c^{(0)}}{4}\tan\left(\frac{\phi^{\mathrm{dc}}}{2}\right), \tag{3.32}$$

and we neglected a c-valued term. In Eq. (3.32), we set parameters so that p may be positive.

Rotating frame

We can transform Eq. (3.30) to the Hamiltonian of a KPO by moving to the rotating frame. We first explain the relation between a state and a Hamiltonian in the laboratory frame and ones in a rotating frame. The Schrödinger equation in the laboratory frame is written in the form

$$\frac{\mathrm{d}}{\mathrm{d}t}\left|\psi\right\rangle = -\frac{\mathrm{i}}{\hbar}\hat{H}\left|\psi\right\rangle . \tag{3.33}$$

Let $\hat{R}$ be the unitary operator which maps a state in the laboratory frame to one in the rotating frame. We now derive the Schrödinger equation which $\hat{R}\left|\psi\right\rangle$ obeys. By taking the time derivative of $\hat{R}\left|\psi\right\rangle$, we obtain

$$\begin{aligned}
\frac{\mathrm{d}}{\mathrm{d}t}(\hat{R}\left|\psi\right\rangle) &= \hat{R}\frac{\mathrm{d}}{\mathrm{d}t}\left|\psi\right\rangle + \left(\frac{\mathrm{d}}{\mathrm{d}t}\hat{R}\right)\left|\psi\right\rangle \\
&= \hat{R}\left(-\frac{\mathrm{i}}{\hbar}\hat{H}\left|\psi\right\rangle\right) + \left(\frac{\mathrm{d}}{\mathrm{d}t}\hat{R}\right)\left|\psi\right\rangle \\
&= -\frac{\mathrm{i}}{\hbar}\left[\hat{R}\hat{H}\hat{R}^{\dagger} + \mathrm{i}\hbar\left(\frac{\mathrm{d}}{\mathrm{d}t}\hat{R}\right)\hat{R}^{\dagger}\right]\hat{R}\left|\psi\right\rangle \\
&= -\frac{\mathrm{i}}{\hbar}\hat{H}^{\mathrm{R}}\hat{R}\left|\psi\right\rangle ,
\end{aligned} \tag{3.34}$$

where

$$\hat{H}^{\mathrm{R}} = \hat{R}\hat{H}\hat{R}^{\dagger} + \mathrm{i}\hbar\left(\frac{\mathrm{d}}{\mathrm{d}t}\hat{R}\right)\hat{R}^{\dagger} \tag{3.35}$$

is the Hamiltonian in the rotating frame.

In the rotating frame with

$$\hat{R} = \exp\left(\mathrm{i}\frac{\omega_p}{2}\hat{a}^{\dagger}\hat{a}t\right), \tag{3.36}$$

the SQUID-transmon Hamiltonian in Eq. (3.30) is transformed into

$$\frac{\hat{H}^{\mathrm{R}}}{\hbar} = \left(\omega_c^{(0)} - \frac{\omega_p}{2}\right)\hat{a}^{\dagger}\hat{a} - \frac{K}{12}\left(\hat{a}\mathrm{e}^{-\mathrm{i}\frac{\omega_p}{2}t} + \hat{a}^{\dagger}\mathrm{e}^{\mathrm{i}\frac{\omega_p}{2}t}\right)^4 + p\left(\hat{a}\mathrm{e}^{-\mathrm{i}\frac{\omega_p}{2}t} + \hat{a}^{\dagger}\mathrm{e}^{\mathrm{i}\frac{\omega_p}{2}t}\right)^2\cos\omega_p t. \tag{3.37}$$

By performing the rotating-wave approximation, in which all the oscillating terms are neglected, we arrive at the Hamiltonian of the KPO [10, Table I]:

$$\frac{\hat{H}^{\mathrm{R}}}{\hbar} = \Delta\hat{a}^{\dagger}\hat{a} - \frac{K}{2}\hat{a}^{\dagger 2}\hat{a}^2 + \frac{p}{2}(\hat{a}^2 + \hat{a}^{\dagger 2}), \tag{3.38}$$

where $\Delta = \omega_c - \omega_p/2$ is the detuning, $\omega_c := \omega_c^{(0)} - K$ is the dressed resonator frequency [58, Appendix C], K is the Kerr nonlinearity, and p is the parametric pumping rate [10]. The modulation frequency is set nearly twice the dressed resonator frequency: $\omega_p \approx 2\omega_c$ [58, Sec. I], which means $\Delta \approx 0$; the detuning is sometimes neglected in the literature [11–13].

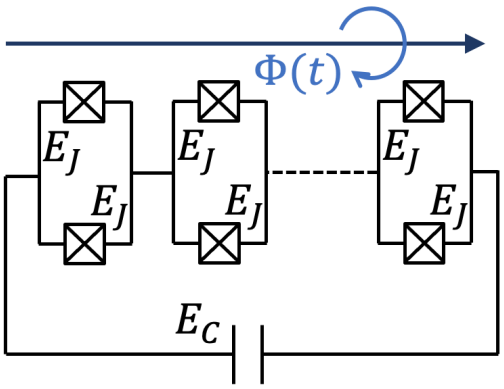

Figure 3.5: A circuit of the KPO with a SQUID array. Each SQUID is threaded by the external magnetic flux $\Phi(t)$.

3.2.2 KPO with multiple SQUIDs

In the previous subsection, we considered the transmon with a single SQUID. A KPO with an array of multiple SQUIDs is also studied in the literature [58, 59]; in fact, it was realized experimentally [58]. The Hamiltonian of the KPO can be derived in a similar way to the case of the single SQUID, as we show briefly in this subsection.

The circuit is shown in Fig. 3.5. The Hamiltonian is given by [58, Appendix C]

$$\hat{H} = 4E_C\hat{n}^2 - NE_J(\Phi(t))\cos\frac{\hat{\varphi}}{N}, \tag{3.39}$$

where $\hat{\varphi}$ is the overall phase across the SQUID array and N is the number of SQUIDs. We here assume that the average phase across each SQUID is $\hat{\varphi}/N$. The Josephson energy for a single SQUID is controlled by the external magnetic flux $\Phi(t)$ as $E_J(\Phi(t)) = E_J + \delta E_J \cos\omega_p t$ with $\delta E_J \ll E_J$. Let us introduce the bosonic annihilation and creation operators as [58, Appendix C]

$$\hat{\varphi} = \left(\frac{2NE_C}{E_J}\right)^{\frac{1}{4}}(\hat{a} + \hat{a}^\dagger), \tag{3.40}$$

$$\hat{n} = -\frac{\mathrm{i}}{2}\left(\frac{E_J}{2NE_C}\right)^{\frac{1}{4}}(\hat{a} - \hat{a}^\dagger). \tag{3.41}$$

Tayler-expanding $\cos\left(\hat{\phi}/N\right)$ to the fourth order in Eq. (3.39) leads to the same form of the Hamiltonian as in Eq. (3.30) [58, Appendix C]:

$$\hat{H} = \hbar\omega_c^{(0)}\hat{a}^\dagger\hat{a} - \frac{\hbar K}{12}(\hat{a} + \hat{a}^\dagger)^4 + \hbar p(\hat{a} + \hat{a}^\dagger)^2\cos\omega_p t \tag{3.42}$$

with $\hbar\omega_c^{(0)} = 2\sqrt{2E_CE_J/N}$, $\hbar K = E_C/N^2$, and $p = \omega_c^{(0)}\delta E_J/4E_J$. Then, the Hamiltonian of the KPO (3.38) is obtained in the same procedure as the previous subsection.

3.2.3 Eigenstates

We here explain the eigenstates of the KPO Hamiltonian in Eq. (3.38). For brevity, we hereafter set $\omega_p = 2\omega_c$, which leads to [10, Sec. 2]

$$\frac{\hat{H}^{\mathrm{R}}}{\hbar} = -\frac{K}{2}\hat{a}^{\dagger 2}\hat{a}^2 + \frac{p}{2}(\hat{a}^2 + \hat{a}^{\dagger 2}) \tag{3.43}$$

$$= -\frac{K}{2}\left(\hat{a}^{\dagger 2} - \alpha^2\right)\left(\hat{a}^2 - \alpha^2\right) + \frac{K}{2}\alpha^4 \tag{3.44}$$

with $\alpha = \sqrt{p/K}$. We see that the two coherent states

$$|\pm\alpha\rangle = \mathrm{e}^{-\frac{|\pm\alpha|^2}{2}} \sum_{n=0}^{\infty} \frac{(\pm\alpha)^n}{\sqrt{n!}} |n\rangle \tag{3.45}$$

are its degenerate eigenstates with the largest eigenenergy $K\alpha^4/2 = p^2/2K$ [11]. Here, $|n\rangle$ is a single-mode bosonic Fock state:

$$\hat{a}\,|0\rangle = 0, \tag{3.46}$$
$$\hat{a}\,|n\rangle = \sqrt{n}\,|n-1\rangle \quad \text{for} \quad n = 1, 2, \ldots, \tag{3.47}$$
$$\hat{a}^\dagger\,|n\rangle = \sqrt{n+1}\,|n+1\rangle \quad \text{for} \quad n = 0, 1, 2, \ldots \tag{3.48}$$

As $\langle\alpha|-\alpha\rangle = \mathrm{e}^{-2\alpha^2}$, $|\alpha\rangle$ and $|-\alpha\rangle$ are quasiorthogonal for $\alpha \gg 1$. Hence, for the realization of a quantum computer, it is proposed to use the KPO as a qubit whose logical states are defined as $|\bar{0}\rangle := |\alpha\rangle$ and $|\bar{1}\rangle := |-\alpha\rangle$ in the regime $p \gg K$ [11,14,15]. The bars of $|\bar{0}\rangle$ and $|\bar{1}\rangle$ distinguish them from the Fock states $|0\rangle$ and $|1\rangle$.

The cats states $|C_\alpha^{0,\pm}\rangle := \mathcal{N}_\alpha^{0,\pm}(|\alpha\rangle \pm |-\alpha\rangle) = \mathcal{N}_\alpha^{0,\pm}(|\bar{0}\rangle \pm |\bar{1}\rangle)$ with $\mathcal{N}_\alpha^{0,\pm} = [2(1 \pm \mathrm{e}^{-2\alpha^2})]^{-1/2}$ are also the degenerate eigenstates [12]. Here, $|C_\alpha^{0,\pm}\rangle$ are called cat states because they are the quantum superpositions of macroscopically distinguishable coherent states $|\alpha\rangle$ and $|-\alpha\rangle$ for large α [60]. Different from $|\pm\alpha\rangle$, the cat states $|C_\alpha^{0,+}\rangle$ and $|C_\alpha^{0,-}\rangle$ are orthogonal to each other. Note that $|C_\alpha^{0,+}\rangle$ and $|C_\alpha^{0,-}\rangle$ have even and odd parities with respect to the number of excitations, respectively. In order to see this, we express $|C_\alpha^{0,\pm}\rangle$ with the Fock states in the form

$$\begin{aligned}
\left|C_\alpha^{0,+}\right\rangle / \mathcal{N}_\alpha^{0,+} &= |\alpha\rangle + |-\alpha\rangle \\
&= \mathrm{e}^{-\frac{|\alpha|^2}{2}} \sum_{n=0}^{\infty} \frac{\alpha^n}{\sqrt{n!}} |n\rangle + \mathrm{e}^{-\frac{|-\alpha|^2}{2}} \sum_{n=0}^{\infty} \frac{(-\alpha)^n}{\sqrt{n!}} |n\rangle \\
&= 2\mathrm{e}^{-\frac{\alpha^2}{2}} \sum_{n=0}^{\infty} \frac{\alpha^{2n}}{\sqrt{(2n)!}} |2n\rangle\,,
\end{aligned} \tag{3.49}$$

$$\left|C_\alpha^{0,-}\right\rangle / \mathcal{N}_\alpha^{0,-} = 2\mathrm{e}^{-\frac{\alpha^2}{2}} \sum_{n=0}^{\infty} \frac{\alpha^{2n+1}}{\sqrt{(2n+1)!}} |2n+1\rangle\,. \tag{3.50}$$

Then we find that $|C_\alpha^{0,+}\rangle$ and $|C_\alpha^{0,-}\rangle$ are the eigenstates of the parity operator $\hat{P} := \exp\left(\mathrm{i}\pi\hat{a}^\dagger\hat{a}\right)$ with the eigenvalues 1 (even) and -1 (odd), respectively. When $p = 0$, the Fock state $|n\rangle$ is the eigenstate of the Hamiltonian (3.43) with eigenenergy $-Kn(n-1)/2$. Then, $|0\rangle$ and $|1\rangle$ are the degenerate eigenstates with the largest eigenenergy 0. Note that $|0\rangle$ and $|1\rangle$ have even and odd parities, respectively. As $\hat{P}$ commutes with the KPO Hamiltonian in Eq. (3.43), the parity is a conserved quantity [12, Sec. II.A]. Thus, preparing the initial states as $|0\rangle$ and $|1\rangle$ and adiabatically increasing the pumping rate from 0 to p, we can generate the cat states $|C_\alpha^{0,+}\rangle$ and $|C_\alpha^{0,-}\rangle$, respectively [10].

Quantum superpositions of the cat states $|C_\alpha^{0,\pm}\rangle$ are a useful resource in quantum computation [13]. In fact, $|C_\alpha^{0,+}\rangle$ is the standard initial state in quantum computation [15]. However, due to the noise from the environment, the quantum superposition is destroyed (decoherence):

$$\left|C_\alpha^{0,+}\right\rangle = \mathcal{N}_\alpha^{0,+}(\,|\bar{0}\rangle + |\bar{1}\rangle) \to \frac{|\bar{0}\rangle\langle\bar{0}| + |\bar{1}\rangle\langle\bar{1}|}{2}. \tag{3.51}$$

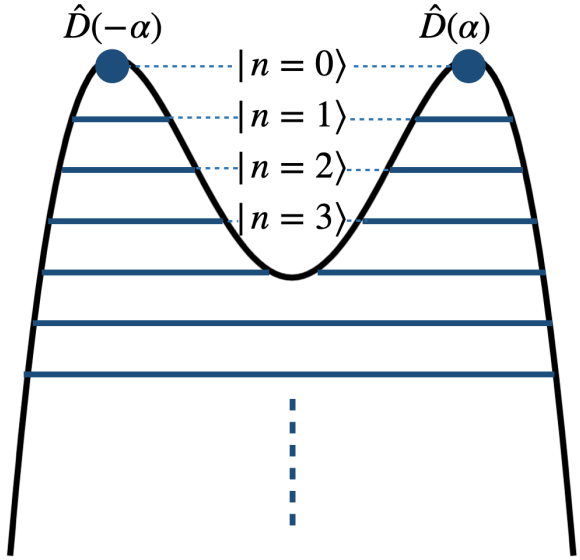

Figure 3.6: Schematic energy diagram of a KPO Hamiltonian in Eq. (3.43).

During this decoherence process, phase-flip error occurs:

$$\left|C_\alpha^{0,+}\right\rangle = \mathcal{N}_\alpha^{0,+}(\,|\bar{0}\rangle + |\bar{1}\rangle) \to \left|C_\alpha^{0,-}\right\rangle = \mathcal{N}_\alpha^{0,-}(\,|\bar{0}\rangle - |\bar{1}\rangle). \tag{3.52}$$

Here, the name "phase flip" comes from the change of the relative phase of $|\bar{1}\rangle$ to $|\bar{0}\rangle$ by π [61, Sec. 2.2.2]. Analyzing and reducing the phase-flip error is important for quantum computation. This is why we calculate the phase-flip rate in Sec. 4.3.2.

The exact forms of the other eigenstates are not known. However, the approximate forms of the high-energy eigenstates can be obtained by transforming the Hamiltonian with the displacement operator $\hat{D}(\pm\alpha) = \mathrm{e}^{\alpha(\hat{a}^\dagger - \hat{a})}$ as [12, Sec. II.A]

$$\begin{aligned}
\frac{\hat{\tilde{H}}^{\mathrm{R}}}{\hbar} &:= \hat{D}(\pm\alpha)\frac{\hat{H}^{\mathrm{R}}}{\hbar}\hat{D}^\dagger(\pm\alpha) \\
&= -\frac{K}{2}\left[(\hat{a}^\dagger \mp \alpha)^2 - \alpha^2\right]\left[(\hat{a} \mp \alpha)^2 - \alpha^2\right] + \frac{K}{2}\alpha^4 \\
&= -\frac{K}{2}(\hat{a}^{\dagger 2} \mp 2\alpha\hat{a}^\dagger)(\hat{a}^2 \mp 2\alpha\hat{a}) + \frac{K}{2}\alpha^4 \\
&= -\frac{K}{2}\hat{a}^{\dagger 2}\hat{a}^2 \pm K\alpha(\hat{a}^{\dagger 2}\hat{a} + \hat{a}^\dagger\hat{a}^2) - 2K\alpha^2\hat{a}^\dagger\hat{a} + \frac{K}{2}\alpha^4 \\
&\approx -2K\alpha^2\hat{a}^\dagger\hat{a} + \frac{K}{2}\alpha^4,
\end{aligned} \tag{3.53}$$

where the last approximation follows from $\alpha \gg 1$. This is the Hamiltonian of an inverted harmonic oscillator [12, Sec. II.A]. The Fock state $|n\rangle$ is an eigenstate of Eq. (3.53) with eigenenergy $-2\hbar K\alpha^2 n + \hbar K\alpha^4/2$. Note that n must be small for the approximation to be good. That is, $|n\rangle$ and $-2\hbar K\alpha^2 n + \hbar K\alpha^4/2$ for small n are the approximate forms of the high-energy eigenstate and eigenenergy, respectively, of $\hat{\tilde{H}}^{\mathrm{R}}$. On the other hand, the approximate high-energy eigenstates of the Hamiltonian (3.43) are the shifted Fock states $\{\hat{D}(\pm\alpha)\,|n\rangle\}$ for small n. Thus, the form of the energy diagram of the Hamiltonian (3.43) is an inverted double well [12, Sec. II.A]; see Fig. 3.6. We can create the eigenstates of the parity operator $\hat{P}$ using

the shifted Fock states as [62, Appendix C]

$$\left|C_\alpha^{n,\pm}\right\rangle := \mathcal{N}_\alpha^{n,\pm}[\hat{D}(\alpha) \pm (-1)^n \hat{D}(-\alpha)]\,|n\rangle\,, \tag{3.54}$$

$$\mathcal{N}_\alpha^{n,\pm} := \left[2\left(1 \pm (-1)^n \mathrm{e}^{-2|\alpha|^2} L_n(4|\alpha|^2)\right)\right]^{-1/2}, \tag{3.55}$$

$$\hat{P}\left|C_\alpha^{n,\pm}\right\rangle = \pm\left|C_\alpha^{n,\pm}\right\rangle, \tag{3.56}$$

where $L_n(x)$ is the Laguerre polynomial. Note that $|C_\alpha^{n,+}\rangle$ and $|C_\alpha^{m,-}\rangle$ are orthogonal to each other because they have different parities with respect to the number of excitations [62, Appendix C]. However, any two states in $\{|C_\alpha^{n,\pm}\rangle\}$ with the same parity are not exactly orthogonal to each other [62, Appendix C]:

$$\left\langle C_\alpha^{m,\pm}\middle|C_\alpha^{n,\pm}\right\rangle = 2\mathcal{N}_\alpha^{m,\pm}\mathcal{N}_\alpha^{n,\pm}[\delta_{m,n} \pm (-1)^m D_{m,n}(2\alpha)], \tag{3.57}$$

$$\begin{aligned} D_{m,n}(2\alpha) &:= \langle m|\hat{D}(2\alpha)|n\rangle \\ &= \mathrm{e}^{-2|\alpha|^2}\sqrt{\frac{\min(m,n)!}{\max(m,n)!}}L_{\min(m,n)}^{(|m-n|)}(4|\alpha|^2) \times \begin{cases} (2\alpha)^{m-n} & m \geq n \\ (-2\alpha^*)^{n-m} & m < n \end{cases}, \end{aligned} \tag{3.58}$$

where $L_n^{(\beta)}(x)$ is the generalized (associated) Laguerre polynomial. Note that $L_n^{(0)}(x) = L_n(x)$.

In addition to the phase-flip error ($|C_\alpha^{0,+}\rangle \leftrightarrow |C_\alpha^{0,-}\rangle$) and the bit flip error ($|\alpha\rangle \leftrightarrow |-\alpha\rangle$, or $|\bar{0}\rangle \leftrightarrow |\bar{1}\rangle$), the noise from the environment can excite the state of a KPO out of the cat subspace C_0, which is spanned by $|C_\alpha^{0,\pm}\rangle$, to the other eigenstates $|C_\alpha^{n,\pm}\rangle$ for $n = 1, 2, \ldots$. This excitation should be reduced in order to efficiently use a KPO as a qubit. We calculate the excitation rate from $|C_\alpha^{0,+}\rangle$ to $|C_\alpha^{1,\pm}\rangle$ in Sec. 4.3.2.

Chapter 4

Decoherence of a Kerr-nonlinear parametric oscillator

In this Chapter, we derive the GKSL equation for a Kerr-nonlinear parametric oscillator (KPO) from the microscopic Hamiltonian and compare it with the GKSL equation in the literature. The latter uses a decoherence part of the damped harmonic oscillator; we review this in Sec. 4.1. Then in Sec. 4.2, we derive the GKSL equation using KPO's two degenerate exact ground states and two degenerate approximate first-excited states. We compare the two GKSL equations in Sec. 4.3; we find that a KPO under our GKSL equation is more robust to excitation errors than that under the GKSL equation in the literature.

4.1 Decoherence of a KPO in the literature

The dominant source of noise in a KPO is a single-photon loss [12, Appendix B]. In order to describe the decoherence due to the noise, the following master equation is often used in the literature (see, for example, Eq. (7) in Ref. [11] and Sec. III in Ref. [12]):

$$\frac{\mathrm{d}\hat{\rho}(t)}{\mathrm{d}t} = -\frac{\mathrm{i}}{\hbar}[\hat{H}, \hat{\rho}(t)] + \kappa\left(2\hat{a}\hat{\rho}(t)\hat{a}^\dagger - \left\{\hat{a}^\dagger\hat{a}, \hat{\rho}(t)\right\}\right), \tag{4.1}$$

where $\hat{H}$ is the KPO Hamiltonian in Eq. (3.43) and κ is a real parameter that is supposed to mean the decay rate. When a single-photon gain is also taken into account, the following master equation is used (see, for example, Eq. (11) in Ref. [12] and Eq. (S21) in the supplementary material of Ref. [13]):

$$\begin{aligned}\frac{\mathrm{d}\hat{\rho}(t)}{\mathrm{d}t} = &-\frac{\mathrm{i}}{\hbar}[\hat{H}, \hat{\rho}(t)] + \kappa(\bar{n}+1)\left(2\hat{a}\hat{\rho}(t)\hat{a}^\dagger - \left\{\hat{a}^\dagger\hat{a}, \hat{\rho}(t)\right\}\right) \\ &+ \kappa\bar{n}\left(2\hat{a}^\dagger\hat{\rho}(t)\hat{a} - \left\{\hat{a}\hat{a}^\dagger, \hat{\rho}(t)\right\}\right),\end{aligned} \tag{4.2}$$

where $\bar{n}$ is the thermal occupation number. Note that Eq. (4.1) corresponds to the case $\bar{n} = 0$ in Eq. (4.2). Since the temperature of the environment of a KPO is finite in experiments (for example, 18 mK in Ref. [13]; see Sec. VI.A in its supplementary material), Eq. (4.2) is preferable to Eq. (4.1).

We find that the decoherence part in Eq. (4.2) has the same form as that of a damped harmonic oscillator in Eq. (2.99). The GKSL equation for the damped harmonic oscillator is derived from a microscopic Hamiltonian as we explained in Sec. 2.5. However, the master equation for the KPO in Eq. (4.2) is not derived from a microscopic Hamiltonian, but naively

adopts the decoherence part of a damped harmonic oscillator; the derivation of Eq. (4.1) (the $\bar{n} = 0$ case) is explained in Appendix B in Ref. [12]. We are not satisfied with it, however, as we explain in the next section.

4.2 Decoherence of a KPO in our treatment

4.2.1 KPO coupled to a bath

Let us incorporate the effect of the environment (namely, the bath). We refer to the KPO (namely, the system) and the bath as A and B, respectively. The bath B consists of N harmonic oscillators; let ω_k and g_k respectively denote the angular frequency and the interaction strength with the system A of the kth harmonic oscillator in the bath B. The total Hamiltonian of the system and the bath in the laboratory frame is given by

$$\hat{H} = \hat{H}_A + \hat{H}_B + \hat{H}_I \tag{4.3}$$

with

$$\hat{H}_A = \hbar\omega_c^{(0)}\hat{a}^\dagger\hat{a} - \frac{\hbar K}{12}(\hat{a}+\hat{a}^\dagger)^4 + \hbar p(\hat{a}+\hat{a}^\dagger)^2\cos\omega_p t, \tag{4.4}$$

$$\hat{H}_B = \sum_{k=1}^{N}\hat{H}_k, \quad \hat{H}_k = \hbar\omega_k\hat{b}_k^\dagger\hat{b}_k, \tag{4.5}$$

$$\hat{H}_I = \sum_{k=1}^{N}\hbar g_k(\hat{a}^\dagger+\hat{a})(\hat{b}_k^\dagger+\hat{b}_k), \tag{4.6}$$

where $\hat{b}_k$ denotes the bosonic annihilation operator of the kth harmonic oscillator. In the rotating frame with

$$\hat{R} = \exp\left[-\mathrm{i}\frac{\omega_p}{2}\left(\hat{a}^\dagger\hat{a} + \sum_{k=1}^{N}\hat{b}_k^\dagger\hat{b}_k\right)t\right], \tag{4.7}$$

the total Hamiltonian is transformed to

$$\hat{H}^{\mathrm{R}} = \hat{H}_A^{\mathrm{R}} + \hat{H}_B^{\mathrm{R}} + \hat{H}_I^{\mathrm{R}} \tag{4.8}$$

with

$$\frac{\hat{H}_A^{\mathrm{R}}}{\hbar} = -\frac{K}{2}\hat{a}^{\dagger 2}\hat{a}^2 + \frac{p}{2}(\hat{a}^2+\hat{a}^{\dagger 2}), \tag{4.9}$$

$$\hat{H}_B^{\mathrm{R}} = \sum_{k=1}^{N}\hbar\left(\omega_k - \frac{\omega_p}{2}\right)\hat{b}_k^\dagger\hat{b}_k, \tag{4.10}$$

$$\hat{H}_I^{\mathrm{R}} = \sum_{k=1}^{N}\hbar g_k\left(\hat{a}^\dagger\hat{b}_k + \hat{a}\hat{b}_k^\dagger\right), \tag{4.11}$$

where we performed the rotating-wave approximation and set $\omega_p = 2\omega_c$.

We prepare the following initial state in the laboratory frame:

$$\hat{\rho}(0) = \hat{\rho}_A(0)\otimes\hat{\rho}_B^{\mathrm{th}} := \hat{\rho}_A(0)\otimes\frac{\mathrm{e}^{-\beta_B^0\hat{H}_B}}{\mathrm{Tr}\left[\mathrm{e}^{-\beta_B^0\hat{H}_B}\right]}. \tag{4.12}$$

In the rotating frame, it is transformed to

$$\hat{\rho}^{\mathrm{R}}(0) = \hat{R}\hat{\rho}(0)\hat{R}^\dagger = \hat{R}_A\hat{\rho}_A(0)\hat{R}_A^\dagger \otimes \hat{R}_B\hat{\rho}_B^{\mathrm{th}}\hat{R}_B^\dagger = \hat{\rho}_A^{\mathrm{R}}(0) \otimes \hat{\rho}_B^{\mathrm{th}}, \tag{4.13}$$

where

$$\hat{R}_A = \exp\left[-\mathrm{i}\frac{\omega_p}{2}\hat{a}^\dagger\hat{a}t\right], \tag{4.14}$$

$$\hat{R}_B = \exp\left[-\mathrm{i}\frac{\omega_p}{2}\sum_k \hat{b}_k^\dagger\hat{b}_k t\right]. \tag{4.15}$$

Note that the initial state of the bath does not change by the transformation $\hat{R}$, since $\hat{R}_B$ and $\hat{\rho}_B^{\mathrm{th}}$ commute with each other. Since we are interested in the bit-flip rate ($|\alpha\rangle \leftrightarrow |-\alpha\rangle$, or $|\bar{0}\rangle \leftrightarrow |\bar{1}\rangle$) and the phase-flip rate ($|C_\alpha^{0,+}\rangle \leftrightarrow |C_\alpha^{0,-}\rangle$), the initial state of the system $\hat{\rho}_A^{\mathrm{R}}(0)$ is chosen from states in the cat subspace C^0 spanned by $|C_\alpha^{0,+}\rangle$ ($\propto |\alpha\rangle + |-\alpha\rangle$) and $|C_\alpha^{0,-}\rangle$ ($\propto |\alpha\rangle - |-\alpha\rangle$). We focus on a short interaction time in which the state of the system is mostly confined to the cat subspace C^0, because after that, the KPO is useless as a qubit.

Incidentally, in Appendix B in Ref. [12], the authors derived Eq. (4.1) by starting from the following interaction Hamiltonian in the interaction picture:

$$\hat{H}_I^I(t) = \sum_k \hbar g_k(\hat{a}\hat{b}_k^\dagger \mathrm{e}^{\mathrm{i}(\omega_k-\omega_c)t} + \hat{a}^\dagger\hat{b}_k\mathrm{e}^{-\mathrm{i}(\omega_k-\omega_c)t}), \tag{4.16}$$

where $\omega_c = \omega_c^{(0)} - K$ is the dressed resonator frequency [58, Appendix C]. This interaction Hamiltonian would be obtained if the total Hamiltonian in the Schrödinger picture were given by

$$\hat{H} = \hat{H}_A + \hat{H}_B + \hat{H}_I \tag{4.17}$$

with

$$\hat{H}_A = \hbar\omega_c\hat{a}^\dagger\hat{a}, \tag{4.18}$$

$$\hat{H}_B = \sum_{k=1}^N \hat{H}_k, \quad \hat{H}_k = \hbar\omega_k\hat{b}_k^\dagger\hat{b}_k, \tag{4.19}$$

$$\hat{H}_I = \sum_{k=1}^N \hbar g_k(\hat{a}^\dagger\hat{b}_k + \hat{a}\hat{b}_k^\dagger). \tag{4.20}$$

If the total Hamiltonian in the rotating frame were given by Eq. (4.17), by tracing the same route as in Sec. 2.5, we would have the following form of the decoherence part:

$$\begin{aligned}\mathcal{D}^{\mathrm{lit}}[\hat{\rho}_A^{\mathrm{R}}(t)] = {}& \Gamma\left(\frac{\omega_p}{2}\right)\left[\bar{n}\left(\frac{\omega_p}{2}\right)+1\right]\left(2\hat{a}\hat{\rho}_A^{\mathrm{R}}(t)\hat{a}^\dagger - \left\{\hat{a}^\dagger\hat{a}, \hat{\rho}_A^{\mathrm{R}}(t)\right\}\right) \\ & + \Gamma\left(\frac{\omega_p}{2}\right)\bar{n}\left(\frac{\omega_p}{2}\right)\left(2\hat{a}^\dagger\hat{\rho}_A^{\mathrm{R}}(t)\hat{a} - \left\{\hat{a}\hat{a}^\dagger, \hat{\rho}_A^{\mathrm{R}}(t)\right\}\right),\end{aligned} \tag{4.21}$$

where

$$\bar{n}(\omega) = \frac{1}{\mathrm{e}^{\beta_B^0\hbar\omega}-1}, \tag{4.22}$$

$$\Gamma(\omega) = \pi J(\omega), \tag{4.23}$$

$$J(\omega) = \sum_k g_k^2\delta(\omega-\omega_k) \tag{4.24}$$

and we set $\omega_p = 2\omega_c$. Note that Eq. (4.18) is not the Hamiltonian of a KPO, but of a harmonic oscillator. Hence, we do not accept Eq. (4.21) as the decoherence part of a GKSL equation for a KPO.

4.2.2 Our GKSL equation for a KPO

We now derive the GKSL equation for a KPO in a way similar to that of the damped harmonic oscillator in Sec. 2.5. Let us rewrite the interaction Hamiltonian (4.11) in the form of Eq. (2.11):

$$\hat{H}_I^{\mathrm{R}} = \hbar \sum_{\bar{\alpha}=1}^{2} \hat{A}_{\bar{\alpha}}^{\mathrm{R}} \otimes \hat{B}_{\bar{\alpha}}^{\mathrm{R}}, \tag{4.25}$$

$$\hat{A}_1^{\mathrm{R}} = \hat{a}^\dagger + \hat{a}, \tag{4.26}$$

$$\hat{A}_2^{\mathrm{R}} = \mathrm{i}(\hat{a}^\dagger - \hat{a}), \tag{4.27}$$

$$\hat{B}_1^{\mathrm{R}} = \sum_{k=1}^{N} \frac{g_k}{2}(\hat{b}_k^\dagger + \hat{b}_k), \tag{4.28}$$

$$\hat{B}_2^{\mathrm{R}} = \sum_{k=1}^{N} \frac{\mathrm{i}g_k}{2}(\hat{b}_k^\dagger - \hat{b}_k), \tag{4.29}$$

where we put the bar in the subscript $\bar{\alpha}$ in order to distinguish it from $\alpha = \sqrt{p/K}$. In the interaction picture, we have

$$\hat{H}_I^{\mathrm{R},I}(t) = \hbar \sum_{\bar{\alpha}=1}^{2} \hat{A}_{\bar{\alpha}}^{\mathrm{R},I}(t) \otimes \hat{B}_{\bar{\alpha}}^{\mathrm{R},I}(t), \tag{4.30}$$

$$\hat{A}_{\bar{\alpha}}^{\mathrm{R},I}(t) = \mathrm{e}^{\frac{\mathrm{i}}{\hbar}\hat{H}_A^{\mathrm{R}}t} \hat{A}_{\bar{\alpha}}^{\mathrm{R}} \mathrm{e}^{-\frac{\mathrm{i}}{\hbar}\hat{H}_A^{\mathrm{R}}t}, \tag{4.31}$$

$$\hat{B}_{\bar{\alpha}}^{\mathrm{R},I}(t) = \mathrm{e}^{\frac{\mathrm{i}}{\hbar}\hat{H}_B^{\mathrm{R}}t} \hat{B}_{\bar{\alpha}}^{\mathrm{R}} \mathrm{e}^{-\frac{\mathrm{i}}{\hbar}\hat{H}_B^{\mathrm{R}}t}. \tag{4.32}$$

We can calculate $\gamma_{\bar{\alpha},\bar{\beta}}^{\mathrm{R}}(\omega_A)$ in Eq. (2.50) as (see Appendix A)

$$\gamma_{1,1}^{\mathrm{R}}(\omega_A) = \Gamma(\omega_p/2 + \omega_A)\frac{\bar{n}(\omega_p/2 + \omega_A) + 1}{2} + \Gamma(\omega_p/2 - \omega_A)\frac{\bar{n}(\omega_p/2 - \omega_A)}{2}, \tag{4.33}$$

$$\gamma_{1,2}^{\mathrm{R}}(\omega_A) = \mathrm{i}\Gamma(\omega_p/2 + \omega_A)\frac{\bar{n}(\omega_p/2 + \omega_A) + 1}{2} - \mathrm{i}\Gamma(\omega_p/2 - \omega_A)\frac{\bar{n}(\omega_p/2 - \omega_A)}{2}, \tag{4.34}$$

$$\gamma_{2,1}^{\mathrm{R}}(\omega_A) = \gamma_{1,2}^{\mathrm{R}*}(\omega_A) = -\gamma_{1,2}^{\mathrm{R}}(\omega_A), \tag{4.35}$$

$$\gamma_{2,2}^{\mathrm{R}}(\omega_A) = \gamma_{1,1}^{\mathrm{R}}(\omega_A), \tag{4.36}$$

where

$$\bar{n}(\omega) = \frac{1}{\mathrm{e}^{\beta_B^0 \hbar\omega} - 1}, \tag{4.37}$$

$$\Gamma(\omega) = \pi J(\omega), \tag{4.38}$$

$$J(\omega) = \sum_k g_k^2 \delta(\omega - \omega_k). \tag{4.39}$$

Let us rewrite $\hat{A}_{\bar{\alpha}}^{\mathrm{R},I}(t)$ as

$$\begin{aligned}
\hat{A}_{\bar{\alpha}}^{\mathrm{R},I}(t) &= \mathrm{e}^{\frac{\mathrm{i}}{\hbar}\hat{H}_A^{\mathrm{R}}t} \hat{A}_{\bar{\alpha}}^{\mathrm{R}} \mathrm{e}^{-\frac{\mathrm{i}}{\hbar}\hat{H}_A^{\mathrm{R}}t} \\
&= \sum_{j,k} \mathrm{e}^{\frac{\mathrm{i}}{\hbar}\hat{H}_A^{\mathrm{R}}t} \left|\psi_j^{\mathrm{R}}\right\rangle\!\left\langle\psi_j^{\mathrm{R}}\right| \hat{A}_{\bar{\alpha}}^{\mathrm{R}} \left|\psi_k^{\mathrm{R}}\right\rangle\!\left\langle\psi_k^{\mathrm{R}}\right| \mathrm{e}^{-\frac{\mathrm{i}}{\hbar}\hat{H}_A^{\mathrm{R}}t} \\
&= \sum_{j,k} \mathrm{e}^{-\frac{\mathrm{i}}{\hbar}(\epsilon_k^{\mathrm{R}} - \epsilon_j^{\mathrm{R}})t} \left\langle\psi_j^{\mathrm{R}}\right| \hat{A}_{\bar{\alpha}}^{\mathrm{R}} \left|\psi_k^{\mathrm{R}}\right\rangle \left|\psi_j^{\mathrm{R}}\right\rangle\!\left\langle\psi_k^{\mathrm{R}}\right|
\end{aligned}$$

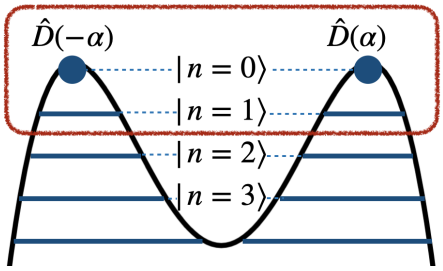

Figure 4.1: Four-level approximation. We consider only four levels in the red frame.

$$= \sum_{\omega_A} \mathrm{e}^{-\mathrm{i}\omega_A t} \hat{A}^{\mathrm{R}}_{\bar{\alpha}}(\omega_A), \tag{4.40}$$

$$\hat{A}^{\mathrm{R}}_{\bar{\alpha}}(\omega_A) := \sum_{\substack{j,k \\ \epsilon^{\mathrm{R}}_k - \epsilon^{\mathrm{R}}_j = \hbar\omega_A}} \left\langle \psi^{\mathrm{R}}_j \middle| \hat{A}^{\mathrm{R}}_{\bar{\alpha}} \middle| \psi^{\mathrm{R}}_k \right\rangle \left| \psi^{\mathrm{R}}_j \middle\rangle\middle\langle \psi^{\mathrm{R}}_k \right|, \tag{4.41}$$

where $\{\epsilon^{\mathrm{R}}_j\}$ and $\{\left|\psi^{\mathrm{R}}_j\right\rangle\}$ are the eigenenergies and the eigenstates of $\hat{H}^{\mathrm{R}}_A$, respectively. If we knew the exact forms of $\{\epsilon^{\mathrm{R}}_j\}$ and $\{\left|\psi^{\mathrm{R}}_j\right\rangle\}$, we could obtain the exact form of the master equation for the KPO in the rotating frame in the Schrödinger picture:

$$\frac{\mathrm{d}\hat{\rho}^{\mathrm{R}}_A(t)}{\mathrm{d}t} = -\frac{\mathrm{i}}{\hbar}[\hat{H}^{\mathrm{R}}_A, \hat{\rho}^{\mathrm{R}}_A(t)] + \mathcal{D}[\hat{\rho}^{\mathrm{R}}_A(t)], \tag{4.42}$$

$$\mathcal{D}[\hat{\rho}^{\mathrm{R}}_A(t)] = \sum_{\omega_A} \sum_{\bar{\alpha},\bar{\beta}} \gamma^{\mathrm{R}}_{\bar{\alpha},\bar{\beta}}(\omega_A) \left(\hat{A}^{\mathrm{R}}_{\bar{\beta}}(\omega_A) \hat{\rho}^{\mathrm{R}}_A(t) \hat{A}^{\mathrm{R}\dagger}_{\bar{\alpha}}(\omega_A) - \frac{1}{2}\{\hat{A}^{\mathrm{R}\dagger}_{\bar{\alpha}}(\omega_A)\hat{A}^{\mathrm{R}}_{\bar{\beta}}(\omega_A), \hat{\rho}^{\mathrm{R}}_A(t)\} \right), \tag{4.43}$$

where we neglected the Lamb-shift Hamiltonian $\hat{H}^{\mathrm{R}}_{\mathrm{LS}}$ for brevity. In fact, the Lamb-shift Hamiltonian is often neglected in the literature because it has only a small effect in general [3]. We are interested in the early-time dynamics in which the population probability of the system in the cat subspace C^0 is very high. Thus, in Eq. (4.41), which appears in the decoherence part, Eq. (4.43), we neglect all the terms except for ones which induce the transitions between high-energy levels. We assume that $|C^{1,\pm}_\alpha\rangle$ are good approximations of the first two excited eigenstates of the Hamiltonian of the system in Eq. (4.9). We hence approximate Eq. (4.41) as

$$\hat{A}^{\mathrm{R}}_{\bar{\alpha}}(\omega_A) \approx \sum_{\substack{j,k=0 \\ \epsilon^{\mathrm{R}}_k - \epsilon^{\mathrm{R}}_j = \hbar\omega_A}}^{3} \left\langle \psi^{\mathrm{R}}_j \middle| \hat{A}^{\mathrm{R}}_{\bar{\alpha}} \middle| \psi^{\mathrm{R}}_k \right\rangle \left| \psi^{\mathrm{R}}_j \middle\rangle\middle\langle \psi^{\mathrm{R}}_k \right| \tag{4.44}$$

with

$$\left|\psi^{\mathrm{R}}_0\right\rangle = \left|C^{0,+}_\alpha\right\rangle, \quad \left|\psi^{\mathrm{R}}_1\right\rangle = \left|C^{0,-}_\alpha\right\rangle, \tag{4.45}$$

$$\left|\psi^{\mathrm{R}}_2\right\rangle \approx \left|C^{1,+}_\alpha\right\rangle, \quad \left|\psi^{\mathrm{R}}_3\right\rangle \approx \left|C^{1,-}_\alpha\right\rangle; \tag{4.46}$$

see Fig. 4.1. The eigenenergies are given by

$$\epsilon^{\mathrm{R}}_0 = \epsilon^{\mathrm{R}}_1 = \frac{1}{2}\hbar K\alpha^4, \tag{4.47}$$

$$\epsilon^{\mathrm{R}}_2 \approx \epsilon^{\mathrm{R}}_3 \approx -2\hbar K\alpha^2 + \frac{1}{2}\hbar K\alpha^4 = -2\hbar p + \frac{1}{2}\hbar K\alpha^4. \tag{4.48}$$

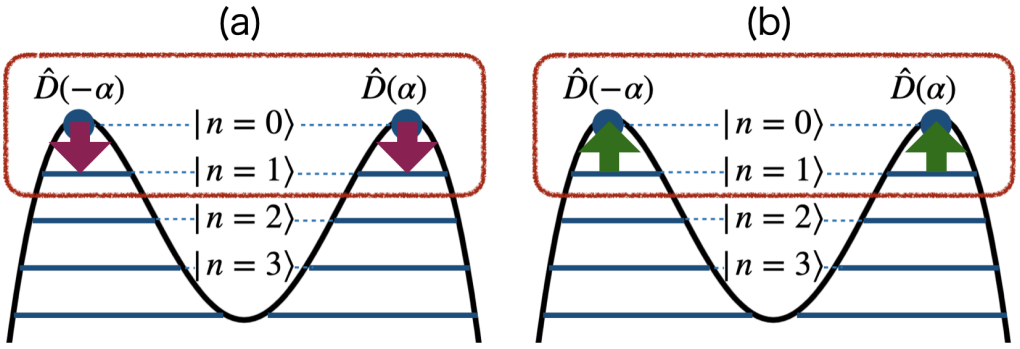

Figure 4.2: (a) The excitation induced by $\hat{A}_1^{\mathrm{R}}(2p)$. (b) The deexcitation induced by $\hat{A}_1^{\mathrm{R}}(-2p)$.

Then, we need to consider the three cases: $\omega_A = 0, \pm 2p$ in Eq. (4.44). After a lengthy calculation (see Appendix B), we arrive at the following form of the decoherence part:

$$\begin{aligned}\mathcal{D}^{\mathrm{ours}}[\hat{\rho}_A^{\mathrm{R}}(t)] \approx{}& \Gamma\left(\frac{\omega_p}{2}\right)\left[\bar{n}\left(\frac{\omega_p}{2}\right)+\frac{1}{2}\right]\left(\hat{A}_1^{\mathrm{R}}(0)\hat{\rho}_A^{\mathrm{R}}(t)\hat{A}_1^{\mathrm{R}\dagger}(0)-\frac{1}{2}\{(\hat{A}_1^{\mathrm{R}\dagger}(0)\hat{A}_1^{\mathrm{R}}(0),\hat{\rho}_A^{\mathrm{R}}(t)\}\right)\\
&+2\Gamma\left(\frac{\omega_p}{2}-2p\right)\bar{n}\left(\frac{\omega_p}{2}-2p\right)\\
&\times\left(\hat{A}_1^{\mathrm{R}}(2p)\hat{\rho}_A^{\mathrm{R}}(t)\hat{A}_1^{\mathrm{R}\dagger}(2p)-\frac{1}{2}\{\hat{A}_1^{\mathrm{R}\dagger}(2p)\hat{A}_1^{\mathrm{R}}(2p),\hat{\rho}_A^{\mathrm{R}}(t)\}\right)\\
&+2\Gamma\left(\frac{\omega_p}{2}-2p\right)\left[\bar{n}\left(\frac{\omega_p}{2}-2p\right)+1\right]\\
&\times\left(\hat{A}_1^{\mathrm{R}}(-2p)\hat{\rho}_A^{\mathrm{R}}(t)\hat{A}_1^{\mathrm{R}\dagger}(-2p)-\frac{1}{2}\{\hat{A}_1^{\mathrm{R}\dagger}(-2p)\hat{A}_1^{\mathrm{R}}(-2p),\hat{\rho}_A^{\mathrm{R}}(t)\}\right), \qquad (4.49)\end{aligned}$$

where

$$\begin{aligned}\hat{A}_1^{\mathrm{R}}(0) &\approx \sum_{n=0}^{1} 2\alpha\left(\left|C_\alpha^{n,-}\right\rangle\!\left\langle C_\alpha^{n,+}\right| + \left|C_\alpha^{n,+}\right\rangle\!\left\langle C_\alpha^{n,-}\right|\right)\\
&\approx 2\alpha\left(|\alpha\rangle\langle\alpha| - |-\alpha\rangle\langle-\alpha| + \hat{D}(\alpha)\,|1\rangle\langle 1|\,\hat{D}^\dagger(\alpha) - \hat{D}(-\alpha)\,|1\rangle\langle 1|\,\hat{D}^\dagger(-\alpha)\right), \qquad (4.50)\\
\hat{A}_1^{\mathrm{R}}(2p) &\approx \left|C_\alpha^{1,-}\right\rangle\!\left\langle C_\alpha^{0,+}\right| + \left|C_\alpha^{1,+}\right\rangle\!\left\langle C_\alpha^{0,-}\right| \approx \hat{D}(\alpha)\,|1\rangle\langle\alpha| + \hat{D}(-\alpha)\,|1\rangle\langle-\alpha|\,, \qquad (4.51)\\
\hat{A}_1^{\mathrm{R}}(-2p) &\approx \left|C_\alpha^{0,-}\right\rangle\!\left\langle C_\alpha^{1,+}\right| + \left|C_\alpha^{0,+}\right\rangle\!\left\langle C_\alpha^{1,-}\right| \approx |\alpha\rangle\langle 1|\,\hat{D}^\dagger(\alpha) + |-\alpha\rangle\langle 1|\,\hat{D}^\dagger(-\alpha), \qquad (4.52)\\
\left|C_\alpha^{n,\pm}\right\rangle &\approx \frac{1}{\sqrt{2}}[\hat{D}(\alpha)\pm(-1)^n\hat{D}(-\alpha)]\,|n\rangle\,. \qquad (4.53)\end{aligned}$$

Note that $\hat{A}_1^{\mathrm{R}}(0)$ does not change energy, $\hat{A}_1^{\mathrm{R}}(2p)$ induces the excitation, and $\hat{A}_1^{\mathrm{R}}(-2p)$ induces the deexcitation; see Fig. 4.2. We find that our decoherence part in Eq. (4.49) does not cause the bit flip ($|\alpha\rangle \leftrightarrow |-\alpha\rangle$, or $|\bar{0}\rangle \leftrightarrow |\bar{1}\rangle$). This is because we made the approximation $|C_\alpha^{n,\pm}\rangle \approx \frac{1}{\sqrt{2}}[\hat{D}(\alpha)\pm(-1)^n\hat{D}(-\alpha)]\,|n\rangle$. In order to calculate the bit-flip rate correctly, we must adopt

$$\begin{aligned}\left|C_\alpha^{n,\pm}\right\rangle &= \mathcal{N}_\alpha^{n,\pm}[\hat{D}(\alpha)\pm(-1)^n\hat{D}(-\alpha)]\,|n\rangle\,, \qquad (4.54)\\
\mathcal{N}_\alpha^{n,\pm} &= \left[2\left(1\pm(-1)^n e^{-2|\alpha|^2}L_n(4|\alpha|^2)\right)\right]^{-1/2}, \qquad (4.55)\end{aligned}$$

where $L_n(x)$ is the Laguerre polynomial. This is left as our future work.

4.3 Comparison between our GKSL equation and the GKSL equation in the literature

Let us compare our GKSL equation

$$\frac{\mathrm{d}\hat{\rho}_A^{\mathrm{R}}(t)}{\mathrm{d}t} = -\frac{\mathrm{i}}{\hbar}[\hat{H}_A^{\mathrm{R}}, \hat{\rho}_A^{\mathrm{R}}(t)] + \mathcal{D}^{\mathrm{ours}}[\hat{\rho}_A^{\mathrm{R}}(t)] \tag{4.56}$$

and the GKSL equation in the literature

$$\frac{\mathrm{d}\hat{\rho}_A^{\mathrm{R}}(t)}{\mathrm{d}t} = -\frac{\mathrm{i}}{\hbar}[\hat{H}_A^{\mathrm{R}}, \hat{\rho}_A^{\mathrm{R}}(t)] + \mathcal{D}^{\mathrm{lit}}[\hat{\rho}_A^{\mathrm{R}}(t)], \tag{4.57}$$

where the two decoherence parts $\mathcal{D}^{\mathrm{ours}}[\hat{\rho}_A^{\mathrm{R}}(t)]$ and $\mathcal{D}^{\mathrm{lit}}[\hat{\rho}_A^{\mathrm{R}}(t)]$ are given by Eqs. (4.49) and (4.21), respectively. We compare analytical forms of Eqs. (4.49) and (4.21) in Sec. 4.3.1. Then, we compare the dynamics of a KPO under Eqs. (4.56) and (4.57) in Sec. 4.3.2.

4.3.1 Analytical comparison

To begin with, we transform Eq. (4.21) by expressing $\hat{a}$ and $\hat{a}^\dagger$ in terms of $\hat{A}_1^{\mathrm{R}}(0)$ and $\hat{A}_1^{\mathrm{R}}(\pm 2p)$ in order to make clear the difference between Eq. (4.21) and (4.49). The action of $\hat{a}$ on $|C_\alpha^{n,\pm}\rangle$ for $n = 0, 1$ is

$$\hat{a}\,|C_\alpha^{0,\pm}\rangle = \alpha\,|C_\alpha^{0,\mp}\rangle\,, \tag{4.58}$$
$$\hat{a}\,|C_\alpha^{1,\pm}\rangle = \alpha\,|C_\alpha^{1,\mp}\rangle + |C_\alpha^{0,\mp}\rangle\,. \tag{4.59}$$

Restricting the Hilbert space to the subspace spanned by $|C_\alpha^{0,\pm}\rangle$ and $|C_\alpha^{1,\pm}\rangle$, we approximate $\hat{a}$ as

$$\begin{aligned}\hat{a} &\approx \alpha\left(|C_\alpha^{0,+}\rangle\langle C_\alpha^{0,-}| + |C_\alpha^{0,-}\rangle\langle C_\alpha^{0,+}|\right) + \left(\alpha\,|C_\alpha^{1,-}\rangle + |C_\alpha^{0,-}\rangle\right)\langle C_\alpha^{1,+}| + \left(\alpha\,|C_\alpha^{1,+}\rangle + |C_\alpha^{0,+}\rangle\right)\langle C_\alpha^{1,-}| \\ &= \frac{1}{2}\hat{A}_1^{\mathrm{R}}(0) + \hat{A}_1^{\mathrm{R}}(-2p) = \frac{1}{2}\hat{A}_1^{\mathrm{R}\dagger}(0) + \hat{A}_1^{\mathrm{R}\dagger}(2p).\end{aligned} \tag{4.60}$$

We then approximate $\hat{a}^\dagger$ as

$$\hat{a}^\dagger \approx \frac{1}{2}\hat{A}_1^{\mathrm{R}}(0) + \hat{A}_1^{\mathrm{R}}(2p) = \frac{1}{2}\hat{A}_1^{\mathrm{R}\dagger}(0) + \hat{A}_1^{\mathrm{R}\dagger}(-2p). \tag{4.61}$$

Using Eqs. (4.60) and (4.61), we approximate $\mathcal{D}^{\mathrm{lit}}[\hat{\rho}_A^{\mathrm{R}}(t)]$ in Eq. (4.21) as

$$\begin{aligned}\mathcal{D}^{\mathrm{lit}}[\hat{\rho}_A^{\mathrm{R}}(t)] \approx\ & \Gamma\left(\frac{\omega_p}{2}\right)\left[\bar{n}\left(\frac{\omega_p}{2}\right) + \frac{1}{2}\right]\left(\hat{A}_1^{\mathrm{R}}(0)\hat{\rho}_A^{\mathrm{R}}(t)\hat{A}_1^{\mathrm{R}\dagger}(0) - \frac{1}{2}\{(\hat{A}_1^{\mathrm{R}\dagger}(0)\hat{A}_1^{\mathrm{R}}(0), \hat{\rho}_A^{\mathrm{R}}(t)\}\right) \\ &+ 2\Gamma\left(\frac{\omega_p}{2}\right)\bar{n}\left(\frac{\omega_p}{2}\right)\left(\hat{A}_1^{\mathrm{R}}(2p)\hat{\rho}_A^{\mathrm{R}}(t)\hat{A}_1^{\mathrm{R}\dagger}(2p) - \frac{1}{2}\{\hat{A}_1^{\mathrm{R}\dagger}(2p)\hat{A}_1^{\mathrm{R}}(2p), \hat{\rho}_A^{\mathrm{R}}(t)\}\right) \\ &+ 2\Gamma\left(\frac{\omega_p}{2}\right)\left[\bar{n}\left(\frac{\omega_p}{2}\right) + 1\right] \\ &\times\left(\hat{A}_1^{\mathrm{R}}(-2p)\hat{\rho}_A^{\mathrm{R}}(t)\hat{A}_1^{\mathrm{R}\dagger}(-2p) - \frac{1}{2}\{\hat{A}_1^{\mathrm{R}\dagger}(-2p)\hat{A}_1^{\mathrm{R}}(-2p), \hat{\rho}_A^{\mathrm{R}}(t)\}\right) \\ &+ \Gamma\left(\frac{\omega_p}{2}\right)\bar{n}\left(\frac{\omega_p}{2}\right)\left(\hat{A}_1^{\mathrm{R}}(2p)\hat{\rho}_A^{\mathrm{R}}(t)\hat{A}_1^{\mathrm{R}\dagger}(0) - \frac{1}{2}\{\hat{A}_1^{\mathrm{R}\dagger}(0)\hat{A}_1^{\mathrm{R}}(2p), \hat{\rho}_A^{\mathrm{R}}(t)\}\right) \\ &+ \Gamma\left(\frac{\omega_p}{2}\right)\bar{n}\left(\frac{\omega_p}{2}\right)\left(\hat{A}_1^{\mathrm{R}}(0)\hat{\rho}_A^{\mathrm{R}}(t)\hat{A}_1^{\mathrm{R}\dagger}(2p) - \frac{1}{2}\{\hat{A}_1^{\mathrm{R}\dagger}(2p)\hat{A}_1^{\mathrm{R}}(0), \hat{\rho}_A^{\mathrm{R}}(t)\}\right)\end{aligned}$$

$$
\begin{aligned}
&+\Gamma\left(\frac{\omega_p}{2}\right)\left[\bar{n}\left(\frac{\omega_p}{2}\right)+1\right]\\
&\times\left(\hat{A}_1^{\mathrm{R}}(-2p)\hat{\rho}_A^{\mathrm{R}}(t)\hat{A}_1^{\mathrm{R}\dagger}(0)-\frac{1}{2}\{\hat{A}_1^{\mathrm{R}\dagger}(0)\hat{A}_1^{\mathrm{R}}(-2p),\hat{\rho}_A^{\mathrm{R}}(t)\}\right)\\
&+\Gamma\left(\frac{\omega_p}{2}\right)\left[\bar{n}\left(\frac{\omega_p}{2}\right)+1\right]\\
&\times\left(\hat{A}_1^{\mathrm{R}}(0)\hat{\rho}_A^{\mathrm{R}}(t)\hat{A}_1^{\mathrm{R}\dagger}(-2p)-\frac{1}{2}\{\hat{A}_1^{\mathrm{R}\dagger}(-2p)\hat{A}_1^{\mathrm{R}}(0),\hat{\rho}_A^{\mathrm{R}}(t)\}\right). \qquad (4.62)
\end{aligned}
$$

On the other hand, we transform Eq. (4.49) as follows. Assuming $p \ll \omega_p$ as in the experiments [13, 58], we make the approximation $\omega_p/2 - 2p \approx \omega_p/2$ in Eq. (4.49), so that we have

$$
\begin{aligned}
\mathcal{D}^{\mathrm{ours}}[\hat{\rho}_A^{\mathrm{R}}(t)] \approx{}& \Gamma\left(\frac{\omega_p}{2}\right)\left[\bar{n}\left(\frac{\omega_p}{2}\right)+\frac{1}{2}\right]\left(\hat{A}_1^{\mathrm{R}}(0)\hat{\rho}_A^{\mathrm{R}}(t)\hat{A}_1^{\mathrm{R}\dagger}(0)-\frac{1}{2}\{(\hat{A}_1^{\mathrm{R}\dagger}(0)\hat{A}_1^{\mathrm{R}}(0),\hat{\rho}_A^{\mathrm{R}}(t)\}\right)\\
&+2\Gamma\left(\frac{\omega_p}{2}\right)\bar{n}\left(\frac{\omega_p}{2}\right)\left(\hat{A}_1^{\mathrm{R}}(2p)\hat{\rho}_A^{\mathrm{R}}(t)\hat{A}_1^{\mathrm{R}\dagger}(2p)-\frac{1}{2}\{\hat{A}_1^{\mathrm{R}\dagger}(2p)\hat{A}_1^{\mathrm{R}}(2p),\hat{\rho}_A^{\mathrm{R}}(t)\}\right)\\
&+2\Gamma\left(\frac{\omega_p}{2}\right)\left[\bar{n}\left(\frac{\omega_p}{2}\right)+1\right]\\
&\times\left(\hat{A}_1^{\mathrm{R}}(-2p)\hat{\rho}_A^{\mathrm{R}}(t)\hat{A}_1^{\mathrm{R}\dagger}(-2p)-\frac{1}{2}\{\hat{A}_1^{\mathrm{R}\dagger}(-2p)\hat{A}_1^{\mathrm{R}}(-2p),\hat{\rho}_A^{\mathrm{R}}(t)\}\right). \qquad (4.63)
\end{aligned}
$$

We find that $\mathcal{D}^{\mathrm{lit}}[\hat{\rho}_A^{\mathrm{R}}(t)]$ in Eq. (4.62) contains all the terms in $\mathcal{D}^{\mathrm{ours}}[\hat{\rho}_A^{\mathrm{R}}(t)]$ in Eq. (4.63). The difference is

$$
\begin{aligned}
\mathcal{D}^{\mathrm{lit}}[\hat{\rho}_A^{\mathrm{R}}(t)]-\mathcal{D}^{\mathrm{ours}}[\hat{\rho}_A^{\mathrm{R}}(t)] \approx{}& \Gamma\left(\frac{\omega_p}{2}\right)\bar{n}\left(\frac{\omega_p}{2}\right)\left(\hat{A}_1^{\mathrm{R}}(2p)\hat{\rho}_A^{\mathrm{R}}(t)\hat{A}_1^{\mathrm{R}\dagger}(0)-\frac{1}{2}\{\hat{A}_1^{\mathrm{R}\dagger}(0)\hat{A}_1^{\mathrm{R}}(2p),\hat{\rho}_A^{\mathrm{R}}(t)\}\right)\\
&+\Gamma\left(\frac{\omega_p}{2}\right)\bar{n}\left(\frac{\omega_p}{2}\right)\left(\hat{A}_1^{\mathrm{R}}(0)\hat{\rho}_A^{\mathrm{R}}(t)\hat{A}_1^{\mathrm{R}\dagger}(2p)-\frac{1}{2}\{\hat{A}_1^{\mathrm{R}\dagger}(2p)\hat{A}_1^{\mathrm{R}}(0),\hat{\rho}_A^{\mathrm{R}}(t)\}\right)\\
&+\Gamma\left(\frac{\omega_p}{2}\right)\left[\bar{n}\left(\frac{\omega_p}{2}\right)+1\right]\\
&\times\left(\hat{A}_1^{\mathrm{R}}(-2p)\hat{\rho}_A^{\mathrm{R}}(t)\hat{A}_1^{\mathrm{R}\dagger}(0)-\frac{1}{2}\{\hat{A}_1^{\mathrm{R}\dagger}(0)\hat{A}_1^{\mathrm{R}}(-2p),\hat{\rho}_A^{\mathrm{R}}(t)\}\right)\\
&+\Gamma\left(\frac{\omega_p}{2}\right)\left[\bar{n}\left(\frac{\omega_p}{2}\right)+1\right]\\
&\times\left(\hat{A}_1^{\mathrm{R}}(0)\hat{\rho}_A^{\mathrm{R}}(t)\hat{A}_1^{\mathrm{R}\dagger}(-2p)-\frac{1}{2}\{\hat{A}_1^{\mathrm{R}\dagger}(-2p)\hat{A}_1^{\mathrm{R}}(0),\hat{\rho}_A^{\mathrm{R}}(t)\}\right). \qquad (4.64)
\end{aligned}
$$

Let us see the effect of this difference on the dynamics of the KPO in the next subsection.

4.3.2 Numerical comparison

For numerical calculations, we used QuTiP, the Quantum Toolbox in Python [63, 64]. We show the parameters that we used in Table 4.1. Here, d is the dimension at which we truncated bosonic excited states. We employ an Ohmic bath whose spectral density is given by

$$
J(\omega) = \eta\omega \mathrm{e}^{-\omega/\omega_{\mathrm{cut}}}, \qquad (4.65)
$$

where η is the coupling strength and ω_{cut} is the cutoff frequency. We calculated the fidelity [61, Sec. 9.2.2] listed in Table 4.2. This table shows that the approximation in Eq. (4.46) is good; hence we can use our GKSL equation in (4.56), which is based on Eq. (4.46). Note that neither $F(|\psi_0^{\mathrm{R}}\rangle, |C_\alpha^{0,+}\rangle)$ nor $F(|\psi_1^{\mathrm{R}}\rangle, |C_\alpha^{0,-}\rangle)$ is exactly equal to one because we truncated bosonic excited states.

Table 4.1: The parameters of the KPO and the bath.

d	50
$\alpha = \sqrt{p/K}$	5
$K/2\pi$	1 MHz
$\omega_p/2\pi$	12 GHz
η	10^{-4}
$\omega_{\rm cut}/2\pi$	48 GHz

Table 4.2: Fidelity $F(|\psi\rangle, |\phi\rangle) = |\langle\psi|\phi\rangle|$.

$F(\|\psi_0^{\rm R}\rangle, \|C_\alpha^{0,+}\rangle)$	0.9999998
$F(\|\psi_1^{\rm R}\rangle, \|C_\alpha^{0,-}\rangle)$	0.999994
$F(\|\psi_2^{\rm R}\rangle, \|C_\alpha^{1,+}\rangle)$	0.989
$F(\|\psi_3^{\rm R}\rangle, \|C_\alpha^{1,-}\rangle)$	0.989

Phase-flip rate and excitation rate

Let us prepare the initial state of the system as $\hat{\rho}_A^{\rm R}(0) = |C_\alpha^{0,+}\rangle\langle C_\alpha^{0,+}|$. We here consider the phase-flip rate ($|C_\alpha^{0,+}\rangle \to |C_\alpha^{0,-}\rangle$) and the excitation rate ($|C_\alpha^{0,+}\rangle \to |C_\alpha^{1,\pm}\rangle$). We calculate the population of each level in the form $p_n^\pm(t) := \langle C_\alpha^{n,\pm}|\hat{\rho}_A^{\rm R}(t)|C_\alpha^{n,\pm}\rangle$ for $n = 0, 1$. For the initial temperature of the bath, we consider two cases: $T_B^0 = 18\,{\rm mK}$ and $180\,{\rm mK}$.

First, we set $T_B^0 = 18\,{\rm mK}$. We show in Fig. 4.3 the time dependence of the population of each level $p_n^\pm(t)$ for $n = 0, 1$ under our GKSL equation (4.56) and under the GKSL equation (4.57) in the literature. Under our GKSL equation (4.56) (see the left panel), the phase-flip rate $p_0^-(t)$ increases from $p_0^-(0) = 0$ to $p_0^-(5\,{\rm ns}) \approx 0.5$ and becomes almost constant after $t \approx 5\,{\rm ns}$. The excitation rates $p_1^\pm(t)$ are very low, although not exactly zero; see Fig. 4.4. On the other hand, under the GKSL equation (4.57) in the literature (see the right panel in Fig. 4.3), the population in the ground states $p_0^\pm(t)$ decreases after $t = 5\,{\rm ns}$ due to the excitation to $|C_\alpha^{1,\pm}\rangle$.

The difference between the two panels in Fig. 4.3 comes from the difference between $\mathcal{D}^{\rm ours}[\hat{\rho}_A^{\rm R}(t)]$ and $\mathcal{D}^{\rm lit}[\hat{\rho}_A^{\rm R}(t)]$ in Eq. (4.64). Let us focus on this difference under the parameters in Table 4.1 and $T_B^0 = 18\,{\rm mK}$. Since $\bar{n}(\omega_p/2) = [{\rm e}^{\hbar\omega_p/2k_BT_B^0} - 1]^{-1} \approx 1.1 \times 10^{-7} \ll 1$, we can approximate Eq. (4.63) as

$$\mathcal{D}^{\rm ours}[\hat{\rho}_A^{\rm R}(t)] \approx \frac{1}{2}\Gamma\left(\frac{\omega_p}{2}\right)\left(\hat{A}_1^{\rm R}(0)\hat{\rho}_A^{\rm R}(t)\hat{A}_1^{\rm R\dagger}(0) - \frac{1}{2}\{(\hat{A}_1^{\rm R\dagger}(0)\hat{A}_1^{\rm R}(0), \hat{\rho}_A^{\rm R}(t)\}\right) + 2\Gamma\left(\frac{\omega_p}{2}\right)\left(\hat{A}_1^{\rm R}(-2p)\hat{\rho}_A^{\rm R}(t)\hat{A}_1^{\rm R\dagger}(-2p) - \frac{1}{2}\{\hat{A}_1^{\rm R\dagger}(-2p)\hat{A}_1^{\rm R}(-2p), \hat{\rho}_A^{\rm R}(t)\}\right). \quad (4.66)$$

This decoherence part does not induce the excitation to $|C_\alpha^{1,\pm}\rangle$. On the other hand, $\bar{n}(\omega_p/2) \ll 1$ leads to

$$\mathcal{D}^{\rm lit}[\hat{\rho}_A^{\rm R}(t)] - \mathcal{D}^{\rm ours}[\hat{\rho}_A^{\rm R}(t)] \approx \Gamma\left(\frac{\omega_p}{2}\right)\left(\hat{A}_1^{\rm R}(-2p)\hat{\rho}_A^{\rm R}(t)\hat{A}_1^{\rm R\dagger}(0) - \frac{1}{2}\{\hat{A}_1^{\rm R\dagger}(0)\hat{A}_1^{\rm R}(-2p), \hat{\rho}_A^{\rm R}(t)\}\right) + \Gamma\left(\frac{\omega_p}{2}\right)\left(\hat{A}_1^{\rm R}(0)\hat{\rho}_A^{\rm R}(t)\hat{A}_1^{\rm R\dagger}(-2p) - \frac{1}{2}\{\hat{A}_1^{\rm R\dagger}(-2p)\hat{A}_1^{\rm R}(0), \hat{\rho}_A^{\rm R}(t)\}\right)$$

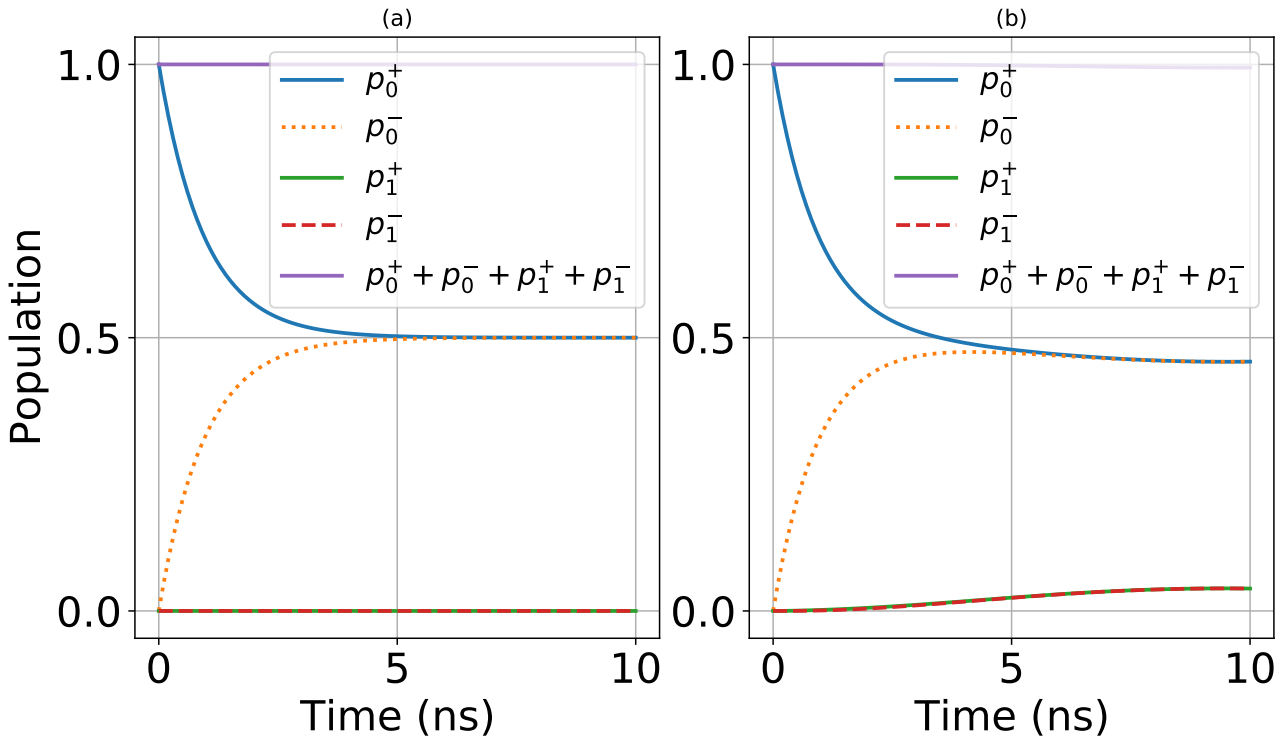

Figure 4.3: The time dependence of the population of each level $p_n^{\pm}(t) := \langle C_\alpha^{n,\pm} | \hat{\rho}_A^{\mathrm{R}}(t) | C_\alpha^{n,\pm} \rangle$ for $n = 0, 1$: (a) Under our GKSL equation (4.56); (b) Under the GKSL equation (4.57) in the literature. The initial temperature of the bath is $T_B^0 = 18\,\mathrm{mK}$. The other parameters are shown in Table 4.1.

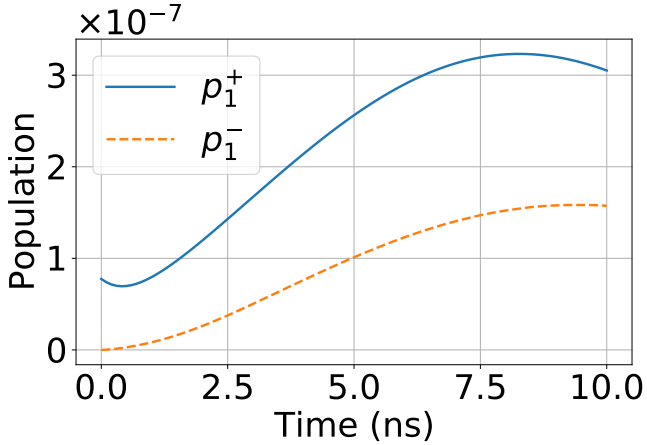

Figure 4.4: The excitation rates $p_1^{\pm}(t)$ under our GKSL equation (4.56). The parameters are the same as those in Fig. 4.3

$$= \Gamma\left(\frac{\omega_p}{2}\right)\left(\hat{A}_1^{\mathrm{R}}(-2p)\hat{\rho}_A^{\mathrm{R}}(t)\hat{A}_1^{\mathrm{R}\dagger}(0) - \frac{1}{2}\{\hat{A}_1^{\mathrm{R}\dagger}(0)\hat{A}_1^{\mathrm{R}\dagger}(2p), \hat{\rho}_A^{\mathrm{R}}(t)\}\right)$$
$$+ \Gamma\left(\frac{\omega_p}{2}\right)\left(\hat{A}_1^{\mathrm{R}}(0)\hat{\rho}_A^{\mathrm{R}}(t)\hat{A}_1^{\mathrm{R}\dagger}(-2p) - \frac{1}{2}\{\hat{A}_1^{\mathrm{R}}(2p)\hat{A}_1^{\mathrm{R}}(0), \hat{\rho}_A^{\mathrm{R}}(t)\}\right) \tag{4.67}$$

and

$$\mathcal{D}^{\mathrm{lit}}[\hat{\rho}_A^{\mathrm{R}}(t)] \approx \frac{1}{2}\Gamma\left(\frac{\omega_p}{2}\right)\left(\hat{A}_1^{\mathrm{R}}(0)\hat{\rho}_A^{\mathrm{R}}(t)\hat{A}_1^{\mathrm{R}\dagger}(0) - \frac{1}{2}\{(\hat{A}_1^{\mathrm{R}\dagger}(0)\hat{A}_1^{\mathrm{R}}(0), \hat{\rho}_A^{\mathrm{R}}(t)\}\right)$$
$$+ 2\Gamma\left(\frac{\omega_p}{2}\right)\left(\hat{A}_1^{\mathrm{R}}(-2p)\hat{\rho}_A^{\mathrm{R}}(t)\hat{A}_1^{\mathrm{R}\dagger}(-2p) - \frac{1}{2}\{\hat{A}_1^{\mathrm{R}\dagger}(-2p)\hat{A}_1^{\mathrm{R}}(-2p), \hat{\rho}_A^{\mathrm{R}}(t)\}\right)$$
$$+ \Gamma\left(\frac{\omega_p}{2}\right)\left(\hat{A}_1^{\mathrm{R}}(-2p)\hat{\rho}_A^{\mathrm{R}}(t)\hat{A}_1^{\mathrm{R}\dagger}(0) - \frac{1}{2}\{\hat{A}_1^{\mathrm{R}\dagger}(0)\hat{A}_1^{\mathrm{R}\dagger}(2p), \hat{\rho}_A^{\mathrm{R}}(t)\}\right)$$
$$+ \Gamma\left(\frac{\omega_p}{2}\right)\left(\hat{A}_1^{\mathrm{R}}(0)\hat{\rho}_A^{\mathrm{R}}(t)\hat{A}_1^{\mathrm{R}\dagger}(-2p) - \frac{1}{2}\{\hat{A}_1^{\mathrm{R}}(2p)\hat{A}_1^{\mathrm{R}}(0), \hat{\rho}_A^{\mathrm{R}}(t)\}\right). \tag{4.68}$$

Note that $\hat{\rho}_A^{\mathrm{R}}(t)\hat{A}_1^{\mathrm{R}\dagger}(0)\hat{A}_1^{\mathrm{R}\dagger}(2p)$ in the third line in Eq. (4.68) and $\hat{A}_1^{\mathrm{R}}(2p)\hat{A}_1^{\mathrm{R}}(0)\hat{\rho}_A^{\mathrm{R}}(t)$ in the last line in Eq. (4.68) induce the excitation to $|C_\alpha^{1,\pm}\rangle$. We find that while our decoherence part $\mathcal{D}^{\mathrm{ours}}[\hat{\rho}_A^{\mathrm{R}}(t)]$ in Eq. (4.66) does not induce the excitation to $|C_\alpha^{1,\pm}\rangle$ very much, the decoherence part in the literature $\mathcal{D}^{\mathrm{lit}}[\hat{\rho}_A^{\mathrm{R}}(t)]$ in Eq. (4.68) does. This means that our GKSL equation (4.56) is not only more accurate than the GKSL equation (4.57) in the literature, but also preferable to the latter in the sense that the state of a KPO under our GKSL equation is more confined to the cat subspace C_0 than that under the GKSL equation in the literature. That is, a KPO under our GKSL equation is more robust to excitation errors than that under the GKSL equation in the literature. We can make similar arguments when the initial temperature of the bath is low enough to satisfy $\bar{n}(\omega_p/2) \ll 1$.

Next, we set $T_B^0 = 180\,\mathrm{mK}$. In this case $\bar{n}(\omega_p/2) \approx 0.25$, and

$$2\Gamma(\omega_p/2)\bar{n}(\omega_p/2)\hat{A}_1^{\mathrm{R}}(2p)\hat{\rho}_A^{\mathrm{R}}(t)\hat{A}_1^{\mathrm{R}\dagger}(2p)$$

in our decoherence part (4.63) induces excitation to $|C_\alpha^{1,\pm}\rangle$; see Fig. 4.5. Because of the difference between $\mathcal{D}^{\mathrm{ours}}[\hat{\rho}_A^{\mathrm{R}}(t)]$ and $\mathcal{D}^{\mathrm{lit}}[\hat{\rho}_A^{\mathrm{R}}(t)]$ in Eq. (4.64), the time dependence of the population of each level $p_n^{\pm}(t) := \langle C_\alpha^{n,\pm}|\hat{\rho}_A^{\mathrm{R}}(t)|C_\alpha^{n,\pm}\rangle$ for $n = 0, 1$ under our GKSL equation (4.56) differs from that under the GKSL equation (4.57) in the literature. We can see that $p_1^{\pm}(t)$ under our GKSL equation are smaller than those under the GKSL equation in the literature. Hence, when $T_B^0 = 180\,\mathrm{mK}$, too, a KPO under our GKSL equation is more robust to excitation errors than that under the GKSL equation in the literature.

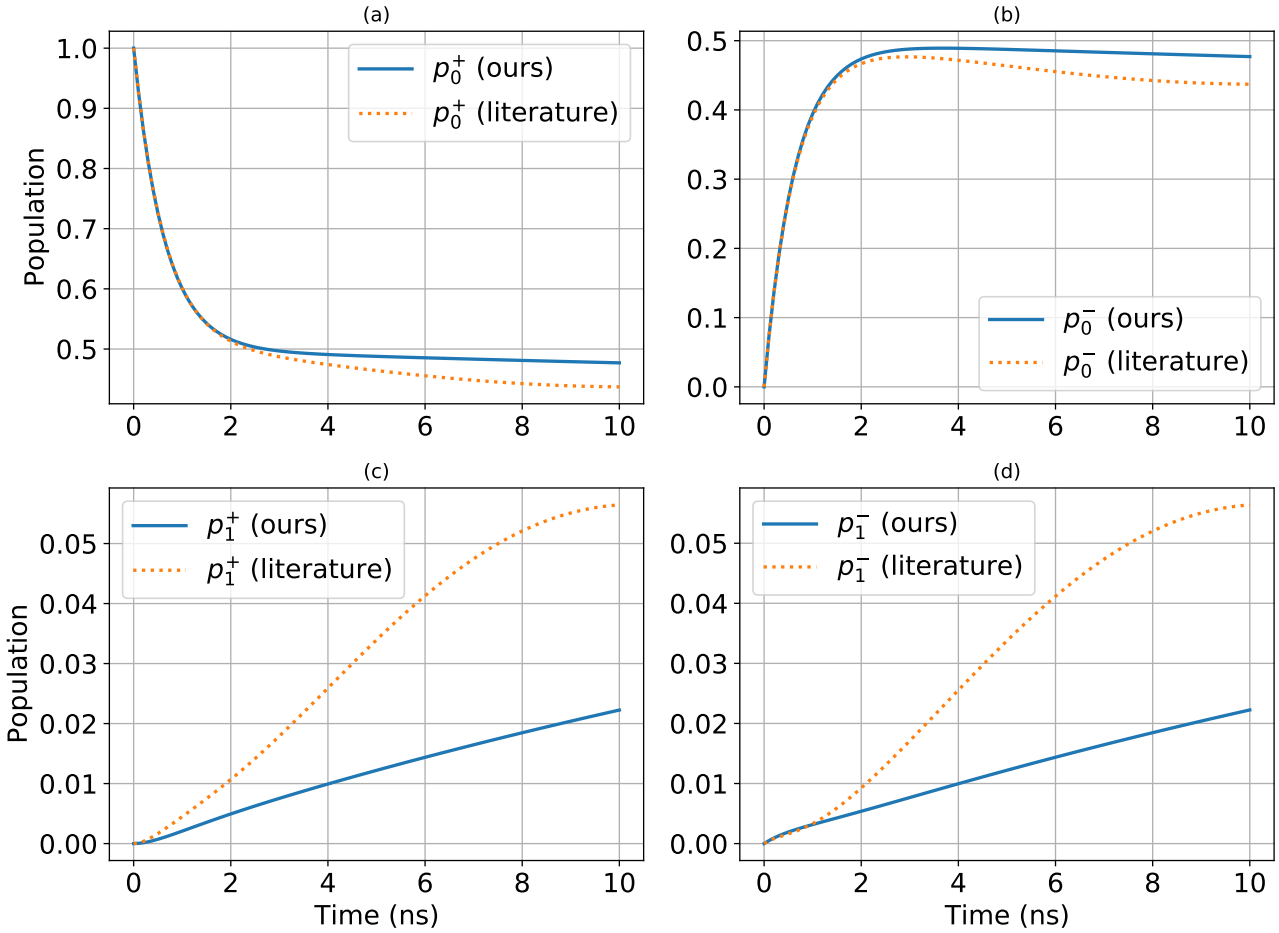

Figure 4.5: The time dependence of the population of each level $p_n^{\pm}(t) := \langle C_\alpha^{n,\pm} | \hat{\rho}_A^{\mathrm{R}}(t) | C_\alpha^{n,\pm} \rangle$ for $n = 0, 1$ under our GKSL equation (4.56) and under the GKSL equation (4.57) in the literature: (a) $p_0^+(t)$; (b) $p_0^-(t)$; (c) $p_1^+(t)$; (d) $p_1^-(t)$. The initial temperature of the bath is $T_B^0 = 180\,\mathrm{mK}$. The other parameters are the same as those in Fig. 4.3.

Chapter 5

Nonequilibrium thermodynamic entropy of a quantum model of coupled harmonic oscillators

In this Chapter, we define and investigate the nonequilibrium thermodynamic entropy of a quantum model of coupled harmonic oscillators in a star configuration, introduced in Sec. 2.5. In Sec. 5.1, we review thermodynamic entropy of a macroscopic bipartite system. In Sec. 5.2, we review the von Neumann entropy production rate. In Sec. 5.3, we introduce the initial state and the dynamics. In Sec. 5.4, we show that every harmonic oscillator is in a Gibbs state with a time-dependent temperature in our settings. We thus define the time-dependent thermodynamic entropy of each harmonic oscillator in a similar way to the definition in equilibrium thermodynamics and statistical mechanics. Then, we define the nonequilibrium thermodynamic entropy of the total system as the summation of them. This total thermodynamic entropy satisfies the third law of thermodynamics. In Sec. 5.5, we set the parameters so that the finite-time dynamics of the system may be well-approximated by the GKSL master equation. We show numerically that our total thermodynamic entropy production rate can take negative values, while our total thermodynamic entropy satisfies the second law of thermodynamics. In Sec. 5.6, we discuss several topics.

5.1 Review of thermodynamic entropy of a macroscopic bipartite system

Equilibrium thermodynamics of macroscopic systems is an established theory [65, 66]. The irreversibility of thermodynamics is expressed by its second law, which can be cast into the form of the principle of increasing total thermodynamic entropy [65, Sec. 14.2] [1]. Let us prepare an adiabatic system in an equilibrium state with some constraints (for example, a system consisting of two subsystems at different temperatures separated by an adiabatic wall). If we get rid of the constraints (e.g. remove the wall) at time $t_{\rm ini}$, the system should change to a new equilibrium state at time $t_{\rm fin}$. The final total thermodynamic entropy $S_{\rm tot}^{\rm th}(t_{\rm fin})$ must be

[1] Throughout this thesis, we intentionally use the term 'thermodynamic entropy' in order to distinguish it from other types of entropy, such as the von Neumann entropy [67], the Rényi entropy [68], and the diagonal entropy [69].

greater than or equal to the initial one $S^{\rm th}_{\rm tot}(t_{\rm ini})$:

$$\Delta S^{\rm th}_{\rm tot}(t_{\rm fin}) = S^{\rm th}_{\rm tot}(t_{\rm fin}) - S^{\rm th}_{\rm tot}(t_{\rm ini}) \geq 0, \tag{5.1}$$

where $\Delta S^{\rm th}_{\rm tot}(t) := S^{\rm th}_{\rm tot}(t) - S^{\rm th}_{\rm tot}(t_{\rm ini})$ denotes the total thermodynamic entropy production from $t_{\rm ini}$ to t. This is the principle of increasing total thermodynamic entropy. Here, the word "total" refers to the adiabatic system itself, excluding its environment, and is used to distinguish $\Delta S^{\rm th}_{\rm tot}(t)$ from the internal thermodynamic entropy production, which we will explain in the next paragraph. Note that the principle is concerned with the difference of thermodynamic entropy between the initial and final equilibrium states; it does not forbid the total thermodynamic entropy from decreasing during the intermediate nonequilibrium processes [65, Sec. 14.2]. In other words, the total thermodynamic entropy production rate $\Pi^{\rm th}_{\rm tot}(t) := {\rm d}S^{\rm th}_{\rm tot}(t)/{\rm d}t$ can be negative for some time t.

Actually, the theory of nonequilibrium thermodynamics of macroscopic systems, including a proper definition of nonequilibrium thermodynamic entropy $S^{\rm th}(t)$, has not been established yet [70]. However, the entropy balance [70, Sec. 2.3] in Eq. (5.2) below is considered to hold universally. Let us consider a system A and its environment B, whose thermodynamic entropies are denoted by $S^{\rm th}_A(t)$ and $S^{\rm th}_B(t)$, respectively. The time derivative of $S^{\rm th}_A(t)$ is written as the sum of the internal thermodynamic entropy production rate of the system $\mathcal{P}^{\rm th}_A(t)$ and the thermodynamic entropy flux into the system $\mathcal{F}^{\rm th}_A(t)$ as follows:

$$\frac{\rm d}{{\rm d}t} S^{\rm th}_A(t) = \mathcal{P}^{\rm th}_A(t) + \mathcal{F}^{\rm th}_A(t). \tag{5.2}$$

This is the entropy balance. We must distinguish the internal thermodynamic entropy production

$$\int_{t_{\rm ini}}^{t_{\rm fin}} {\rm d}t\, \mathcal{P}^{\rm th}_A(t) \tag{5.3}$$

from the total thermodynamic entropy production in the previous paragraph. When the temperature $T_A(t)$ of the system A is defined, the entropy flux into the system A is defined as [70, Sec. 1.3.3.2]

$$\mathcal{F}^{\rm th}_A(t) := \frac{1}{T_A(t)} \frac{\text{đ}Q_A(t)}{{\rm d}t}, \tag{5.4}$$

where $\text{đ}Q_A(t)/{\rm d}t$ is the heat flux into the system A and the bar in $\text{đ}Q_A(t)$ means that it is an inexact differential [70, Sec. 1.3.2]. Then, the internal entropy production rate of the system A is determined from Eqs. (5.2) and (5.4). On the other hand, when the temperature $T_A(t)$ of the system A is not defined uniquely because of being out of equilibrium, it is a subject of research how to define each of $\mathcal{P}^{\rm th}_A(t)$ and $\mathcal{F}^{\rm th}_A(t)$. A similar relation to Eq. (5.2) holds for the environment:

$$\frac{\rm d}{{\rm d}t} S^{\rm th}_B(t) = \mathcal{P}^{\rm th}_B(t) + \mathcal{F}^{\rm th}_B(t). \tag{5.5}$$

The point is that the entropy flux into the system is not equal to that out of the environment in general:

$$\mathcal{F}^{\rm th}_A(t) \neq -\mathcal{F}^{\rm th}_B(t). \tag{5.6}$$

In order to recognize this point, let us consider the following example [66, Sec. 4.3] [70, Sec. 7.1.1]. We prepare an isolated system composed of the two subsystems A and B which are

separated by two fixed walls, namely an adiabatic wall and a diathermal wall. The subsystems A and B are in equilibrium states with temperatures T_A^0 and T_B^0, respectively, with $T_A^0 < T_B^0$. The total system is also at equilibrium. Then, we remove the adiabatic wall at time $t_{\rm ini}$, so that heat begins to flow from B to A through the diathermal wall and continues flowing until the two subsystems are at an equal temperature at time $t_{\rm fin}$. Let us assume that the thermal conductivity of the diathermal wall is so small that each of the two subsystems should be always in an equilibrium state and that their temperatures $T_A(t)$ and $T_B(t)$ change very slowly during the process. We call this process as quasistatic [66, Sec. 4.3] for both A and B in the sense that each of them is always in an equilibrium state. We note that there are other definitions of quasistatic processes; see, for example, Sec. 12.6 in Ref. [65].

Let us describe the internal energy of the subsystem A as $E_A(t)$. From the first law of thermodynamics, the change of $E_A(t)$ is equal to the sum of the heat Q_A into A and the work W_A done on A: $\Delta E_A(t) = Q_A + W_A$. In the present example, W_A is always zero because of the fixed diathermal wall. Hence the heat flux into the subsystem A is given by $\mathrm{d}E_A(t)/\mathrm{d}t$. From the law of energy conservation, the heat flux into the subsystem B is given by $-\mathrm{d}E_A(t)/\mathrm{d}t$. Then the entropy fluxes into the two subsystems are given by

$$\mathcal{F}_A^{\rm th}(t) = \frac{1}{T_A(t)} \frac{\mathrm{d}E_A(t)}{\mathrm{d}t}, \tag{5.7}$$

$$\mathcal{F}_B^{\rm th}(t) = -\frac{1}{T_B(t)} \frac{\mathrm{d}E_A(t)}{\mathrm{d}t}. \tag{5.8}$$

These equations show that the entropy flux into A is not equal to that out of B at $t \neq t_{\rm fin}$ because $T_A(t) \neq T_B(t)$. As the process is quasistatic for both A and B, the time derivatives of the thermodynamic entropies of the two subsystems are given by [66, Sec. 4.3]

$$\frac{\mathrm{d}}{\mathrm{d}t} S_A^{\rm th}(t) = \frac{1}{T_A(t)} \frac{\mathrm{d}E_A(t)}{\mathrm{d}t}, \tag{5.9}$$

$$\frac{\mathrm{d}}{\mathrm{d}t} S_B^{\rm th}(t) = -\frac{1}{T_B(t)} \frac{\mathrm{d}E_A(t)}{\mathrm{d}t}. \tag{5.10}$$

Combining Eqs. (5.2), (5.5), and (5.7)-(5.10), we find that the internal thermodynamic entropy production rates of the two subsystems are both zero:

$$\mathcal{P}_A^{\rm th}(t) = \mathcal{P}_B^{\rm th}(t) = 0. \tag{5.11}$$

We regard this as a sign that the process is quasistatic for both A and B.

Let us confirm that the above example satisfies the principle of increasing total thermodynamic entropy (5.1). The total thermodynamic entropy production rate is the sum of the variation rates of the thermodynamic entropies of the two subsystems:

$$\Pi_{\rm tot}^{\rm th}(t) = \frac{\mathrm{d}}{\mathrm{d}t} S_{\rm tot}^{\rm th}(t) = \frac{\mathrm{d}}{\mathrm{d}t} S_A^{\rm th}(t) + \frac{\mathrm{d}}{\mathrm{d}t} S_B^{\rm th}(t) = \frac{T_B(t) - T_A(t)}{T_A(t) T_B(t)} \frac{\mathrm{d}E_A(t)}{\mathrm{d}t} \geq 0, \tag{5.12}$$

where the last inequality follows from $T_B(t) \geq T_A(t)$ and $\mathrm{d}E_A(t)/\mathrm{d}t \geq 0$. This leads to the satisfaction of the principle of increasing total thermodynamic entropy:

$$\Delta S_{\rm tot}^{\rm th}(t_{\rm fin}) = \int_{t_{\rm ini}}^{t_{\rm fin}} \mathrm{d}t\, \Pi_{\rm tot}^{\rm th}(t) \geq 0. \tag{5.13}$$

Note that the total thermodynamic entropy production rate is not the sum of the internal thermodynamic entropy production rates:

$$\Pi_{\rm tot}^{\rm th}(t) \neq \mathcal{P}_A^{\rm th}(t) + \mathcal{P}_B^{\rm th}(t). \tag{5.14}$$

5.2 Review of the von Neumann entropy production rate

Let us consider an undriven open quantum system A (different from A in the previous section) which is coupled to a thermal bath B with initial temperature T_B^0. If the coupling is sufficiently weak, the dynamics of the system is well approximated by the GKSL-type Markovian master equation in Eq. (2.40). Then the following von Neumann entropy production rate [35] is typically used:

$$\Pi^{\mathrm{vN}}(t) := -\frac{\mathrm{d}}{\mathrm{d}t} K^{\mathrm{vN}}\left(\hat{\rho}_A(t) || \hat{\rho}_A^{\mathrm{th}}\right), \tag{5.15}$$

where $\hat{\rho}_A(t)$ is the density operator of the system, $\hat{\rho}_A^{\mathrm{th}} = \mathrm{e}^{-\beta_B^0 \hat{H}_A}/\mathrm{Tr}[\mathrm{e}^{-\beta_B^0 \hat{H}_A}]$ is the stationary state in Eq. (2.52), and

$$K^{\mathrm{vN}}\left(\hat{\rho}_1 || \hat{\rho}_2\right) := k_B \mathrm{Tr}\left[\hat{\rho}_1 \left(\ln \hat{\rho}_1 - \ln \hat{\rho}_2\right)\right] = -S^{\mathrm{vN}}(\hat{\rho}_1) - k_B \mathrm{Tr}\left[\hat{\rho}_1 \ln \hat{\rho}_2\right] \tag{5.16}$$

is the von Neumann relative entropy [36, Sec. 11.8] with $S^{\mathrm{vN}}(\hat{\rho}) := -k_B \mathrm{Tr}\left[\hat{\rho} \ln \hat{\rho}\right]$ being the von Neumann entropy.

We can transform Eq. (5.15) as follows [3, Sec. 3.2.5]:

$$\begin{aligned}
\Pi^{\mathrm{vN}}(t) &= -\frac{\mathrm{d}}{\mathrm{d}t} K^{\mathrm{vN}}\left(\hat{\rho}_A(t) || \hat{\rho}_A^{\mathrm{th}}\right) \\
&= \frac{\mathrm{d}}{\mathrm{d}t} S_A^{\mathrm{vN}}(t) + k_B \frac{\mathrm{d}}{\mathrm{d}t} \mathrm{Tr}\left[\hat{\rho}_A(t) \ln \frac{\mathrm{e}^{-\beta_B^0 \hat{H}_A}}{\mathrm{Tr}[\mathrm{e}^{-\beta_B^0 \hat{H}_A}]}\right] \\
&= \frac{\mathrm{d}}{\mathrm{d}t} S_A^{\mathrm{vN}}(t) - \frac{1}{T_B^0} \frac{\mathrm{d}}{\mathrm{d}t} \mathrm{Tr}\left[\hat{\rho}_A(t) \hat{H}_A\right] - k_B \ln \mathrm{Tr}[\mathrm{e}^{-\beta_B^0 \hat{H}_A}] \frac{\mathrm{d}}{\mathrm{d}t} \mathrm{Tr}\left[\hat{\rho}_A(t)\right] \\
&= \frac{\mathrm{d}}{\mathrm{d}t} S_A^{\mathrm{vN}}(t) - \frac{1}{T_B^0} \frac{\mathrm{d}}{\mathrm{d}t} E_A(t) \\
&= \frac{\mathrm{d}}{\mathrm{d}t} S_A^{\mathrm{vN}}(t) + \frac{1}{T_B^0} \frac{\mathrm{d}}{\mathrm{d}t} E_B(t),
\end{aligned} \tag{5.17}$$

where $E_A(t)$ and $E_B(t)$ are the mean energies of the system and the bath, respectively. The last term in the third line of Eq. (5.17) becomes zero because $\mathrm{Tr}\left[\hat{\rho}_A(t)\right] = 1$ all the time. From the conservation of the total energy, we have derived the last line in Eq. (5.17), ignoring the interaction energy due to weak coupling. The first term in the last line of Eq. (5.17) is the time derivative of the von Neumann entropy of the system and the second term is the time-derivative of the thermodynamic entropy of the bath under the quasistatic process. Note that an implicit assumption is made that the temperature of the bath does not change from the initial temperature T_B^0 in this second term. However, when the size of the bath is finite, the temperature of a part of the bath changes as we will show in Sec. 5.5.2. In this case, we cannot use the von Neumann entropy production rate.

If we regarded the von Neumann entropy of the system as its nonequilibrium thermodynamic entropy, the von Neumann entropy production rate (5.17) would be regarded as the total thermodynamic entropy production rate. However, this is a delicate matter, because the von Neumann entropy is not equal to the thermodynamic entropy in general. For example, let us decouple the system from the bath in the middle of the dynamics. Then the system is isolated, in general out of equilibrium, and undergoes the unitary dynamics. If the system shows thermalization [71], its nonequilibrium thermodynamic entropy should change. However, its von Neumann entropy does not change under the unitary dynamics [36, Sec. 11.1.1]. Hence

we do not regard the von Neumann entropy of the system as its thermodynamic entropy in general. However, when the system is in a Gibbs state, its von Neumann entropy coincides with its thermodynamic entropy. Actually, we will consider such a case by adopting special settings in the next section.

It is shown that the von Neumann entropy production rate is always non-negative during the dynamics [35]:

$$\Pi^{\mathrm{vN}}(t) \geq 0 \quad {}^{\forall}t. \tag{5.18}$$

This leads to the non-negative von Neumann entropy production:

$$\Delta S^{\mathrm{vN}}(t) := \int_{t_{\mathrm{ini}}}^{t} \mathrm{d}s\, \Pi^{\mathrm{vN}}(s) \geq 0 \quad {}^{\forall}t \geq t_{\mathrm{ini}}. \tag{5.19}$$

The above two inequalities are often regarded as signs of irreversibility. Here the total system is not necessarily at equilibrium at t_{ini} or t. Hence, the inequality (5.19) with $t = t_{\mathrm{fin}}$ is different from the principle of increasing total thermodynamic entropy (5.1) unless each of the total system and the system A is in an equilibrium state at both t_{ini} and t_{fin}.

5.3 Settings

5.3.1 Hamiltonian

Let us consider the quantum model of coupled harmonic oscillators in a star configuration which was introduced in Sec. 2.5. We can cast the total Hamiltonian in Eq. (2.59) into the form

$$\hat{H} = \sum_{j=1}^{N+1} \frac{\hbar\omega_j}{2} \left(\hat{r}_{2j-1}^2 + \hat{r}_{2j}^2\right) + \sum_{j=2}^{N+1} \hbar g_j \left(\hat{r}_1 \hat{r}_{2j-1} + \hat{r}_2 \hat{r}_{2j}\right) =: \frac{\hbar}{2} \hat{\mathbf{r}}^{\mathrm{T}} H \hat{\mathbf{r}}, \tag{5.20}$$

where we have introduced the modified position operator $\hat{r}_{2j-1}$ and the modified momentum operator $\hat{r}_{2j}$,

$$\hat{r}_{2j-1} := \frac{\hat{a}_j + \hat{a}_j^\dagger}{\sqrt{2}}, \quad \hat{r}_{2j} := \frac{\hat{a}_j - \hat{a}_j^\dagger}{\sqrt{2}\,\mathrm{i}}, \tag{5.21}$$

and their vector representation

$$\hat{\mathbf{r}} = (\hat{r}_1, \hat{r}_2, \ldots, \hat{r}_{2N+1}, \hat{r}_{2N+2})^{\mathrm{T}} \tag{5.22}$$

as well as a $2(N+1)$-dimensional symmetric matrix H, whose nonzero elements are

$$\begin{aligned} H_{2j-1,2j-1} = H_{2j,2j} = \omega_j \quad \text{for} \quad j = 1, \ldots, N+1, \\ H_{1,2j-1} = H_{2j-1,1} = H_{2,2j} = H_{2j,2} = g_j \quad \text{for} \quad j = 2, \ldots, N+1. \end{aligned} \tag{5.23}$$

5.3.2 Initial state and unitary dynamics

Let us impose the constraint $\hat{H}_I = 0$ for $t < 0$ and prepare the following initial state:

$$\hat{\rho}(t \leq 0) = \frac{\mathrm{e}^{-\beta_A^0 \hat{H}_A}}{Z_A} \otimes \frac{\mathrm{e}^{-\beta_B^0 \hat{H}_B}}{Z_B} = \frac{\mathrm{e}^{-\beta_A^0 \hat{H}_A}}{Z_A} \otimes \left(\bigotimes_{j=2}^{N+1} \frac{\mathrm{e}^{-\beta_B^0 \hat{H}_j}}{Z_j} \right), \tag{5.24}$$

where

$$Z_A = \mathrm{Tr}\left[\mathrm{e}^{-\beta_A^0 \hat{H}_A}\right] = \frac{1}{2\sinh(\beta_A^0 \hbar\omega_1/2)}, \quad Z_B = \mathrm{Tr}\left[\mathrm{e}^{-\beta_B^0 \hat{H}_B}\right] = \prod_{j=2}^{N+1} Z_j, \tag{5.25}$$

$$\hat{H}_j = \hbar\omega_j \left(\hat{a}_j^\dagger \hat{a}_j + \frac{1}{2}\right), \quad Z_j = \mathrm{Tr}\left[\mathrm{e}^{-\beta_B^0 \hat{H}_j}\right] = \frac{1}{2\sinh(\beta_B^0 \hbar\omega_j/2)}. \tag{5.26}$$

That is, the system and the bath are both in the Gibbs states with inverse temperatures β_A^0 and β_B^0, respectively, and they are uncorrelated. We calculate Z_A in Eq. (5.25) in Appendix C. We can calculate Z_B and Z_j in a similar way. Because of the constraint $\hat{H}_I = 0$, the initial state (5.24) is an equilibrium state:

$$\hat{\rho}(t_2) = e^{-\mathrm{i}\frac{\hat{H}_A+\hat{H}_B}{\hbar}(t_2-t_1)} \hat{\rho}(t_1) e^{\mathrm{i}\frac{\hat{H}_A+\hat{H}_B}{\hbar}(t_2-t_1)} = \hat{\rho}(t_1) \quad \text{for} \quad t_1 \le t_2 \le 0. \tag{5.27}$$

At time $t = 0$, we remove the constraint $\hat{H}_I = 0$ and let the state of the total system evolve under the total Hamiltonian (5.20). The interaction sets in between the system and the bath, which creates correlations.

As $\hat{H}_A$ and $\hat{H}_B$ are purely quadratic, the initial state (5.24) is a Gaussian state [16–20] with vanishing first moments: $\mathrm{Tr}\left[\hat{\mathbf{r}}\hat{\rho}(0)\right] = \mathbf{0}$. Moreover, as the total Hamiltonian is purely quadratic, the total density operator

$$\hat{\rho}(t) = \hat{U}(t)\hat{\rho}(0)\hat{U}^\dagger(t) \quad \text{with} \quad \hat{U}(t) = \exp\left(-\mathrm{i}\frac{\hat{H}}{\hbar}t\right) \tag{5.28}$$

is always a Gaussian state with vanishing first moments: $\mathrm{Tr}\left[\hat{\mathbf{r}}\hat{\rho}(t)\right] = \mathbf{0}$. Therefore, $\hat{\rho}(t)$ is completely characterized by the $2(N+1)\times 2(N+1)$ covariance matrix $\sigma(t)$ whose (j,k)-element is given by

$$\sigma_{j,k}(t) = \mathrm{Tr}\left[\hat{\rho}(t)\{\hat{r}_j, \hat{r}_k\}\right], \tag{5.29}$$

where the curly parentheses $\{\bullet,\bullet\}$ denote the anticommutator. Note that the covariance matrix is a symmetric matrix. Because of Eq. (5.28), the following relation holds [16, Sec. 5.1.2]:

$$\sigma(t) = V(t)\sigma(0)V(t)^{\mathrm{T}} \quad \text{with} \quad V(t) = \mathrm{e}^{\Omega H t}, \tag{5.30}$$

where

$$\Omega = \bigoplus_{j=1}^{N+1} \Omega_1 = \begin{pmatrix} \Omega_1 & & \\ & \ddots & \\ & & \Omega_1 \end{pmatrix}, \quad \Omega_1 = \begin{pmatrix} 0 & 1 \\ -1 & 0 \end{pmatrix}, \tag{5.31}$$

and H is the $2(N+1)$-dimensional symmetric matrix introduced in Eq. (5.20). We give the derivation of Eq. (5.30) in Appendix D.

If the total system is in a Gaussian state, its subsystems are also in Gaussian states. Thus, each of the states of the system and the bath is Gaussian and is completely characterized by the covariance matrices $\sigma_A(t)$ and $\sigma_B(t)$, respectively, which are the submatrices of $\sigma(t)$ [16, Sec. 5.2]:

$$\sigma(t) = \begin{pmatrix} \sigma_A(t) & \sigma_{AB}(t) \\ \sigma_{AB}(t)^{\mathrm{T}} & \sigma_B(t) \end{pmatrix}, \tag{5.32}$$

where $\sigma_A(t)$ is a two-dimensional symmetric matrix, $\sigma_B(t)$ is a $2N$-dimensional symmetric matrix, and $\sigma_{AB}(t)$ is a $2 \times 2N$ matrix. Each harmonic oscillator in the total system is also in a Gaussian state which is totally determined by the following covariance matrix:

$$\sigma_j(t) := \begin{pmatrix} \sigma_{2j-1,2j-1}(t) & \sigma_{2j-1,2j}(t) \\ \sigma_{2j-1,2j}(t) & \sigma_{2j,2j}(t) \end{pmatrix} \tag{5.33}$$

for $j = 1, \ldots, N+1$. The initial covariance matrix for the state (5.24) is [16, Sec. 3.3]

$$\begin{aligned} \sigma(0) &= \begin{pmatrix} \sigma_A(0) & 0 \\ 0 & \sigma_B(0) \end{pmatrix}, \\ \sigma_A(0) = \sigma_1(0) &= \coth\left(\frac{\hbar\omega_1}{2k_B T_A^0}\right) I_2, \\ \sigma_B(0) = \bigoplus_{j=2}^{N+1} \sigma_j(0), &\quad \sigma_j(0) = \coth\left(\frac{\hbar\omega_j}{2k_B T_B^0}\right) I_2, \end{aligned} \tag{5.34}$$

where $T_A^0 = 1/(k_B\beta_A^0)$, $T_B^0 = 1/(k_B\beta_B^0)$, and I_2 is the two-dimensional identity matrix. We calculate $\sigma_{1,1}(0)$, which is a component of $\sigma_A(0)$, in Appendix C. The other components of $\sigma(0)$ can be calculated in a similar way.

5.3.3 The GKSL master equation

As we explained in Sec. 2.5, If the couplings $\{g_j\}$ of the harmonic oscillators are sufficiently weak, the dynamics of the system is well approximated by the GKSL master equation in Eq. (2.99). As we will show in the next section, the first term in the right-hand side in Eq. (2.99) is always equal to zero in our settings. Then the GKSL master equation (2.99) becomes

$$\begin{aligned} \frac{\mathrm{d}}{\mathrm{d}t}\hat{\rho}_A(t) = \Gamma(\bar{n}(\omega_1)+1)\left(2\hat{a}_1\hat{\rho}_A(t)\hat{a}_1^\dagger - \left\{\hat{a}_1^\dagger\hat{a}_1, \hat{\rho}_A(t)\right\}\right) \\ + \Gamma\bar{n}(\omega_1)\left(2\hat{a}_1^\dagger\hat{\rho}_A(t)\hat{a}_1 - \left\{\hat{a}_1\hat{a}_1^\dagger, \hat{\rho}_A(t)\right\}\right). \end{aligned} \tag{5.35}$$

Under this GKSL master equation and the initial covariance matrix in Eq. (5.34), the covariance matrix of the system at time t is written as [20, Sec. 4.1.1]

$$\sigma_A(t) = \left[\coth\left(\frac{\hbar\omega_1}{2k_B T_A^0}\right)\mathrm{e}^{-2\Gamma t} + \coth\left(\frac{\hbar\omega_1}{2k_B T_B^0}\right)\left(1 - \mathrm{e}^{-2\Gamma t}\right)\right] I_2. \tag{5.36}$$

We derive Eq. (5.36) in Appendix E.

5.4 Analytical results

5.4.1 Gibbs states

We show that each harmonic oscillator is always in a Gibbs state with a time-dependent temperature under the unitary dynamics (5.28) of the total system. Note that there is a one-to-one correspondence between the density operator and the covariance matrix of each harmonic oscillator. As the covariance matrix is easier to calculate than the density matrix, we first calculate the covariance matrix. By substituting Eq. (5.34) into Eq. (5.30), we find (see Appendix F)

$$\sigma_j(t) = \sigma_{2j-1,2j-1}(t) I_2 \quad \text{for} \quad j = 1, \ldots, N+1. \tag{5.37}$$

According to the calculation in Appendix F, the density operator is expressed with the covariance matrix (5.37) in the following form:

$$\hat{\rho}_j(t) = \frac{\mathrm{e}^{-\beta_j(t)\hat{H}_j}}{Z_j(t)}, \tag{5.38}$$

$$Z_j(t) = \mathrm{Tr}\left[\mathrm{e}^{-\beta_j(t)\hat{H}_j}\right] = \frac{1}{2}\sqrt{\sigma_{2j-1,2j-1}(t)^2 - 1}, \tag{5.39}$$

$$\begin{aligned}\beta_j(t) &= \frac{1}{k_B T_j(t)} = \frac{2}{\hbar\omega_j}\coth^{-1}\left[\sigma_{2j-1,2j-1}(t)\right] \\ &= \frac{1}{\hbar\omega_j}\ln\left(\frac{\sigma_{2j-1,2j-1}(t)+1}{\sigma_{2j-1,2j-1}(t)-1}\right) = \frac{1}{\hbar\omega_j}\ln\left(\frac{2E_j(t)+\hbar\omega_j}{2E_j(t)-\hbar\omega_j}\right),\end{aligned} \tag{5.40}$$

where $E_j(t)$ is the mean energy of the jth harmonic oscillator:

$$E_j(t) = \mathrm{Tr}\left[\hat{H}_j\hat{\rho}_j(t)\right] = \frac{\hbar\omega_j}{2}\sigma_{2j-1,2j-1}(t). \tag{5.41}$$

We find that each harmonic oscillator is always in a Gibbs (thermal equilibrium) state with a time-dependent temperature $T_j(t)$. In this meaning, the dynamics is quasistatic for every harmonic oscillator.

As the system is always in a Gibbs state, the relation $[(\omega_1+\Delta)\hat{a}_1^\dagger\hat{a}_1, \hat{\rho}_A(t)] = [(\omega_1+\Delta)\hat{a}_1^\dagger\hat{a}_1, \mathrm{e}^{-\beta_A(t)\hbar\omega_1\hat{a}_1^\dagger\hat{a}_1}/Z_A(t)] = 0$ holds all the time. Therefore the GKSL master equation (2.99) transforms into Eq. (5.35). Using Eq. (5.36) for the time-dependent temperature $T_j(t)$ in Eq. (5.40), we find that the system under the GKSL master equation is equilibrated with the bath in the limit $t \to \infty$:

$$T_A(\infty) = T_1(\infty) = T_B^0; \tag{5.42}$$

we will plot this in Fig. 5.4 below.

5.4.2 Thermodynamic entropy

We define the time-dependent free energy and the time-dependent thermodynamic entropy of the jth harmonic oscillator simply following the analog of equilibrium statistical mechanics and thermodynamics:

$$F_j(t) := -k_B T_j(t)\ln Z_j(t), \tag{5.43}$$

$$S_j^{\mathrm{th}}(t) := \frac{E_j(t)-F_j(t)}{T_j(t)}. \tag{5.44}$$

In fact, the von Neumann entropy of the jth harmonic oscillator coincides with its thermodynamic entropy because it is in a Gibbs state [65, Sec. 21.1]:

$$\begin{aligned}S_j^{\mathrm{vN}}(t) &:= -k_B\mathrm{Tr}\left[\hat{\rho}_j(t)\ln\hat{\rho}_j(t)\right] \\ &= -k_B\mathrm{Tr}\left[\hat{\rho}_j(t)\ln\left(\frac{\mathrm{e}^{-\beta_j(t)\hat{H}_j}}{Z_j(t)}\right)\right] \\ &= \frac{1}{T_j(t)}\mathrm{Tr}\left[\hat{\rho}_j(t)\hat{H}_j\right] + k_B\ln Z_j(t) \\ &= \frac{E_j(t)-F_j(t)}{T_j(t)} = S_j^{\mathrm{th}}(t).\end{aligned} \tag{5.45}$$

We can rewrite $S_j^{\rm th}(t)$ in Eq. (5.44) as a strictly monotonically increasing function of $E_j(t)$:

$$\frac{S_j^{\rm th}(t)}{k_B} = \frac{2E_j(t)+\hbar\omega_j}{2\hbar\omega_j}\ln\left(\frac{2E_j(t)+\hbar\omega_j}{2\hbar\omega_j}\right) - \frac{2E_j(t)-\hbar\omega_j}{2\hbar\omega_j}\ln\left(\frac{2E_j(t)-\hbar\omega_j}{2\hbar\omega_j}\right). \tag{5.46}$$

This is followed by

$$\frac{\partial S_j^{\rm th}(t)}{\partial E_j(t)} = \frac{k_B}{\hbar\omega_j}\ln\left(\frac{2E_j(t)+\hbar\omega_j}{2E_j(t)-\hbar\omega_j}\right) = \frac{1}{T_j(t)} \tag{5.47}$$

and

$$\frac{\rm d}{{\rm d}t}S_j^{\rm th}(t) = \frac{1}{T_j(t)}\frac{\rm d}{{\rm d}t}E_j(t), \tag{5.48}$$

where the last equality in Eq. (5.47) comes from Eq. (5.40). We regard ${\rm d}E_j(t)/{\rm d}t$ as the heat flux into the jth harmonic oscillator because its Hamiltonian $\hat{H}_j$ is time independent [22, Sec. 2.1]. Then, Eq. (5.48) is a manifestation of the quasistatic process; see Eq. (5.9). We define the thermodynamic entropy flux into the jth harmonic oscillator as

$$\mathcal{F}_j^{\rm th}(t) = \frac{1}{T_j(t)}\frac{\rm d}{{\rm d}t}E_j(t), \tag{5.49}$$

just as Eq. (5.7). Then we find that the internal thermodynamic entropy production rate of the jth harmonic oscillator is zero:

$$\mathcal{P}_j^{\rm th}(t) = \frac{\rm d}{{\rm d}t}S_j^{\rm th}(t) - \mathcal{F}_j^{\rm th}(t) = 0, \tag{5.50}$$

which is also a manifestation of the quasistatic process.

In order to define the nonequilibrium thermodynamic entropy of the total system, we impose the additivity of the thermodynamic entropy, which is satisfied in equilibrium thermodynamics of macroscopic systems (see Secs. 11.5 and 13.11 in Ref. [65]). We thereby arrive at

$$\begin{aligned} S_{\rm tot}^{\rm th}(t) &:= \sum_{j=1}^{N+1} S_j^{\rm th}(t) \\ &= k_B \sum_{j=1}^{N+1}\left[\frac{2E_j(t)+\hbar\omega_j}{2\hbar\omega_j}\ln\left(\frac{2E_j(t)+\hbar\omega_j}{2\hbar\omega_j}\right) - \frac{2E_j(t)-\hbar\omega_j}{2\hbar\omega_j}\ln\left(\frac{2E_j(t)-\hbar\omega_j}{2\hbar\omega_j}\right)\right]. \end{aligned} \tag{5.51}$$

We analytically confirm that our thermodynamic entropy (5.51) satisfies the third law of thermodynamics [65, Sec. 23.7] as follows. The temperature $T_j(t)$ in Eq. (5.40) and the thermodynamic entropy $S_j^{\rm th}(t)$ in Eq. (5.46) become zero for the vacuum state:

$$T_j(t) \to +0, \quad S_j^{\rm th}(t) \to +0 \quad \text{as} \quad E_j(t) \to \frac{\hbar\omega_j}{2} + 0. \tag{5.52}$$

As $T_j(t)$ and $S_j^{\rm th}(t)$ are both strictly monotonically increasing functions of $E_j(t)$, the thermodynamic entropy $S_j^{\rm th}(t)$ becomes zero if and only if $T_j(t)$ becomes zero:

$$S_j^{\rm th}(t) \to +0 \quad \text{as} \quad T_j(t) \to +0. \tag{5.53}$$

This and Eq. (5.51) lead to the third law of thermodynamics:

$$S_{\rm tot}^{\rm th}(t) \to +0 \quad \text{as} \quad T_j(t) \to +0 \quad {}^\forall j, \tag{5.54}$$

which supports the validity of our definition of the total thermodynamic entropy in Eq. (5.51).

5.4.3 Total thermodynamic entropy production and its rate

We define the total thermodynamic entropy production as

$$\Delta S^{\rm th}_{\rm tot}(t) := S^{\rm th}_{\rm tot}(t) - S^{\rm th}_{\rm tot}(0) = S^{\rm th}_A(t) - S^{\rm th}_A(0) + \sum_{j=2}^{N+1}\left[S^{\rm th}_j(t) - S^{\rm th}_j(0)\right] \tag{5.55}$$

and its rate as

$$\Pi^{\rm th}_{\rm tot}(t) := \frac{\mathrm{d}}{\mathrm{d}t}S^{\rm th}_{\rm tot}(t) = \sum_{j=1}^{N+1}\frac{1}{T_j(t)}\frac{\mathrm{d}}{\mathrm{d}t}E_j(t) = \frac{1}{T_A(t)}\frac{\mathrm{d}}{\mathrm{d}t}E_A(t) + \sum_{j=2}^{N+1}\frac{1}{T_j(t)}\frac{\mathrm{d}}{\mathrm{d}t}E_j(t). \tag{5.56}$$

Let us transform this into the form which we can easily calculate in terms of the covariance matrix. Using Eqs. (G.5) and (G.6) in Appendix G, we obtain

$$\begin{aligned}\Pi^{\rm th}_{\rm tot}(t) &= \frac{\hbar\omega_1}{T_A(t)}\sum_{j=2}^{N+1} g_j\sigma_{1,2j}(t) - \sum_{j=2}^{N+1}\frac{\hbar\omega_j}{T_j(t)}g_j\sigma_{1,2j}(t)\\ &= k_B\sum_{j=2}^{N+1} g_j\sigma_{1,2j}(t)\left[\ln\left(\frac{\sigma_{1,1}(t)+1}{\sigma_{1,1}(t)-1}\right) - \ln\left(\frac{\sigma_{2j-1,2j-1}(t)+1}{\sigma_{2j-1,2j-1}(t)-1}\right)\right].\end{aligned} \tag{5.57}$$

This total thermodynamic entropy production rate can be negative as we will see in Fig. 5.3.

5.4.4 The difference between our total thermodynamic entropy production rate and the conventional one

Let us consider the weak-coupling regime so that the finite-time dynamics of the system is well approximated by the GKSL master equation in Eq. (5.35). In our settings, the von Neumann entropy of the system coincides with its thermodynamic entropy as in Eq. (5.45), and hence the conventional entropy production rate $\Pi^{\rm vN}(t)$ in Eq. (5.17) has the following form:

$$\Pi^{\rm vN}(t) = \frac{1}{T_A(t)}\frac{\mathrm{d}}{\mathrm{d}t}E_A(t) + \frac{1}{T_B^0}\frac{\mathrm{d}}{\mathrm{d}t}E_B(t) = \frac{1}{T_A(t)}\frac{\mathrm{d}}{\mathrm{d}t}E_A(t) + \sum_{j=2}^{N+1}\frac{1}{T_B^0}\frac{\mathrm{d}}{\mathrm{d}t}E_j(t). \tag{5.58}$$

Let us transform Eq. (5.58) into the form which we can easily calculate. As we consider the weak-coupling regime, we neglect the interaction energy: $\mathrm{d}E_B(t)/\mathrm{d}t = -\mathrm{d}E_A(t)/\mathrm{d}t$. From the first equality in Eq. (5.58), we obtain

$$\Pi^{\rm vN}(t) = \left(\frac{1}{T_A(t)} - \frac{1}{T_B^0}\right)\frac{\mathrm{d}}{\mathrm{d}t}E_A(t) \tag{5.59}$$

$$\begin{aligned}&= \hbar\omega_1\Gamma\left(\frac{1}{T_B^0} - \frac{1}{T_A(t)}\right)\left[\frac{2E_A(t)}{\hbar\omega_1} - \coth\left(\frac{\hbar\omega_1}{2k_BT_B^0}\right)\right]\\ &= \hbar\omega_1\Gamma\left(\frac{1}{T_B^0} - \frac{1}{T_A(t)}\right)\left[\coth\left(\frac{\hbar\omega_1}{2k_BT_A(t)}\right) - \coth\left(\frac{\hbar\omega_1}{2k_BT_B^0}\right)\right],\end{aligned} \tag{5.60}$$

where the second line follows from Eqs. (5.41) and (5.36), and the last line follows from Eq. (5.40). The difference between our total thermodynamic entropy production rate $\Pi^{\rm th}_{\rm tot}(t)$ in Eq. (5.56) and the conventional entropy production rate $\Pi^{\rm vN}(t)$ in Eq. (5.58) arises from the gaps between $\{T_j(t)\}$ and T_B^0:

$$\Pi^{\rm vN}(t) - \Pi^{\rm th}_{\rm tot}(t) = \sum_{j=2}^{N+1}\left(\frac{1}{T_B^0} - \frac{1}{T_j(t)}\right)\frac{\mathrm{d}}{\mathrm{d}t}E_j(t). \tag{5.61}$$

5.5 Numerical results

5.5.1 Parameters

For a numerical example, we use an Ohmic bath [6, 34], whose spectral density is

$$J(\omega) = \sum_{j=2}^{N+1} g_j^2 \delta(\omega - \omega_j) = \eta\omega \mathrm{e}^{-\omega/\omega_{\mathrm{cut}}}, \tag{5.62}$$

where η is the coupling strength between the system and the bath, and ω_{cut} is the cutoff frequency. Here, we discretize the bath by equal spaces as in Appendix A in Ref. [6]:

$$\omega_j = \omega_{\mathrm{min}} + (j-2)\Delta\omega, \quad \Delta\omega = \frac{\omega_{\mathrm{max}} - \omega_{\mathrm{min}}}{N-1} \tag{5.63}$$

for $j = 2, \ldots, N+1$. Adopting a logarithmic discretization [72] yields qualitatively same results as those obtained in this section; see Sec. 5.6.4. We set the coupling constant g_j by integrating Eq. (5.62) over ω as in

$$\sum_{j=2}^{N+1} g_j^2 = \int_{\omega_{\mathrm{min}}-\epsilon}^{\omega_{\mathrm{max}}+\epsilon} \mathrm{d}\omega\, \eta\omega \mathrm{e}^{-\omega/\omega_{\mathrm{cut}}} \simeq \sum_{j=2}^{N+1} \eta\Delta\omega\omega_j \mathrm{e}^{-\omega_j/\omega_{\mathrm{cut}}}, \tag{5.64}$$

which gives

$$g_j = \sqrt{\eta\Delta\omega\, \omega_j \mathrm{e}^{-\omega_j/\omega_{\mathrm{cut}}}} \tag{5.65}$$

for $j = 2, \ldots, N+1$. For numerical demonstration, we fix the parameters as follows:

$$\begin{gathered} \omega_1 = 4\,\mathrm{MHz},\ \omega_{\mathrm{cut}} = 3\,\mathrm{MHz},\ \omega_{\mathrm{min}} = 0.026\,\mathrm{MHz}, \omega_{\mathrm{max}} = 20\,\mathrm{MHz}, \\ \eta = 10^{-3},\ T_A^0 = 10\,\mu\mathrm{K},\ T_B^0 = 50\,\mu\mathrm{K}. \end{gathered} \tag{5.66}$$

Let us check whether the finite-time dynamics of the system is well-approximated by the GKSL master equation when $N = 4000$, 6000, and 8000. Note that the quantum state of the system is totally determined only by $\sigma_{1,1}(t)$. Thus, in Fig. 5.1 we compare $\sigma_{1,1}(t)$ which we calculate from the unitary dynamics of the total system (5.30) and that we calculate from the GKSL master equation (5.36). We find that the two curves coincide with each other for $t \lesssim 2\pi/\Delta\omega$, and hence we conclude that the dynamics of the system is well approximated by the GKSL master equation in that time range. However, the dynamics of the system no longer obeys the GKSL master equation for $t \gtrsim 2\pi/\Delta\omega$ because at $t = t_1 := 2\pi/\Delta\omega$, we have $\mathrm{e}^{\mathrm{i}\omega_j t_1} = \mathrm{e}^{2\pi \mathrm{i}\omega_{\mathrm{min}}/\Delta\omega}$ for $j = 2, \ldots, N+1$, and hence all harmonic oscillators in the bath have almost the same phase and recurrencelike behavior happens; see Fig. 5.1. This means that the dynamics of the system is non-Markovian as a map. Hence we restrict ourselves to $t_{\mathrm{max}} < t_1 = 2\pi/\Delta\omega$ in the following calculations. Note that t_1 is almost proportional to N for large N because $\Delta\omega = (\omega_{\mathrm{max}} - \omega_{\mathrm{min}})/(N-1)$; we thus need not worry about the recurrencelike behavior for sufficiently large N. We also remark that the interaction energy $E_I(t) := \mathrm{Tr}[\hat{\rho}(t)\hat{H}_I]$ is negligibly small under the parameters in Eq. (5.66) for large N; see Fig. 5.2. This justifies the transformation from the first equality of Eq. (5.58) to that of Eq. (5.60).

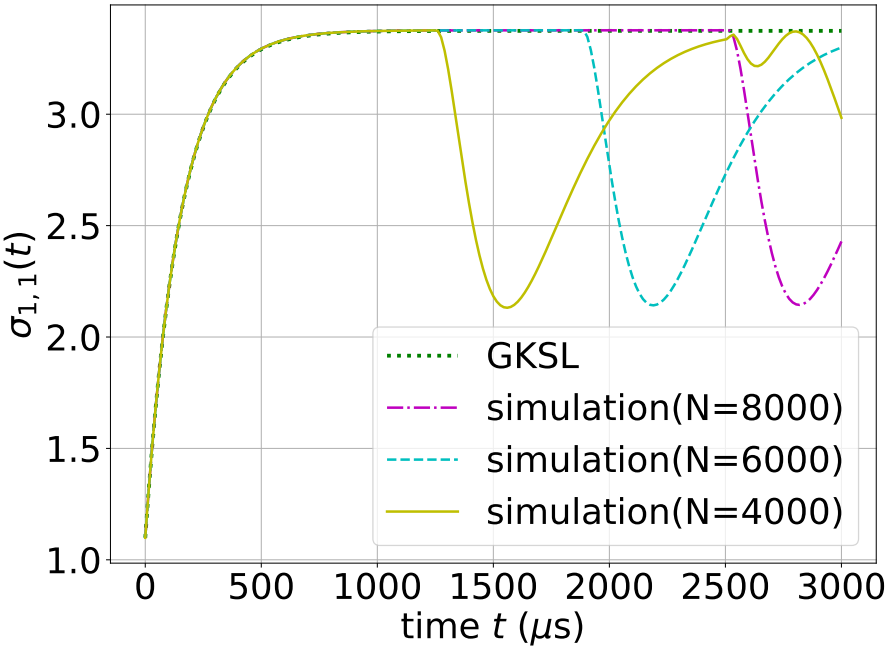

Figure 5.1: The time evolution of $\sigma_{1,1}(t)$. We adopt the Ohmic bath separated by equal spaces; see Eqs. (5.63) and (5.65). The parameters are shown in Eq. (5.66). The green dotted line is obtained from the solution of the GKSL master equation in Eq. (5.36). The other lines are obtained from the unitary dynamics of the total system in Eq. (5.30).

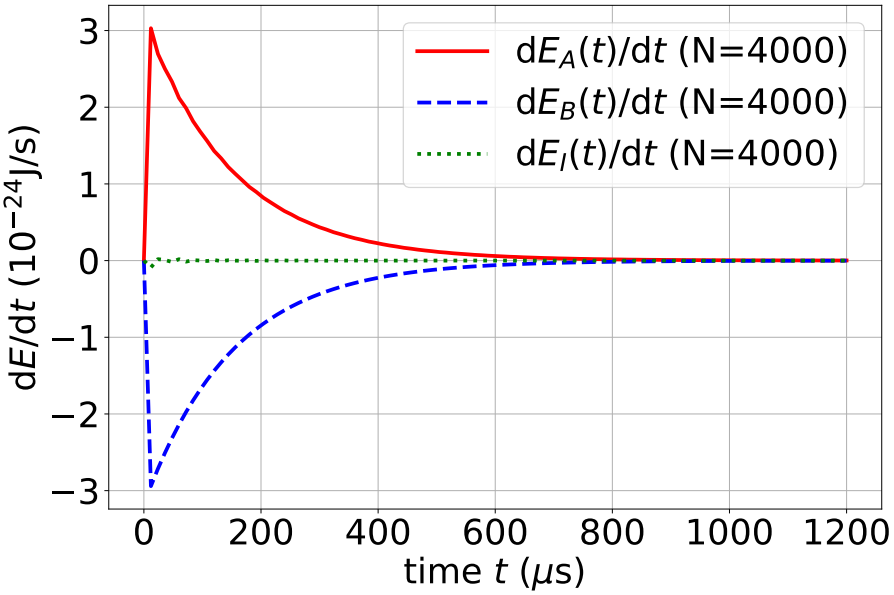

Figure 5.2: The time evolution of $\mathrm{d}E_A(t)/\mathrm{d}t$ in Eq. (G.5), $\mathrm{d}E_B(t)/\mathrm{d}t$ in Eq. (G.9), and $\mathrm{d}E_I(t)/\mathrm{d}t$ in Eq. (G.10) when $N = 4000$ under the unitary dynamics of the total system in Eq. (5.30). The setting and all the parameters except N are the same as those in Fig. 5.1.

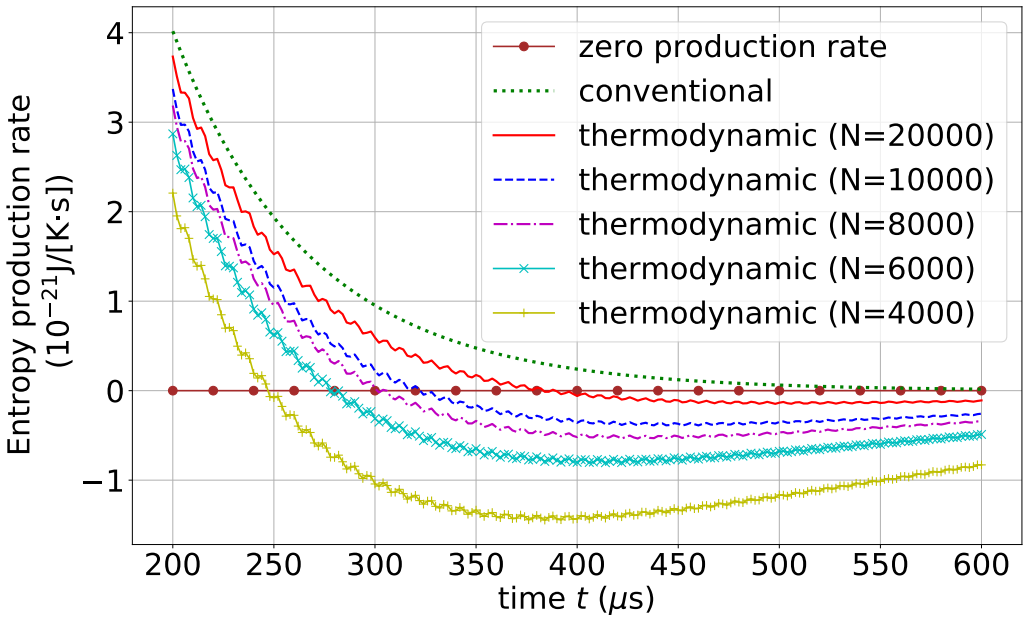

Figure 5.3: The total thermodynamic entropy production rate $\Pi^{\rm th}_{\rm tot}(t)$ in Eq. (5.57) under the unitary dynamics of the total system in Eq. (5.30) and the conventional entropy production rate $\Pi^{\rm vN}(t)$ in Eq. (5.60) under the GKSL master equation in Eq. (5.36). The setting and all the parameters except N are the same as those in Fig. 5.1.

5.5.2 Negative total thermodynamic entropy production rate

We compare in Fig. 5.3 our total thermodynamic entropy production rate $\Pi^{\rm th}_{\rm tot}(t)$ in Eq. (5.57) with the conventional entropy production rate $\Pi^{\rm vN}(t)$ in Eq. (5.60). We find that our total thermodynamic entropy production rate $\Pi^{\rm th}_{\rm tot}(t)$ is negative in a certain time range, in contrast to the conventional entropy production rate $\Pi^{\rm vN}(t)$, which is always non-negative. As we said in Sec. 5.4.4, $\Pi^{\rm th}_{\rm tot}(t)$ differs from $\Pi^{\rm vN}(t)$ because some of $\{T_j(t)\}$ differ from T_B^0; see Eq. (5.61). Let us see the behaviors of $\{T_j(t)\}$ below.

We find in Fig. 5.4 that the temperature of the system $T_A(t)$ relaxes to the initial temperature of the bath T_B^0, while some of the temperatures $\{T_j(t)\}$ of the harmonic oscillators in the bath decrease. The harmonic oscillators which show temperature decreasing have almost the same frequency as the system (Fig. 5.5). This can be explained as follows. The mean energy of the system $E_A(t)$ is a strictly monotonically increasing function of the temperature of the system $T_A(t)$, and hence $E_A(t)$ increases as $T_A(t)$ relaxes to T_B^0, which is higher than the initial temperature of the system T_A^0. In order for $E_A(t)$ to increase, the system must receive particles with energy $\hbar\omega_1$. Note that the total particle number operator $\sum_{j=1}^{N+1}\hat{a}_j^\dagger\hat{a}_j$ commutes with the total Hamiltonian (5.20), so that the total particle number is conserved. Thus, in order for the system to receive a particle with energy $\hbar\omega_1$, the bath must provide the particle, and only the harmonic oscillators whose frequencies are almost the same as the system can do so. When the harmonic oscillators provide the particle, their mean energies $\{E_j(t)\}$ decrease. Hence, the time-dependent temperature $T_j(t)$, which is a strictly monotonically increasing function of $E_j(t)$, also decreases.

We see from Fig. 5.5 that as $|\omega_j-\omega_1|$ becomes smaller, $[T_B^0-T_j(t)]$ and $|{\rm d}E_j(t)/{\rm d}t|$ become larger, and so does $[1/T_B^0-1/T_j(t)]{\rm d}E_j(t)/{\rm d}t$. As N becomes larger, more harmonic oscillators in the bath take part in the energy exchange with the system, and hence $[T_B^0-T_j(t)]$ and $|{\rm d}E_j(t)/{\rm d}t|$ for each harmonic oscillator become smaller; see Fig. 5.5. In addition, $\sum_{j=2}^{N+1}{\rm d}E_j(t)/{\rm d}t =$

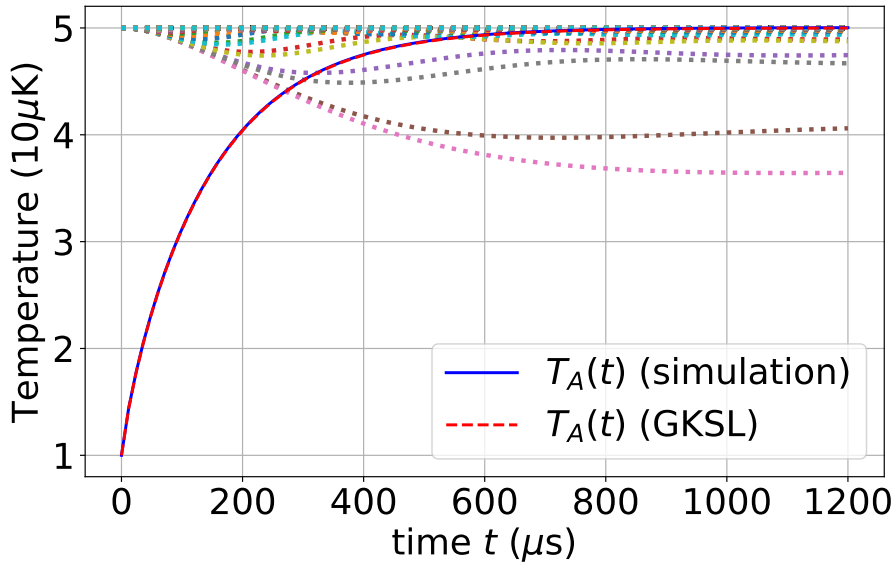

Figure 5.4: Time-dependent temperature $T_j(t)$ in Eq. (5.40) of each harmonic oscillator. We set $N = 4000$. The setting and all the parameters except N are the same as those in Fig. 5.1. The blue solid line is the time-dependent temperature of the system obtained from the unitary dynamics of the total system in Eq. (5.30). The red dashed line, which is almost identical to the blue solid line, is the time-dependent temperature of the system obtained from the solution of the GKSL master equation in Eq. (5.36). The dotted lines are the time-dependent temperatures of all the harmonic oscillators in the bath obtained from the unitary dynamics of the total system in Eq. (5.30).

$\mathrm{d}E_B(t)/\mathrm{d}t = -\mathrm{d}E_A(t)/\mathrm{d}t$ does not depend on N as long as the dynamics of the system obeys the GKSL master equation. Therefore as N becomes larger, $\Pi^{\mathrm{vN}}(t) - \Pi^{\mathrm{th}}_{\mathrm{tot}}(t)$ in Eq. (5.61) becomes smaller as in Fig. 5.3.

5.5.3 The second law of thermodynamics

We compare in Fig. 5.6 our total thermodynamic entropy production $\Delta S^{\mathrm{th}}_{\mathrm{tot}}(t)$ in Eq. (5.55) with the conventional entropy production, which in our settings is given by

$$\Delta S^{\mathrm{vN}}(t) := \int_0^t \mathrm{d}t\, \Pi^{\mathrm{vN}}(t) = S^{\mathrm{th}}_A(t) - S^{\mathrm{th}}_A(0) - \frac{E_A(t) - E_A(0)}{T^0_B}. \tag{5.67}$$

As the entropy production is the time integral of the entropy production rate, our total thermodynamic entropy production approaches the conventional entropy production as N becomes larger, which is similar to the case of the total entropy production rate. In fact, the difference

$$\Delta S^{\mathrm{vN}}(t) - \Delta S^{\mathrm{th}}_{\mathrm{tot}}(t) = \frac{E_A(0) - E_A(t)}{T^0_B} + \sum_{j=2}^{N+1} \left[S^{\mathrm{th}}_j(0) - S^{\mathrm{th}}_j(t) \right] \tag{5.68}$$

is almost proportional to N^{-1} for large N; see Fig. 5.7. This suggests that $\Delta S^{\mathrm{th}}_{\mathrm{tot}}(t)$ may converge to $\Delta S^{\mathrm{vN}}(t)$ in the limit $N \to \infty$.

Our total thermodynamic entropy production changes little for $800\,\mu\mathrm{s} \lesssim t \leq 1200\,\mu\mathrm{s}$, as shown in Fig. 5.6. We therefore regard the quantum state of the total system $\hat{\rho}(t)$ in this time range as an equilibrium state. Since $\Delta S^{\mathrm{th}}_{\mathrm{tot}}(t) > 0$ for $800\,\mu\mathrm{s} \lesssim t \leq 1200\,\mu\mathrm{s}$, we judge that our

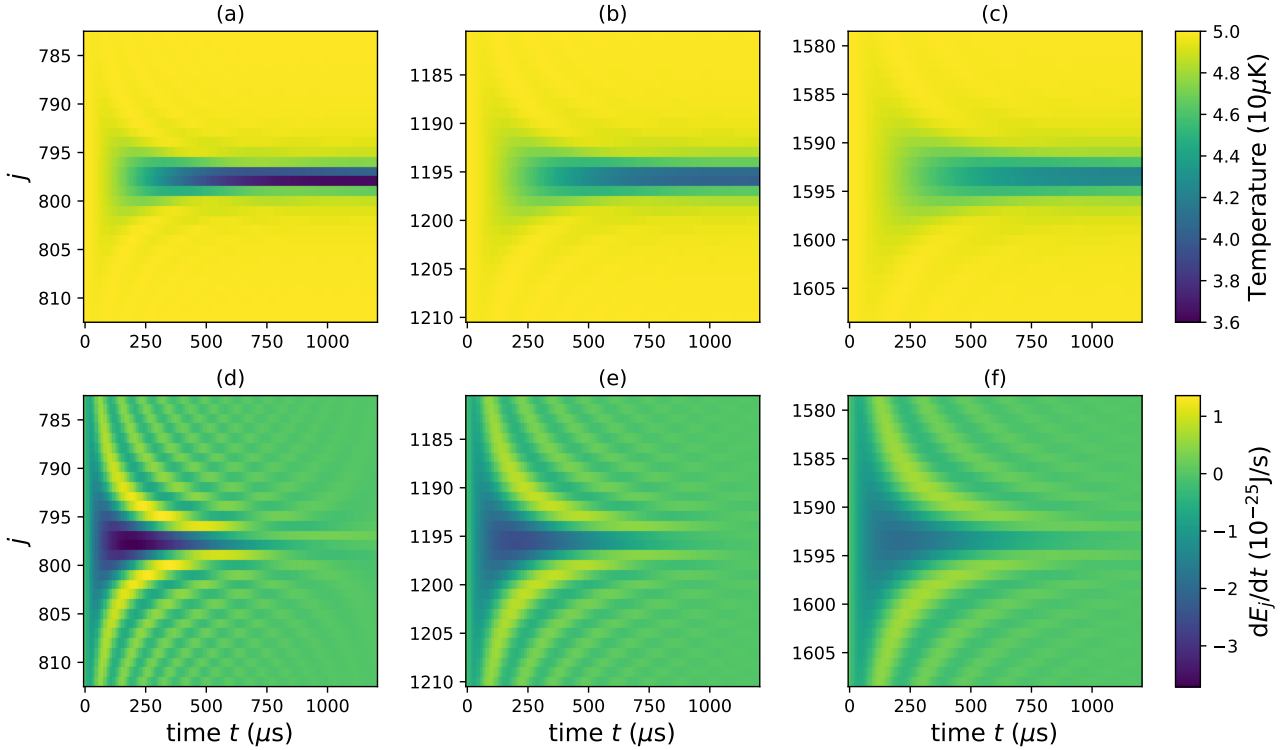

Figure 5.5: The time-dependent temperatures $\{T_j(t)\}$ (upper panels) and the time derivatives of the mean energies $\{\mathrm{d}E_j(t)/\mathrm{d}t\}$ (lower panels) of the harmonic oscillators in the bath which have almost the same frequencies as that of the system. The color expresses the value of $T_j(t)$ ($\mathrm{d}E_j(t)/\mathrm{d}t$) in the upper (lower) panels. The vertical axis corresponds to the number j of each harmonic oscillator. The horizontal axis corresponds to time. We set $N = 4000$ in (a) and (d), $N = 6000$ in (b) and (e), and $N = 8000$ in (c) and (f). The setting and the other parameters are the same as those in Fig. 5.1.

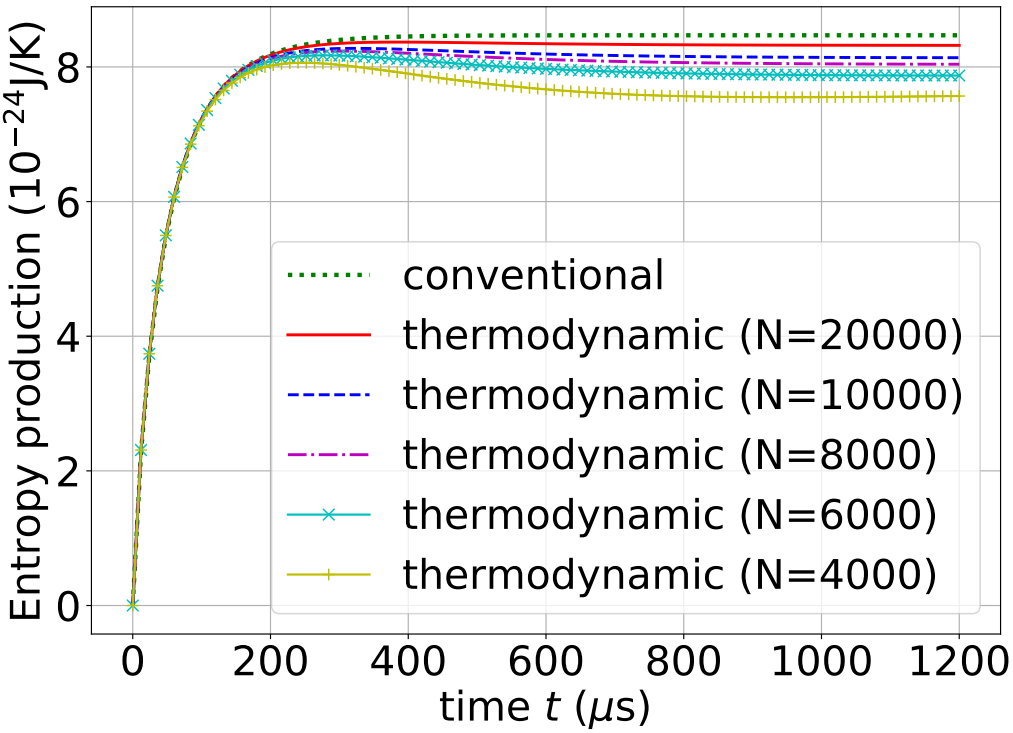

Figure 5.6: The thermodynamic entropy production $\Delta S^{\rm th}_{\rm tot}(t)$ in Eq. (5.55) under the unitary dynamics of the total system in Eq. (5.30) and the conventional entropy production $\Delta S^{\rm vN}(t)$ in Eq. (5.67) under the GKSL master equation in Eq. (5.36). The setting and all the parameters except N are the same as those in Fig. 5.1.

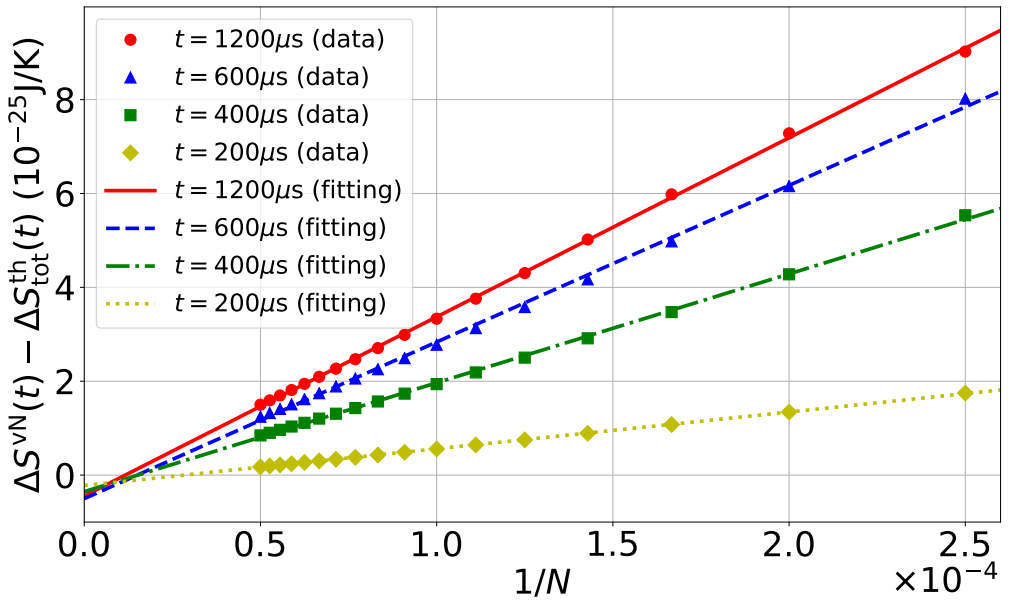

Figure 5.7: The difference $\Delta S^{\rm vN}(t) - \Delta S^{\rm th}_{\rm tot}(t)$ in Eq. (5.68) against N^{-1} for four different times. The setting and all the parameters except N are the same as those in Fig. 5.1.

total thermodynamic entropy $S_{\rm tot}^{\rm th}(t)$ satisfies the principle of increasing total thermodynamic entropy (5.1).

5.6 Discussions

5.6.1 Conventional entropy production rate

We compare in Fig. 5.8 the conventional entropy production rate $\Pi^{\rm vN}(t)$ in Eq. (5.59) under the unitary dynamics of the total system in Eq. (5.30) and the conventional entropy production rate $\Pi^{\rm vN}(t)$ in Eq. (5.60) under the GKSL master equation in Eq. (5.36). We find that the former is close to the latter and is positive for $t \lesssim 1030\,\mu$s. The negative values of the former for $1030\,\mu{\rm s} \lesssim t \leq 1200\,\mu$s are much smaller than its positive values for $t \lesssim 950\,\mu$s. Moreover, the system is almost in equilibrium with the bath for $1030\,\mu{\rm s} \lesssim t \leq 1200\,\mu$s. This also supports that the dynamics of the system for $0 \leq t \leq 1200\,\mu$s is well-approximated by the GKSL equation.

5.6.2 Protocol dependence of our total thermodynamic entropy production

The definition of our nonequilibrium thermodynamic entropy $S_{\rm tot}^{\rm th}(t)$ in Eq. (5.51) is based on the initial state of the total system in Eq. (5.34). Here, let us consider a different initial state. As an example, we focus on the state of the total system with $N = 4000$ in Sec. 5.5 at $t = 204\,\mu$s:

$$\sigma(204\,\mu{\rm s}) = \begin{pmatrix} \sigma_A(204\,\mu{\rm s}) & \sigma_{AB}(204\,\mu{\rm s}) \\ \sigma_{AB}(204\,\mu{\rm s})^{\rm T} & \sigma_B(204\,\mu{\rm s}) \end{pmatrix}. \tag{5.69}$$

If we get rid of the correlation between the system and the bath, we will have

$$\bar{\sigma}(204\,\mu{\rm s}) = \begin{pmatrix} \sigma_A(204\,\mu{\rm s}) & 0 \\ 0 & \sigma_B(204\,\mu{\rm s}) \end{pmatrix}. \tag{5.70}$$

Note that our total nonequilibrium thermodynamic entropy of the state in Eq. (5.69) is equal to that of the state in Eq. (5.70). However, it is not obvious whether our total nonequilibrium thermodynamic entropy of the state

$$\sigma(t) = V(t - 204\,\mu{\rm s})\sigma(204\,\mu{\rm s})V(t - 204\,\mu{\rm s})^{\rm T} \tag{5.71}$$

is equal to the total nonequilibrium thermodynamic entropy of the state

$$\bar{\sigma}(t) = V(t - 204\,\mu{\rm s})\bar{\sigma}(204\,\mu{\rm s})V(t - 204\,\mu{\rm s})^{\rm T}. \tag{5.72}$$

Note that the state in Eq. (5.71) for $t \geq 204\,\mu$s is the same as that used in Sec. 5.5. Thus, if we prepare the state in Eq. (5.69) as the initial state of the total system, each harmonic oscillator at $t \geq 204\,\mu$s is in a Gibbs state. On the other hand, if we prepare the state in Eq. (5.70) as the initial state of the total system, we do not know whether each harmonic oscillator at $t \geq 204\,\mu$s is in a Gibbs state.

If we assume that each harmonic oscillator at $t \geq 204\,\mu$s is in a Gibbs state in the case of the initial state in Eq. (5.70), the temperature of each harmonic oscillator time-evolves as in Fig. 5.9. We find that the time evolution of the temperature $T_A(t)$ of the system in Fig. 5.9 is

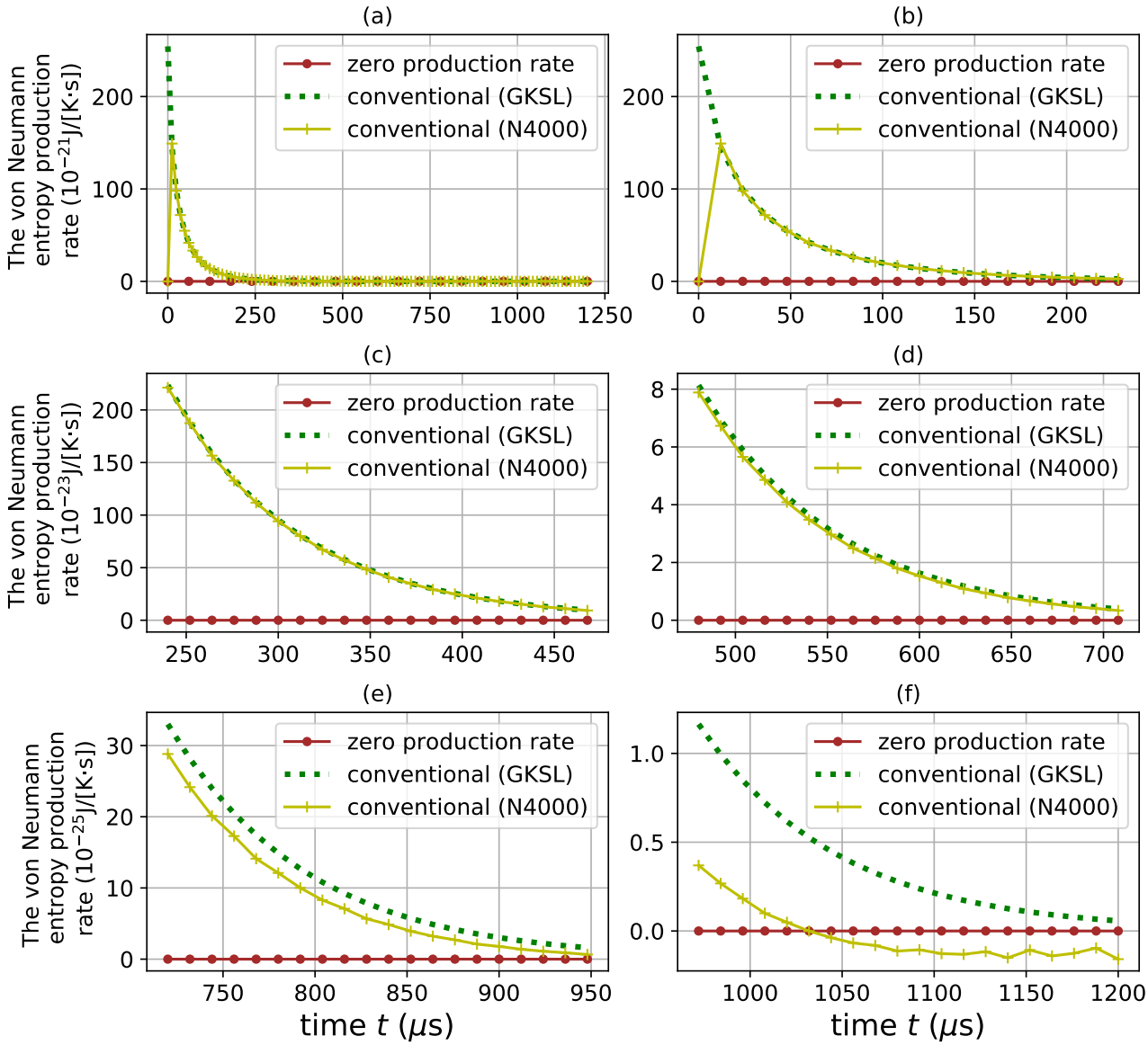

Figure 5.8: The conventional entropy production rate $\Pi^{\mathrm{vN}}(t)$ in Eq. (5.59) under the unitary dynamics of the total system in Eq. (5.30) and the conventional entropy production rate $\Pi^{\mathrm{vN}}(t)$ in Eq. (5.60) under the GKSL master equation in Eq. (5.36): (a) $0 \leq t \leq 1200\,\mu$s; (b) $0 \leq t \leq 228\,\mu$s; (c) $240\,\mu\mathrm{s} \leq t \leq 468\,\mu$s; (d) $480\,\mu\mathrm{s} \leq t \leq 708\,\mu$s; (e) $720\,\mu\mathrm{s} \leq t \leq 948\,\mu$s; (f) $960\,\mu\mathrm{s} \leq t \leq 1200\,\mu$s. We set $N = 4000$. The setting and all the parameters except N are the same as those in Fig. 5.1.

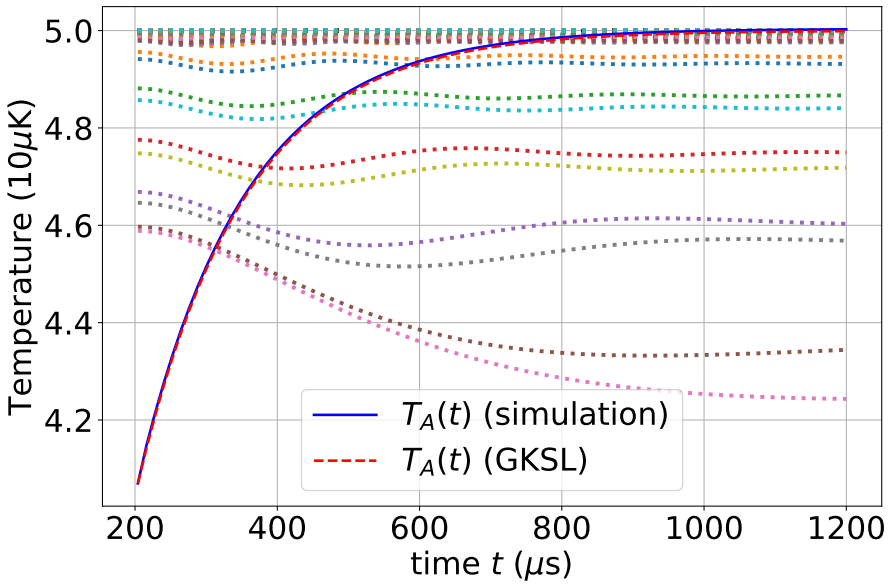

Figure 5.9: Time-dependent temperature $T_j(t)$ of each harmonic oscillator assuming that they are in Gibbs states. We adopt the Ohmic bath separated by equal spaces; see Eqs. (5.63) and (5.65). We set $N = 4000$. The blue solid line is the time-dependent temperature of the system obtained from the unitary dynamics of the total system in Eq. (5.72). The red dashed line here, which is almost identical to the blue solid line, is the same as the red dashed line in Fig. 5.4. The dotted lines are the time-dependent temperatures of all the harmonic oscillators in the bath obtained from the unitary dynamics of the total system in Eq. (5.72).

almost the same as that in Fig. 5.4. As the conventional entropy production

$$\Delta S^{\mathrm{vN}}(t) = S_A^{\mathrm{th}}(t) - S_A^{\mathrm{th}}(204\,\mu\mathrm{s}) - \frac{E_A(t) - E_A(204\,\mu\mathrm{s})}{T_B^0} \tag{5.73}$$

depends on the state of the system only, the conventional entropy production of the state in Eq. (5.72) is almost the same as that of the state in Eq. (5.71).

On the other hand, the time evolutions of the temperatures $T_j(t)$ of the harmonic oscillators in the bath in Fig. 5.9 are different from those in Fig. 5.4. As our total thermodynamic entropy production

$$\Delta S_{\mathrm{tot}}^{\mathrm{th}}(t) = S_A^{\mathrm{th}}(t) - S_A^{\mathrm{th}}(204\,\mu\mathrm{s}) + \sum_{j=2}^{N+1} \left[S_j^{\mathrm{th}}(t) - S_j^{\mathrm{th}}(204\,\mu\mathrm{s}) \right] \tag{5.74}$$

depends not only on the state of the system, but also on the states of the harmonic oscillators in the bath, our total thermodynamic entropy production of the state in Eq. (5.72) is different from that of the state in Eq. (5.71); see Fig. 5.10.

5.6.3 The same initial temperatures of the system and the bath

Let us investigate how does the temperature of the system change if the initial temperature of the system is equal to that of the bath. Here, we fix the parameters as follows:

$$\begin{gathered} \omega_1 = 4\,\mathrm{MHz},\ \omega_{\mathrm{cut}} = 3\,\mathrm{MHz},\ \omega_{\mathrm{min}} = 0.026\,\mathrm{MHz},\ \omega_{\mathrm{max}} = 20\,\mathrm{MHz}, \\ N = 4000,\ T_A^0 = T_B^0 = 50\,\mu\mathrm{K}. \end{gathered} \tag{5.75}$$

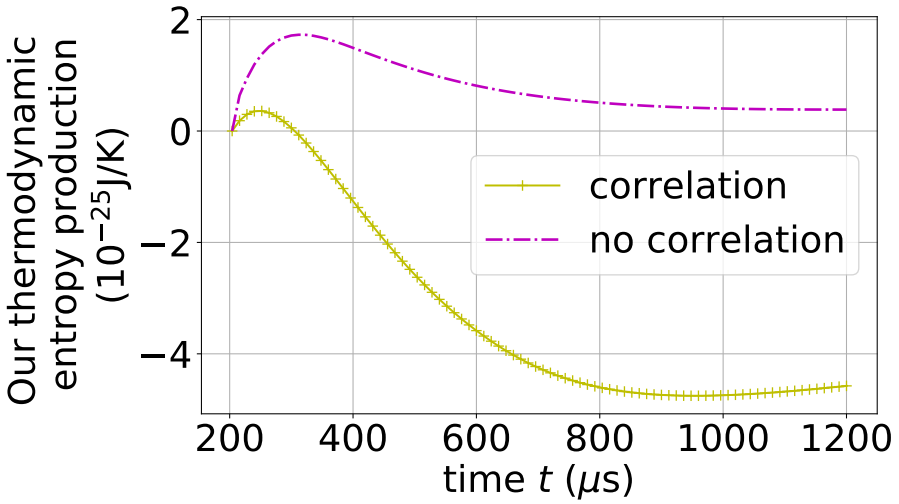

Figure 5.10: Our total thermodynamic entropy production $\Delta S_{\rm tot}^{\rm th}(t)$ in Eq. (5.74) of the state in Eq. (5.72) (the dashed magenta line) and that of the state in Eq. (5.71) (the yellow line), which is the same as the yellow line in Fig. 5.6. The parameters are the same as those in Fig. 5.9.

For the coupling strength η, we consider two cases: $\eta = 10^{-3}$ (weak coupling) and $\eta = 0.1$ (strong coupling). When the coupling is weak, the interaction energy $E_I(t)$ is small; see Fig. 5.11. Hence, the mean energy $E_A(t)$ of the system changes little, nor does the temperature $T_A(t)$ of the system; see Fig. 5.12. On the other hand, when the coupling is strong, the interaction energy $E_I(t)$ is large and negative; see Fig. 5.13. Hence, the mean energy $E_A(t)$ of the system increases much and so does the temperature $T_A(t)$ of the system; see Fig. 5.14.

5.6.4 Discretization of a bosonic bath

In Sec. 5.5.1, we discretized the bath by eqaul spaces; see Eq. (5.63). Here, let us adopt a logarithmic discretization [72]:

$$\omega_{j+1} = \omega_j + \Delta\omega_j, \tag{5.76}$$

$$\Delta\omega_{j+1} = l\Delta\omega_j = l^{j-1}\Delta\omega_2 \tag{5.77}$$

for $j = 2, \ldots, N$ with $l > 0$. Using these equations, we obtain

$$\omega_{N+1} = \omega_2 + \sum_{j=2}^{N} \Delta\omega_j = \omega_2 + \Delta\omega_2 \sum_{j=2}^{N} l^{j-2} = \omega_2 + \frac{l^{N-1}-1}{l-1}\Delta\omega_2, \tag{5.78}$$

or

$$\Delta\omega_2 = \frac{l-1}{l^{N-1}-1}(\omega_{N+1} - \omega_2) \tag{5.79}$$

and

$$\Delta\omega_j = l^{j-2}\Delta\omega_2 = \frac{(l-1)l^{j-2}}{l^{N-1}-1}(\omega_{N+1} - \omega_2), \tag{5.80}$$

$$\omega_j = \omega_2 + \Delta\omega_2 \sum_{k=2}^{j-1} l^{k-2} = \omega_2 + \frac{l^{j-2}-1}{l^{N-1}-1}(\omega_{N+1} - \omega_2) \tag{5.81}$$

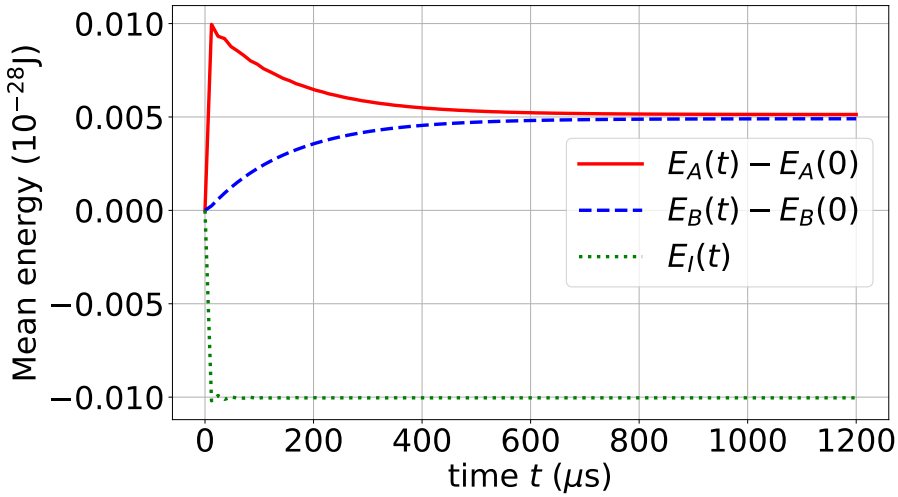

Figure 5.11: The time evolution of $E_A(t) - E_A(0)$, $E_B(t) - E_B(0)$, and $E_I(t)$ under the unitary dynamics of the total system in Eq. (5.30). We adopt the Ohmic bath separated by equal spaces; see Eqs. (5.63) and (5.65). We set $\eta = 10^{-3}$. The other parameters are shown in Eq. (5.75).

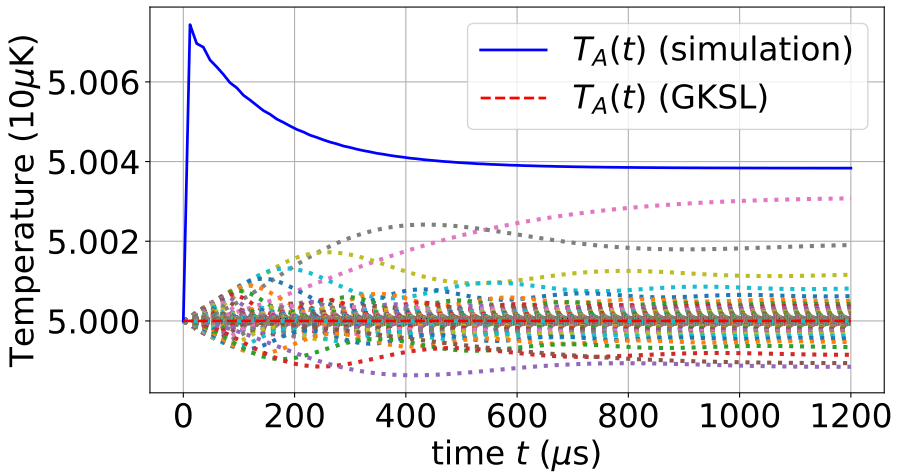

Figure 5.12: Time-dependent temperature $T_j(t)$ in Eq. (5.40) of each harmonic oscillator. The setting and all the parameters are the same as those in Fig. 5.11. The blue solid line is the time-dependent temperature of the system obtained from the unitary dynamics of the total system in Eq. (5.30). The red dashed line is the time-dependent temperature of the system obtained from the solution of the GKSL master equation in Eq. (5.36). The dotted lines are the time-dependent temperatures of all the harmonic oscillators in the bath obtained from the unitary dynamics of the total system in Eq. (5.30).

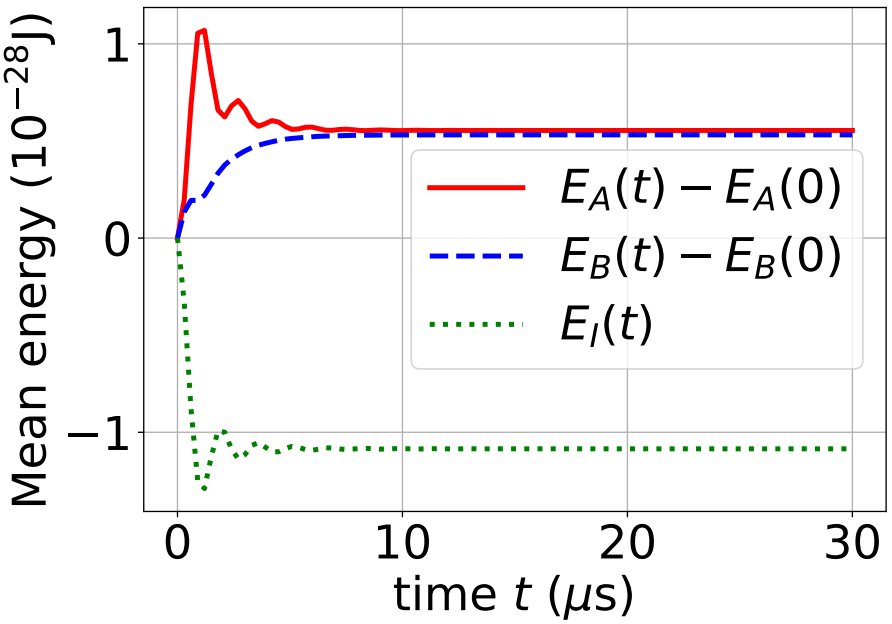

Figure 5.13: The time evolution of $E_A(t) - E_A(0)$, $E_B(t) - E_B(0)$, and $E_I(t)$ under the unitary dynamics of the total system in Eq. (5.30). We set $\eta = 0.1$. The setting and all the parameters except η are the same as those in Fig. 5.11.

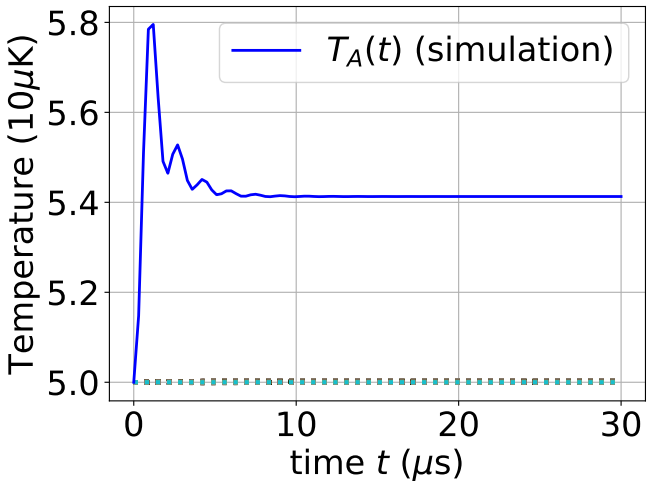

Figure 5.14: Time-dependent temperature $T_j(t)$ in Eq. (5.40) of each harmonic oscillator. The setting and all the parameters are the same as those in Fig. 5.13. The blue solid line is the time-dependent temperature of the system obtained from the unitary dynamics of the total system in Eq. (5.30). The dotted lines are the time-dependent temperatures of all the harmonic oscillators in the bath obtained from the unitary dynamics of the total system in Eq. (5.30).

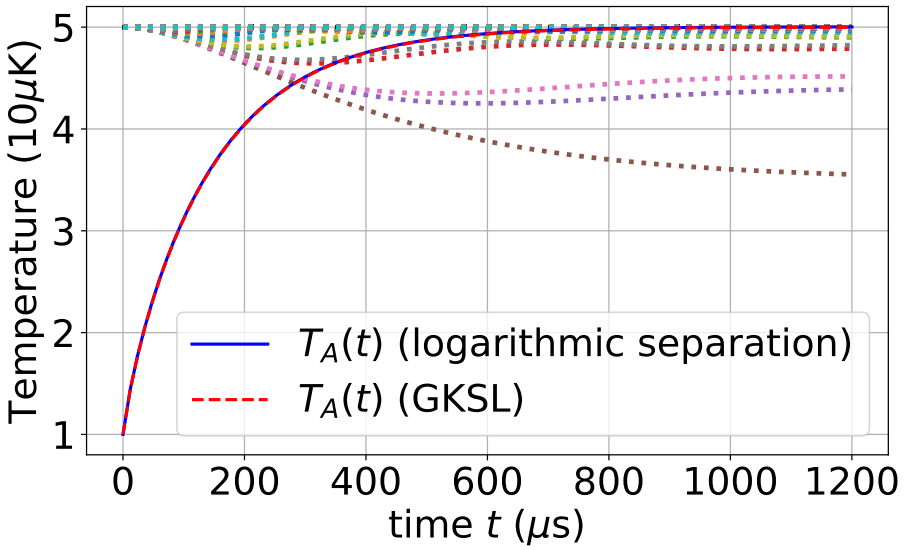

Figure 5.15: Time-dependent temperature $T_j(t)$ in Eq. (5.40) of each harmonic oscillator. We adopt the Ohmic bath separated logarithmically; see Eqs. (5.82) and (5.83). The parameters are shown in Eq. (5.84). The blue solid line is the time-dependent temperature of the system obtained from the unitary dynamics of the total system in Eq. (5.30). The red dashed line, which is almost identical to the blue solid line, is the time-dependent temperature of the system obtained from the solution of the GKSL master equation in Eq. (5.36). The dotted lines are the time-dependent temperatures of all the harmonic oscillators in the bath obtained from the unitary dynamics of the total system in Eq. (5.30).

for $j = 3, \ldots, N+1$. In summary, the logarithmic discretization in Eqs. (5.76) and (5.77) is equivalent to

$$\omega_j = \omega_{\min} + \frac{l^{j-2} - 1}{l^{N-1} - 1}(\omega_{\max} - \omega_{\min}) \tag{5.82}$$

for $j = 2, \ldots, N+1$. A procedure similar to Eq. (5.64) leads to

$$g_j = \sqrt{\eta \Delta \omega_j \, \omega_j e^{-\omega_j/\omega_{\rm cut}}} \tag{5.83}$$

for $j = 2, \ldots, N+1$. we fix the parameters as follows:

$$\begin{aligned} &\omega_1 = 4\,\text{MHz},\ \omega_{\rm cut} = 3\,\text{MHz},\ \omega_{\min} = 0.026\,\text{MHz},\ \omega_{\max} = 20\,\text{MHz}, \\ &N = 4000,\ l = 1.001,\ \eta = 10^{-3},\ T_A^0 = 10\,\mu\text{K},\ T_B^0 = 50\,\mu\text{K}. \end{aligned} \tag{5.84}$$

We show in Fig. 5.15 the time evolution of the temperature $T_j(t)$ of each harmonic oscillator. We compare in Fig. 5.16 our total thermodynamic entropy production rate $\Pi_{\rm tot}^{\rm th}(t)$ in Eq. (5.57) with the conventional entropy production rate $\Pi^{\rm vN}(t)$ in Eq. (5.60). We compare in Fig. 5.17 our total thermodynamic entropy production $\Delta S_{\rm tot}^{\rm th}(t)$ in Eq. (5.55) with the conventional entropy production $\Delta S^{\rm vN}(t)$ in Eq. (5.67). We have obtained with the logarithmically separated bath the qualitatively same results as those with the equally separated bath in Sec. 5.5; see Figs. 5.3, 5.4, and 5.6.

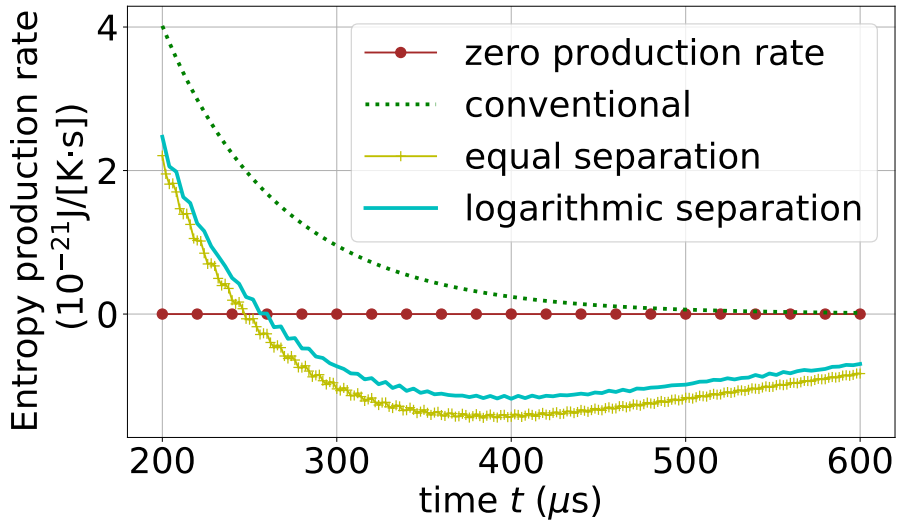

Figure 5.16: The total thermodynamic entropy production rate $\Pi^{\rm th}_{\rm tot}(t)$ in Eq. (5.57) and the conventional entropy production rate $\Pi^{\rm vN}(t)$ in Eq. (5.60). The green dotted line labeled "conventional" here is the same as that in Fig. 5.3. The yellow line labeled "equal separation" here is the same as the yellow line labeled "thermodynamic ($N = 4000$) in Fig. 5.3. The cyan line labeled "logarithmic separation" is $\Pi^{\rm th}_{\rm tot}(t)$ calculated under the same setting and parameters as those in Fig. 5.15.

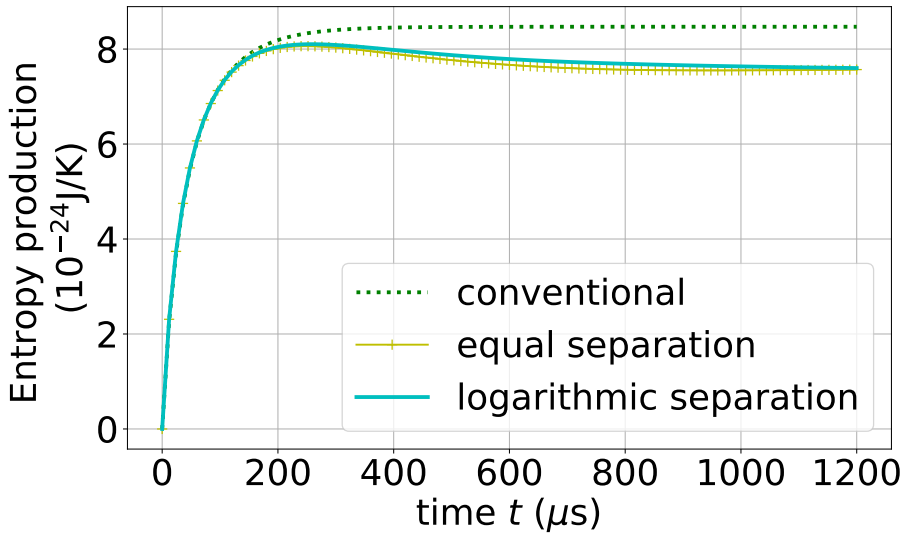

Figure 5.17: The total thermodynamic entropy production $\Delta S^{\rm th}_{\rm tot}(t)$ in Eq. (5.55) and the conventional entropy production $\Delta S^{\rm vN}(t)$ in Eq. (5.67). The green dotted line labeled "conventional" here is the same as that in Fig. 5.6. The yellow line labeled "equal separation" here is the same as the yellow line labeled "thermodynamic ($N = 4000$) in Fig. 5.6. The cyan line labeled "logarithmic separation" is $\Delta S^{\rm th}_{\rm tot}(t)$ calculated under the same setting and parameters as those in Fig. 5.15.

Chapter 6

Conclusions

In this thesis, we have studied dynamics and thermodynamics of coupled quantum oscillators, based on the Hamiltonian of the total system which consists of a system of interest and a bath. Our main results are in Chapters 4 and 5. As the system of interest, we consider a Kerr-nonlinear parametric oscillator (KPO) in Chapter 4 and a quantum harmonic oscillator in Chapter 5. In both cases, the bath is comprised of many quantum harmonic oscillators. The coupling between the system and the bath is weak enough for the dynamics of the system to be well-approximated by the Gorini-Kossakowski-Sudarshan-Lindblad (GKSL)-type Markovian master equation.

In Chapter 4, we have microscopically derived the GKSL equation (4.56) for a KPO, starting from the Hamiltonian (4.8) of the total system. By doing so, the relationship between the dynamics of the KPO and the Hamiltonian of the total system has become clear. On the other hand, the decoherence part of the GKSL equation (4.57) in the literature is obtained under the assumption that the system is a quantum harmonic oscillator, which is not true. Therefore, it is questionable whether the GKSL equation in the literature describes the decoherence of a KPO correctly. We have compared the dynamics of a KPO under our GKSL equation and that under the GKSL equation in the literature. As a result, we have found that the excitation error of a KPO under our GKSL equation is smaller than that under the GKSL equation in the literature. In particular, in the low-temperature limit of the bath, we have found that the state of a KPO under our GKSL equation is mostly confined to the cat subspace C_0, which is spanned by KPO's two degenerate ground states, $|C_\alpha^{0,\pm}\rangle$. This is desirable when we use a KPO as a qubit for a quantum computer, whose mission is to reduce as many errors as possible. We claim that it is essential to employ our more accurate GKSL equation to reproduce this desirable result.

Let us describe future prospects regarding the decoherence of a KPO. First, in the derivation of our GKSL equation (4.56), we assumed the following: (i) $\alpha \gg 1$; (ii) four-level approximation is good (see Fig. 4.1); (iii) $|C_\alpha^{n,\pm}\rangle \approx \frac{1}{\sqrt{2}}[\hat{D}(\alpha) \pm (-1)^n \hat{D}(-\alpha)]\,|n\rangle$ [Eq. (4.53)]. As we explained in Sec. 4.2.2, due to the assumption (iii), we cannot calculate the bit-flip rate ($|\alpha\rangle \leftrightarrow |-\alpha\rangle$, or $|\bar{0}\rangle \leftrightarrow |\bar{1}\rangle$) correctly with our GKSL equation (4.56). To amend this point, we would like to derive the GKSL equation for a KPO adopting Eq. (4.54). In Ref. [73], it was shown that making use of higher effective excited states $|C_\alpha^{n,\pm}\rangle$ for $n = 2, 3$ achieves a faster R_x gate, which exchanges the populations between $|\alpha\rangle = |\bar{0}\rangle$ and $|-\alpha\rangle = |\bar{1}\rangle$. In this case, the assumption (ii) is broken. We would like to expand our GKSL equation so that we can also treat the transitions to and from $|C_\alpha^{n,\pm}\rangle$ for $n = 2, 3, \ldots$.

As another prospect, we want to compare our GKSL equation with experiments. Until now, experiments of a KPO have been done with small α (for instance $\alpha \approx 1.6$ in Ref. [13]). On the

other hand, owing to the assumption (i), we cannot use our GKSL equation when α is small. To amend this, we would like to derive the GKSL equation for a KPO with small α. For this purpose, we need the forms of the excited states of the KPO. Unfortunately, even approximate forms of the excited states are not known when α is small. Searching for the forms of the excited states of a KPO with small α is left as our future work.

In Chapter 5, we have defined and analyzed the nonequilibrium thermodynamic entropy for the quantum model of coupled harmonic oscillators in a star configuration. As the initial state of the total system, we have prepared the tensor product of the Gibbs states of the system and the bath. As a result, we have found that every harmonic oscillator is always in a Gibbs state with a time-dependent temperature. This allows us to define the thermodynamic entropy for each harmonic oscillator in a similar way to the definition in equilibrium thermodynamics and statistical mechanics. We can treat every harmonic oscillator on an equal footing thanks to the initial state that we adopted. We have defined the nonequilibrium thermodynamic entropy of the total system as the summation of the thermodynamic entropy of each harmonic oscillator. We have analytically confirmed that our total thermodynamic entropy satisfies the third law of thermodynamics. We have found numerically that our total thermodynamic entropy production rate can be negative though the finite-time dynamics of the central harmonic oscillator (the system of interest) is well approximated by the GKSL-type Markovian master equation, while our total thermodynamic entropy satisfies the second law of thermodynamics. This contrasts with the von Neumann entropy production rate, which is always positive. This difference originates in our microscopically treating the harmonic oscillators in the bath. We can pursue the time evolution of the temperature of each harmonic oscillator in our formulation. We hence found that the temperatures of the harmonic oscillators in the bath which have almost the same frequency as the system change due to the interaction. Our thermodynamic entropy production rate takes this into account; see Eq. (5.56). On the other hand, the form of the von Neumann entropy production rate does not take the temperature changes into account;. see Eq. (5.58). Therefore, when the size of the bath is finite, our thermodynamic entropy production rate is preferable.

Let us discuss the future prospect regarding the nonequilibrium thermodynamic entropy of the quantum model of coupled harmonic oscillators. If we prepare a different initial state from the tensor product of the Gibbs states of the system and the bath, each harmonic oscillator will be no longer in a Gibbs state. That is, each harmonic oscillator is out of equilibrium. Then we cannot define the nonequilibrium thermodynamic entropy of each harmonic oscillator in a similar way to the definition in equilibrium thermodynamics and statistical mechanics. Studying how to define the nonequilibrium thermodynamic entropy for a nonequilibrium harmonic oscillator can be an interesting future work. As another issue, when we summed the thermodynamic entropy of each harmonic oscillator to define the nonequilibrium thermodynamic entropy of the total system, we assumed the additivity of the thermodynamic entropy because of the weak couplings between the system and the harmonic oscillators in the bath. However, if the couplings are strong, the contribution of the interaction between the system and the harmonic oscillators in the bath to the nonequilibrium thermodynamic entropy of the total system will not be negligible. How to incorporate the effect of the couplings is left as our future work.

Appendix A

Derivation of $\gamma^{\mathrm{R}}_{1,1}(\omega_A)$ in Eq. (4.33)

In this Appendix, we derive $\gamma^{\mathrm{R}}_{1,1}(\omega_A)$ in Eq. (4.33). Let us calculate $\hat{B}^{\mathrm{R},I}_{\bar{\alpha}}(t)$ in Eq. (4.32) as

$$\begin{aligned}
\hat{B}^{\mathrm{R},I}_1(t) &= \sum_{k=1}^{N}\left(\mathrm{e}^{-\mathrm{i}(\omega_k-\omega_p/2)t}\frac{g_k}{2}\hat{b}_k + \mathrm{e}^{\mathrm{i}(\omega_k-\omega_p/2)t}\frac{g_k}{2}\hat{b}^\dagger_k\right) \\
&= \sum_{\omega_B\in\{\omega_k-\omega_p/2,-(\omega_k-\omega_p/2)|k=1,\ldots,N\}} \mathrm{e}^{-\mathrm{i}\omega_B t}\hat{B}^{\mathrm{R}}_1(\omega_B), \qquad \text{(A.1)} \\
\hat{B}^{\mathrm{R}}_1(\omega_k-\omega_p/2) &= \frac{g_k}{2}\hat{b}_k, \quad \hat{B}_1(-(\omega_k-\omega_p/2)) = \frac{g_k}{2}\hat{b}^\dagger_k \qquad \text{(A.2)} \\
\hat{B}^{\mathrm{R},I}_2(t) &= \sum_{k=1}^{N}\left(-\mathrm{i}\mathrm{e}^{-\mathrm{i}(\omega_k-\omega_p/2)t}\frac{g_k}{2}\hat{b}_k + \mathrm{i}\mathrm{e}^{\mathrm{i}(\omega_k-\omega_p/2)t}\frac{g_k}{2}\hat{b}^\dagger_k\right) \\
&= \sum_{\omega_B\in\{\omega_k-\omega_p/2,-(\omega_k-\omega_p/2)|k=1,\ldots,N\}} \mathrm{e}^{-\mathrm{i}\omega_B t}\hat{B}^{\mathrm{R}}_2(\omega_B), \qquad \text{(A.3)} \\
\hat{B}^{\mathrm{R}}_2(\omega_k-\omega_p/2) &= -\mathrm{i}\frac{g_k}{2}\hat{b}_k, \quad \hat{B}^{\mathrm{R}}_2(-(\omega_k-\omega_p/2)) = \mathrm{i}\frac{g_k}{2}\hat{b}^\dagger_k. \qquad \text{(A.4)}
\end{aligned}$$

Using these, we calculate $\gamma^{\mathrm{R}}_{\bar{\alpha},\bar{\beta}}(\omega_A)$ in Eq. (2.50); its (1,1)-component is given by

$$\begin{aligned}
\gamma^{\mathrm{R}}_{1,1}(\omega_A) &= \sum_{\omega_B} 2\pi\delta(\omega_A-\omega_B)\mathrm{Tr}_B[\hat{B}^{\mathrm{R}}_1(\omega_B)\hat{B}^{\mathrm{R}}_1\hat{\rho}^{\mathrm{th}}_B] \\
&= \sum_k\sum_{\omega_B} 2\pi\delta(\omega_A-\omega_B)\mathrm{Tr}_B\left[\hat{B}^{\mathrm{R}}_1(\omega_B)\frac{g_k}{2}(\hat{b}^\dagger_k+\hat{b}_k)\hat{\rho}^{\mathrm{th}}_B\right] \\
&= \sum_k\sum_{\omega_B=\pm(\omega_k-\omega_p/2)} 2\pi\delta(\omega_A-\omega_B)\mathrm{Tr}_k\left[\hat{B}^{\mathrm{R}}_1(\omega_B)\frac{g_k}{2}(\hat{b}^\dagger_k+\hat{b}_k)\hat{\rho}^{\mathrm{th}}_k\right] \\
&= \sum_k 2\pi\delta(\omega_A-(\omega_k-\omega_p/2))\mathrm{Tr}_k\left[\frac{g_k}{2}\hat{b}_k\frac{g_k}{2}(\hat{b}^\dagger_k+\hat{b}_k)\hat{\rho}^{\mathrm{th}}_k\right] \\
&\quad + \sum_k 2\pi\delta(\omega_A+(\omega_k-\omega_p/2))\mathrm{Tr}_k\left[\frac{g_k}{2}\hat{b}^\dagger_k\frac{g_k}{2}(\hat{b}^\dagger_k+\hat{b}_k)\hat{\rho}^{\mathrm{th}}_k\right] \\
&= \sum_k \frac{\pi g_k^2}{2}\delta(\omega_A-(\omega_k-\omega_p/2))\mathrm{Tr}_k\left[(\hat{b}^\dagger_k\hat{b}_k+1)\hat{\rho}^{\mathrm{th}}_k\right] \\
&\quad + \sum_j \frac{\pi g_k^2}{2}\delta(\omega_A+(\omega_k-\omega_p/2))\mathrm{Tr}_k\left[\hat{b}^\dagger_k\hat{b}_k\hat{\rho}^{\mathrm{th}}_k\right] \\
&= \sum_k \frac{\pi g_k^2}{2}[(\bar{n}(\omega_k)+1)\delta(\omega_A-(\omega_k-\omega_p/2)) + \bar{n}(\omega_k)\delta(\omega_A+(\omega_k-\omega_p/2))]
\end{aligned}$$

$$
\begin{aligned}
&= \sum_k \frac{\pi g_k^2}{2}[(\bar{n}(\omega_p/2+\omega_A)+1)\delta(\omega_p/2+\omega_A-\omega_k) \\
&\qquad + \bar{n}(\omega_p/2-\omega_A)\delta(\omega_p/2-\omega_A-\omega_k)] \\
&= \Gamma(\omega_p/2+\omega_A)\frac{\bar{n}(\omega_p/2+\omega_A)+1}{2} + \Gamma(\omega_p/2-\omega_A)\frac{\bar{n}(\omega_p/2-\omega_A)}{2},
\end{aligned} \tag{A.5}
$$

where

$$
\bar{n}(\omega) = \frac{1}{\mathrm{e}^{\beta_B^0 \hbar\omega} - 1}, \tag{A.6}
$$

$$
\Gamma(\omega) = \pi J(\omega), \tag{A.7}
$$

$$
J(\omega) = \sum_k g_k^2 \delta(\omega - \omega_k) \tag{A.8}
$$

and we used

$$
\hat{\rho}_B^{\mathrm{th}} = \frac{\mathrm{e}^{-\beta_B^0 \hat{H}_B}}{\mathrm{Tr}\left[\mathrm{e}^{-\beta_B^0 \hat{H}_B}\right]} = \bigotimes_{k=1}^{N} \frac{\mathrm{e}^{-\beta_B^0 \hat{H}_k}}{\mathrm{Tr}\left[\mathrm{e}^{-\beta_B^0 \hat{H}_k}\right]} =: \bigotimes_{k=1}^{N} \hat{\rho}_k^{\mathrm{th}}. \tag{A.9}
$$

We can calculate the other components similarly.

Appendix B

Derivation of our decoherence part $\mathcal{D}^{\rm ours}[\hat{\rho}^{\rm R}_A(t)]$ in Eq. (4.49)

In this Appendix, we give a detailed calculation related to the derivation of Eq. (4.49). Let us calculate the action of $\hat{a}$ on $|C^{n,\pm}_\alpha\rangle$ for $n=0,1$ as

$$\begin{aligned}
\hat{a}\left|C^{0,+}_\alpha\right\rangle &= \hat{a}\mathcal{N}^{0,+}_\alpha(|\alpha\rangle+|-\alpha\rangle)\\
&= \alpha\mathcal{N}^{0,+}_\alpha(|\alpha\rangle-|-\alpha\rangle)\\
&= \alpha\frac{\mathcal{N}^{0,+}_\alpha}{\mathcal{N}^{0,-}_\alpha}\left|C^{0,-}_\alpha\right\rangle, \qquad \text{(B.1)}\\
\hat{a}\left|C^{0,-}_\alpha\right\rangle &= \alpha\frac{\mathcal{N}^{0,-}_\alpha}{\mathcal{N}^{0,+}_\alpha}\left|C^{0,+}_\alpha\right\rangle, \qquad \text{(B.2)}\\
\hat{a}\left|C^{1,+}_\alpha\right\rangle &= \hat{a}\mathcal{N}^{1,+}_\alpha[\hat{D}(\alpha)-\hat{D}(-\alpha)]\,|1\rangle\\
&= \mathcal{N}^{1,+}_\alpha[\hat{D}(\alpha)(\hat{a}+\alpha)-\hat{D}(-\alpha)(\hat{a}-\alpha)]\,|1\rangle\\
&= \mathcal{N}^{1,+}_\alpha\left([\hat{D}(\alpha)-\hat{D}(-\alpha)]\,|0\rangle+\alpha[\hat{D}(\alpha)+\hat{D}(-\alpha)]\,|1\rangle\right)\\
&= \frac{\mathcal{N}^{1,+}_\alpha}{\mathcal{N}^{0,-}_\alpha}\left|C^{0,-}_\alpha\right\rangle+\alpha\frac{\mathcal{N}^{1,+}_\alpha}{\mathcal{N}^{1,-}_\alpha}\left|C^{1,-}_\alpha\right\rangle, \qquad \text{(B.3)}\\
\hat{a}\left|C^{1,-}_\alpha\right\rangle &= \hat{a}\mathcal{N}^{1,-}_\alpha[\hat{D}(\alpha)+\hat{D}(-\alpha)]\,|1\rangle\\
&= \mathcal{N}^{1,-}_\alpha[\hat{D}(\alpha)(\hat{a}+\alpha)+\hat{D}(-\alpha)(\hat{a}-\alpha)]\,|1\rangle\\
&= \mathcal{N}^{1,-}_\alpha\left([\hat{D}(\alpha)+\hat{D}(-\alpha)]\,|0\rangle+\alpha[\hat{D}(\alpha)-\hat{D}(-\alpha)]\,|1\rangle\right)\\
&= \frac{\mathcal{N}^{1,-}_\alpha}{\mathcal{N}^{0,+}_\alpha}\left|C^{0,+}_\alpha\right\rangle+\alpha\frac{\mathcal{N}^{1,-}_\alpha}{\mathcal{N}^{1,+}_\alpha}\left|C^{1,+}_\alpha\right\rangle, \qquad \text{(B.4)}
\end{aligned}$$

whose Hermitian conjugates are

$$\begin{aligned}
\left\langle C^{0,+}_\alpha\right|\hat{a}^\dagger &= \alpha\frac{\mathcal{N}^{0,+}_\alpha}{\mathcal{N}^{0,-}_\alpha}\left\langle C^{0,-}_\alpha\right|, \qquad \text{(B.5)}\\
\left\langle C^{0,-}_\alpha\right|\hat{a}^\dagger &= \alpha\frac{\mathcal{N}^{0,-}_\alpha}{\mathcal{N}^{0,+}_\alpha}\left\langle C^{0,+}_\alpha\right|, \qquad \text{(B.6)}\\
\left\langle C^{1,+}_\alpha\right|\hat{a}^\dagger &= \frac{\mathcal{N}^{1,+}_\alpha}{\mathcal{N}^{0,-}_\alpha}\left\langle C^{0,-}_\alpha\right|+\alpha\frac{\mathcal{N}^{1,+}_\alpha}{\mathcal{N}^{1,-}_\alpha}\left\langle C^{1,-}_\alpha\right|, \qquad \text{(B.7)}\\
\left\langle C^{1,-}_\alpha\right|\hat{a}^\dagger &= \frac{\mathcal{N}^{1,-}_\alpha}{\mathcal{N}^{0,+}_\alpha}\left\langle C^{0,+}_\alpha\right|+\alpha\frac{\mathcal{N}^{1,-}_\alpha}{\mathcal{N}^{1,+}_\alpha}\left\langle C^{1,+}_\alpha\right|. \qquad \text{(B.8)}
\end{aligned}$$

Note that the action of $\hat{a}^\dagger$ and $\hat{a}$ changes the excitation-number parity and that any two states with different parities are orthogonal to each other. We calculate $\hat{A}_1^{\mathrm{R}}(0)$ as

$$
\begin{aligned}
\hat{A}_1^{\mathrm{R}}(0) \approx & \sum_{\substack{j,k=0 \\ \epsilon_k^{\mathrm{R}}-\epsilon_j^{\mathrm{R}}=0}}^{3} \left\langle \psi_j^{\mathrm{R}} \middle| \hat{A}_1^{\mathrm{R}} \middle| \psi_k^{\mathrm{R}} \right\rangle \left| \psi_j^{\mathrm{R}} \middle\rangle\middle\langle \psi_k^{\mathrm{R}} \right| \\
\approx & \left\langle C_\alpha^{0,-} \middle| (\hat{a}^\dagger + \hat{a}) \middle| C_\alpha^{0,+} \right\rangle \left| C_\alpha^{0,-} \middle\rangle\middle\langle C_\alpha^{0,+} \right| + \left\langle C_\alpha^{0,+} \middle| (\hat{a}^\dagger + \hat{a}) \middle| C_\alpha^{0,-} \right\rangle \left| C_\alpha^{0,+} \middle\rangle\middle\langle C_\alpha^{0,-} \right| \\
& + \left\langle C_\alpha^{1,-} \middle| (\hat{a}^\dagger + \hat{a}) \middle| C_\alpha^{1,+} \right\rangle \left| C_\alpha^{1,-} \middle\rangle\middle\langle C_\alpha^{1,+} \right| + \left\langle C_\alpha^{1,+} \middle| (\hat{a}^\dagger + \hat{a}) \middle| C_\alpha^{1,-} \right\rangle \left| C_\alpha^{1,+} \middle\rangle\middle\langle C_\alpha^{1,-} \right| \\
= & \left(\alpha \frac{\mathcal{N}_\alpha^{0,-}}{\mathcal{N}_\alpha^{0,+}} + \alpha \frac{\mathcal{N}_\alpha^{0,+}}{\mathcal{N}_\alpha^{0,-}} \right) \left| C_\alpha^{0,-} \middle\rangle\middle\langle C_\alpha^{0,+} \right| + \left(\alpha \frac{\mathcal{N}_\alpha^{0,+}}{\mathcal{N}_\alpha^{0,-}} + \alpha \frac{\mathcal{N}_\alpha^{0,-}}{\mathcal{N}_\alpha^{0,+}} \right) \left| C_\alpha^{0,+} \middle\rangle\middle\langle C_\alpha^{0,-} \right| \\
& + \left[\frac{\mathcal{N}_\alpha^{1,-}}{\mathcal{N}_\alpha^{0,+}} \left\langle C_\alpha^{0,+} \middle| C_\alpha^{1,+} \right\rangle + \alpha \frac{\mathcal{N}_\alpha^{1,-}}{\mathcal{N}_\alpha^{1,+}} + \frac{\mathcal{N}_\alpha^{1,+}}{\mathcal{N}_\alpha^{0,-}} \left\langle C_\alpha^{1,-} \middle| C_\alpha^{0,-} \right\rangle + \alpha \frac{\mathcal{N}_\alpha^{1,+}}{\mathcal{N}_\alpha^{1,-}} \right] \left| C_\alpha^{1,-} \middle\rangle\middle\langle C_\alpha^{1,+} \right| \\
& + \left[\frac{\mathcal{N}_\alpha^{1,+}}{\mathcal{N}_\alpha^{0,-}} \left\langle C_\alpha^{0,-} \middle| C_\alpha^{1,-} \right\rangle + \alpha \frac{\mathcal{N}_\alpha^{1,+}}{\mathcal{N}_\alpha^{1,-}} + \frac{\mathcal{N}_\alpha^{1,-}}{\mathcal{N}_\alpha^{0,+}} \left\langle C_\alpha^{1,+} \middle| C_\alpha^{0,+} \right\rangle + \alpha \frac{\mathcal{N}_\alpha^{1,-}}{\mathcal{N}_\alpha^{1,+}} \right] \left| C_\alpha^{1,+} \middle\rangle\middle\langle C_\alpha^{1,-} \right| \\
= & \sum_{n=0}^{1} \alpha \frac{(\mathcal{N}_\alpha^{n,+})^2 + (\mathcal{N}_\alpha^{n,-})^2}{\mathcal{N}_\alpha^{n,+}\mathcal{N}_\alpha^{n,-}} \left(\left| C_\alpha^{n,-} \middle\rangle\middle\langle C_\alpha^{n,+} \right| + \left| C_\alpha^{n,+} \middle\rangle\middle\langle C_\alpha^{n,-} \right| \right) \\
& + \left[2\mathcal{N}_\alpha^{1,-}\mathcal{N}_\alpha^{1,+} D_{0,1}(2\alpha) + 2\mathcal{N}_\alpha^{1,-}\mathcal{N}_\alpha^{1,+} D_{1,0}(2\alpha) \right] \left| C_\alpha^{1,-} \middle\rangle\middle\langle C_\alpha^{1,+} \right| \\
& + \left[-2\mathcal{N}_\alpha^{1,-}\mathcal{N}_\alpha^{1,+} D_{0,1}(2\alpha) - 2\mathcal{N}_\alpha^{1,-}\mathcal{N}_\alpha^{1,+} D_{1,0}(2\alpha) \right] \left| C_\alpha^{1,+} \middle\rangle\middle\langle C_\alpha^{1,-} \right| \\
= & \sum_{n=0}^{1} \alpha \frac{(\mathcal{N}_\alpha^{n,+})^2 + (\mathcal{N}_\alpha^{n,-})^2}{\mathcal{N}_\alpha^{n,+}\mathcal{N}_\alpha^{n,-}} \left(\left| C_\alpha^{n,-} \middle\rangle\middle\langle C_\alpha^{n,+} \right| + \left| C_\alpha^{n,+} \middle\rangle\middle\langle C_\alpha^{n,-} \right| \right), \qquad \text{(B.9)}
\end{aligned}
$$

where in the third equality we have used Eqs. (B.1)-(B.8), in the fourth equality we have used Eq. (3.57) and in the last equality we have used Eq. (3.58). In a similar way, we have

$$
\begin{aligned}
\hat{A}_2^{\mathrm{R}}(0) \approx & \mathrm{i}\alpha \frac{(\mathcal{N}_\alpha^{0,+})^2 - (\mathcal{N}_\alpha^{0,-})^2}{\mathcal{N}_\alpha^{0,+}\mathcal{N}_\alpha^{0,-}} \left(\left| C_\alpha^{0,+} \middle\rangle\middle\langle C_\alpha^{0,-} \right| - \left| C_\alpha^{0,-} \middle\rangle\middle\langle C_\alpha^{0,+} \right| \right) \\
& + \mathrm{i} \left[4\mathcal{N}_\alpha^{1,-}\mathcal{N}_\alpha^{1,+} D_{1,0}(2\alpha) + \alpha \frac{(\mathcal{N}_\alpha^{1,+})^2 - (\mathcal{N}_\alpha^{1,-})^2}{\mathcal{N}_\alpha^{1,+}\mathcal{N}_\alpha^{1,-}} \right] \left(\left| C_\alpha^{1,+} \middle\rangle\middle\langle C_\alpha^{1,-} \right| - \left| C_\alpha^{1,-} \middle\rangle\middle\langle C_\alpha^{1,+} \right| \right). \qquad \text{(B.10)}
\end{aligned}
$$

Note that $\hat{A}_{\bar{\alpha}}^{\mathrm{R}\dagger}(0) = \hat{A}_{\bar{\alpha}}^{\mathrm{R}}(0)$ holds. Then, let us calculate $\hat{A}_{\bar{\alpha}}^{\mathrm{R}}(\pm 2p)$ as

$$
\begin{aligned}
\hat{A}_1^{\mathrm{R}}(2p) \approx & \sum_{\substack{j,k=0 \\ \epsilon_k^{\mathrm{R}}-\epsilon_j^{\mathrm{R}}=2\hbar p}}^{3} \left\langle \psi_j^{\mathrm{R}} \middle| \hat{A}_1^{\mathrm{R}} \middle| \psi_k^{\mathrm{R}} \right\rangle \left| \psi_j^{\mathrm{R}} \middle\rangle\middle\langle \psi_k^{\mathrm{R}} \right| \\
\approx & \left\langle C_\alpha^{1,-} \middle| (\hat{a}^\dagger + \hat{a}) \middle| C_\alpha^{0,+} \right\rangle \left| C_\alpha^{1,-} \middle\rangle\middle\langle C_\alpha^{0,+} \right| + \left\langle C_\alpha^{1,+} \middle| (\hat{a}^\dagger + \hat{a}) \middle| C_\alpha^{0,-} \right\rangle \left| C_\alpha^{1,+} \middle\rangle\middle\langle C_\alpha^{0,-} \right| \\
= & \left[\frac{\mathcal{N}_\alpha^{1,-}}{\mathcal{N}_\alpha^{0,+}} + \alpha \frac{\mathcal{N}_\alpha^{1,-}}{\mathcal{N}_\alpha^{1,+}} \left\langle C_\alpha^{1,+} \middle| C_\alpha^{0,+} \right\rangle + \alpha \frac{\mathcal{N}_\alpha^{0,+}}{\mathcal{N}_\alpha^{0,-}} \left\langle C_\alpha^{1,-} \middle| C_\alpha^{0,-} \right\rangle \right] \left| C_\alpha^{1,-} \middle\rangle\middle\langle C_\alpha^{0,+} \right| \\
& + \left[\frac{\mathcal{N}_\alpha^{1,+}}{\mathcal{N}_\alpha^{0,-}} + \alpha \frac{\mathcal{N}_\alpha^{1,+}}{\mathcal{N}_\alpha^{1,-}} \left\langle C_\alpha^{1,-} \middle| C_\alpha^{0,-} \right\rangle + \alpha \frac{\mathcal{N}_\alpha^{0,-}}{\mathcal{N}_\alpha^{0,+}} \left\langle C_\alpha^{1,+} \middle| C_\alpha^{0,+} \right\rangle \right] \left| C_\alpha^{1,+} \middle\rangle\middle\langle C_\alpha^{0,-} \right| \\
= & \left[\frac{\mathcal{N}_\alpha^{1,-}}{\mathcal{N}_\alpha^{0,+}} - 2\alpha\mathcal{N}_\alpha^{1,-}\mathcal{N}_\alpha^{0,+} D_{1,0}(2\alpha) + 2\alpha\mathcal{N}_\alpha^{1,-}\mathcal{N}_\alpha^{0,+} D_{1,0}(2\alpha) \right] \left| C_\alpha^{1,-} \middle\rangle\middle\langle C_\alpha^{0,+} \right| \\
& + \left[\frac{\mathcal{N}_\alpha^{1,+}}{\mathcal{N}_\alpha^{0,-}} + 2\alpha\mathcal{N}_\alpha^{1,+}\mathcal{N}_\alpha^{0,-} D_{1,0}(2\alpha) - 2\alpha\mathcal{N}_\alpha^{1,+}\mathcal{N}_\alpha^{0,-} D_{1,0}(2\alpha) \right] \left| C_\alpha^{1,+} \middle\rangle\middle\langle C_\alpha^{0,-} \right|
\end{aligned}
$$

$$= \frac{\mathcal{N}_\alpha^{1,-}}{\mathcal{N}_\alpha^{0,+}} \left|C_\alpha^{1,-}\right\rangle\!\left\langle C_\alpha^{0,+}\right| + \frac{\mathcal{N}_\alpha^{1,+}}{\mathcal{N}_\alpha^{0,-}} \left|C_\alpha^{1,+}\right\rangle\!\left\langle C_\alpha^{0,-}\right|, \tag{B.11}$$

$$\begin{aligned}\hat{A}_2^{\mathrm{R}}(2p) &\approx \mathrm{i}\left[\frac{\mathcal{N}_\alpha^{1,-}}{\mathcal{N}_\alpha^{0,+}} - 4\alpha\mathcal{N}_\alpha^{1,-}\mathcal{N}_\alpha^{0,+}D_{1,0}(2\alpha)\right]\left|C_\alpha^{1,-}\right\rangle\!\left\langle C_\alpha^{0,+}\right| \\ &\quad + \mathrm{i}\left[\frac{\mathcal{N}_\alpha^{1,+}}{\mathcal{N}_\alpha^{0,-}} + 4\alpha\mathcal{N}_\alpha^{1,+}\mathcal{N}_\alpha^{0,-}D_{1,0}(2\alpha)\right]\left|C_\alpha^{1,+}\right\rangle\!\left\langle C_\alpha^{0,-}\right|,\end{aligned} \tag{B.12}$$

$$\begin{aligned}\hat{A}_1^{\mathrm{R}}(-2p) &\approx \sum_{\substack{j,k=0 \\ \epsilon_k^{\mathrm{R}}-\epsilon_j^{\mathrm{R}}=-2\hbar p}}^{3} \left\langle\psi_j^{\mathrm{R}}\right|\hat{A}_1^{\mathrm{R}}\left|\psi_k^{\mathrm{R}}\right\rangle \left|\psi_j^{\mathrm{R}}\right\rangle\!\left\langle\psi_k^{\mathrm{R}}\right| \\ &\approx \left\langle C_\alpha^{0,-}\right|(\hat{a}^\dagger+\hat{a})\left|C_\alpha^{1,+}\right\rangle \left|C_\alpha^{0,-}\right\rangle\!\left\langle C_\alpha^{1,+}\right| + \left\langle C_\alpha^{0,+}\right|(\hat{a}^\dagger+\hat{a})\left|C_\alpha^{1,-}\right\rangle \left|C_\alpha^{0,+}\right\rangle\!\left\langle C_\alpha^{1,-}\right| \\ &= \left[\alpha\frac{\mathcal{N}_\alpha^{0,-}}{\mathcal{N}_\alpha^{0,+}}\left\langle C_\alpha^{0,+}\middle|C_\alpha^{1,+}\right\rangle + \frac{\mathcal{N}_\alpha^{1,+}}{\mathcal{N}_\alpha^{0,-}} + \alpha\frac{\mathcal{N}_\alpha^{1,+}}{\mathcal{N}_\alpha^{1,-}}\left\langle C_\alpha^{0,-}\middle|C_\alpha^{1,-}\right\rangle\right]\left|C_\alpha^{0,-}\right\rangle\!\left\langle C_\alpha^{1,+}\right| \\ &\quad + \left[\alpha\frac{\mathcal{N}_\alpha^{0,+}}{\mathcal{N}_\alpha^{0,-}}\left\langle C_\alpha^{0,-}\middle|C_\alpha^{1,-}\right\rangle + \frac{\mathcal{N}_\alpha^{1,-}}{\mathcal{N}_\alpha^{0,+}} + \alpha\frac{\mathcal{N}_\alpha^{1,-}}{\mathcal{N}_\alpha^{1,+}}\left\langle C_\alpha^{0,+}\middle|C_\alpha^{1,+}\right\rangle\right]\left|C_\alpha^{0,+}\right\rangle\!\left\langle C_\alpha^{1,-}\right| \\ &= \left[-2\alpha\mathcal{N}_\alpha^{1,+}\mathcal{N}_\alpha^{0,-}D_{1,0}(2\alpha) + \frac{\mathcal{N}_\alpha^{1,+}}{\mathcal{N}_\alpha^{0,-}} + 2\alpha\mathcal{N}_\alpha^{1,+}\mathcal{N}_\alpha^{0,-}D_{1,0}(2\alpha)\right]\left|C_\alpha^{0,-}\right\rangle\!\left\langle C_\alpha^{1,+}\right| \\ &\quad + \left[2\alpha\mathcal{N}_\alpha^{1,-}\mathcal{N}_\alpha^{0,+}D_{1,0}(2\alpha) + \frac{\mathcal{N}_\alpha^{1,-}}{\mathcal{N}_\alpha^{0,+}} - 2\alpha\mathcal{N}_\alpha^{1,-}\mathcal{N}_\alpha^{0,+}\right]\left|C_\alpha^{0,+}\right\rangle\!\left\langle C_\alpha^{1,-}\right| \\ &= \frac{\mathcal{N}_\alpha^{1,+}}{\mathcal{N}_\alpha^{0,-}}\left|C_\alpha^{0,-}\right\rangle\!\left\langle C_\alpha^{1,+}\right| + \frac{\mathcal{N}_\alpha^{1,-}}{\mathcal{N}_\alpha^{0,+}}\left|C_\alpha^{0,+}\right\rangle\!\left\langle C_\alpha^{1,-}\right|,\end{aligned} \tag{B.13}$$

$$\begin{aligned}\hat{A}_2^{\mathrm{R}}(-2p) &\approx -\mathrm{i}\left[\frac{\mathcal{N}_\alpha^{1,+}}{\mathcal{N}_\alpha^{0,-}} + 4\alpha\mathcal{N}_\alpha^{1,+}\mathcal{N}_\alpha^{0,-}D_{1,0}(2\alpha)\right]\left|C_\alpha^{0,-}\right\rangle\!\left\langle C_\alpha^{1,+}\right| \\ &\quad - \mathrm{i}\left[\frac{\mathcal{N}_\alpha^{1,-}}{\mathcal{N}_\alpha^{0,+}} - 4\alpha\mathcal{N}_\alpha^{1,-}\mathcal{N}_\alpha^{0,+}D_{1,0}(2\alpha)\right]\left|C_\alpha^{0,+}\right\rangle\!\left\langle C_\alpha^{1,-}\right|.\end{aligned} \tag{B.14}$$

Note that $\hat{A}_{\bar{\alpha}}^{\mathrm{R}\dagger}(\pm 2p) = \hat{A}_{\bar{\alpha}}^{\mathrm{R}}(\mp 2p)$ holds.

Substituting $\omega_A = 0, \pm 2p$ into $\gamma_{\bar{\alpha},\bar{\beta}}^{\mathrm{R}}(\omega_A)$ in Eqs. (4.33) and (4.34), we obtain

$$\gamma_{1,1}^{\mathrm{R}}(0) = \Gamma\left(\frac{\omega_p}{2}\right)\left[\bar{n}\left(\frac{\omega_p}{2}\right) + \frac{1}{2}\right], \tag{B.15}$$

$$\gamma_{1,1}^{\mathrm{R}}(2p) = \frac{1}{2}\Gamma\left(\frac{\omega_p}{2}+2p\right)\left[\bar{n}\left(\frac{\omega_p}{2}+2p\right)+1\right] + \frac{1}{2}\Gamma\left(\frac{\omega_p}{2}-2p\right)\bar{n}\left(\frac{\omega_p}{2}-2p\right), \tag{B.16}$$

$$\gamma_{1,1}^{\mathrm{R}}(-2p) = \frac{1}{2}\Gamma\left(\frac{\omega_p}{2}-2p\right)\left[\bar{n}\left(\frac{\omega_p}{2}-2p\right)+1\right] + \frac{1}{2}\Gamma\left(\frac{\omega_p}{2}+2p\right)\bar{n}\left(\frac{\omega_p}{2}+2p\right), \tag{B.17}$$

$$\gamma_{1,2}^{\mathrm{R}}(0) = \frac{\mathrm{i}}{2}\Gamma\left(\frac{\omega_p}{2}\right), \tag{B.18}$$

$$\gamma_{1,2}^{\mathrm{R}}(2p) = \frac{\mathrm{i}}{2}\Gamma\left(\frac{\omega_p}{2}+2p\right)\left[\bar{n}\left(\frac{\omega_p}{2}+2p\right)+1\right] - \frac{\mathrm{i}}{2}\Gamma\left(\frac{\omega_p}{2}-2p\right)\bar{n}\left(\frac{\omega_p}{2}-2p\right), \tag{B.19}$$

$$\gamma_{1,2}^{\mathrm{R}}(-2p) = \frac{\mathrm{i}}{2}\Gamma\left(\frac{\omega_p}{2}-2p\right)\left[\bar{n}\left(\frac{\omega_p}{2}-2p\right)+1\right] - \frac{\mathrm{i}}{2}\Gamma\left(\frac{\omega_p}{2}+2p\right)\bar{n}\left(\frac{\omega_p}{2}+2p\right). \tag{B.20}$$

Hereafter we approximate $\mathrm{e}^{-2\alpha^2} \approx 0$ because we assume $\alpha \gg 1$; for example, $\mathrm{e}^{-2\times 5^2} \approx 2\times 10^{-22}$. Then we have

$$\mathcal{N}_\alpha^{n,\pm} \approx \frac{1}{\sqrt{2}}, \tag{B.21}$$

$$\left|C_\alpha^{n,\pm}\right\rangle \approx \frac{1}{\sqrt{2}}[\hat{D}(\alpha) \pm (-1)^n \hat{D}(-\alpha)]\,|n\rangle\,, \tag{B.22}$$

$$\left\langle C_\alpha^{m,\pm}\middle|C_\alpha^{n,\pm}\right\rangle \approx \delta_{m,n}, \tag{B.23}$$

$$D_{m,n}(2\alpha) \approx 0, \tag{B.24}$$

$$\hat{A}_1^{\mathrm{R}}(0) \approx \sum_{n=0}^{1} 2\alpha \left(\left|C_\alpha^{n,-}\middle\rangle\middle\langle C_\alpha^{n,+}\right| + \left|C_\alpha^{n,+}\middle\rangle\middle\langle C_\alpha^{n,-}\right|\right), \tag{B.25}$$

$$\hat{A}_2^{\mathrm{R}}(0) \approx 0, \tag{B.26}$$

$$\hat{A}_1^{\mathrm{R}}(2p) \approx \left|C_\alpha^{1,-}\middle\rangle\middle\langle C_\alpha^{0,+}\right| + \left|C_\alpha^{1,+}\middle\rangle\middle\langle C_\alpha^{0,-}\right|, \tag{B.27}$$

$$\hat{A}_2^{\mathrm{R}}(2p) \approx \mathrm{i}\left(\left|C_\alpha^{1,-}\middle\rangle\middle\langle C_\alpha^{0,+}\right| + \left|C_\alpha^{1,+}\middle\rangle\middle\langle C_\alpha^{0,-}\right|\right), \tag{B.28}$$

$$\hat{A}_1^{\mathrm{R}}(-2p) \approx \left|C_\alpha^{0,-}\middle\rangle\middle\langle C_\alpha^{1,+}\right| + \left|C_\alpha^{0,+}\middle\rangle\middle\langle C_\alpha^{1,-}\right|, \tag{B.29}$$

$$\hat{A}_2^{\mathrm{R}}(-2p) \approx -\mathrm{i}\left(\left|C_\alpha^{0,-}\middle\rangle\middle\langle C_\alpha^{1,+}\right| + \left|C_\alpha^{0,+}\middle\rangle\middle\langle C_\alpha^{1,-}\right|\right). \tag{B.30}$$

Note that $\hat{A}_2^{\mathrm{R}}(2p) = \mathrm{i}\hat{A}_1^{\mathrm{R}}(2p)$ and $\hat{A}_2^{\mathrm{R}}(-2p) = -\mathrm{i}\hat{A}_1^{\mathrm{R}}(-2p)$ holds. We finally arrive at the following form of the decoherence part in Eq. (4.49):

$$\begin{aligned}
\mathcal{D}^{\mathrm{ours}}[\hat{\rho}_A^{\mathrm{R}}(t)] &\approx \sum_{\omega_A=0,\pm 2p}\sum_{\bar{\alpha},\bar{\beta}=1}^{2} \gamma_{\bar{\alpha},\bar{\beta}}^{\mathrm{R}}(\omega_A)\left(\hat{A}_{\bar{\beta}}^{\mathrm{R}}(\omega_A)\hat{\rho}_A^{\mathrm{R}}(t)\hat{A}_{\bar{\alpha}}^{\mathrm{R}\dagger}(\omega_A) - \frac{1}{2}\{\hat{A}_{\bar{\alpha}}^{\mathrm{R}\dagger}(\omega_A)\hat{A}_{\bar{\beta}}^{\mathrm{R}}(\omega_A), \hat{\rho}_A^{\mathrm{R}}(t)\}\right) \\
&= \gamma_{1,1}^{\mathrm{R}}(0)\left(\hat{A}_1^{\mathrm{R}}(0)\hat{\rho}_A^{\mathrm{R}}(t)\hat{A}_1^{\mathrm{R}\dagger}(0) - \frac{1}{2}\{(\hat{A}_1^{\mathrm{R}\dagger}(0)\hat{A}_1^{\mathrm{R}}(0), \hat{\rho}_A^{\mathrm{R}}(t)\}\right) \\
&\quad + \gamma_{1,1}^{\mathrm{R}}(2p)\left(\hat{A}_1^{\mathrm{R}}(2p)\hat{\rho}_A^{\mathrm{R}}(t)\hat{A}_1^{\mathrm{R}\dagger}(2p) - \frac{1}{2}\{\hat{A}_1^{\mathrm{R}\dagger}(2p)\hat{A}_1^{\mathrm{R}}(2p), \hat{\rho}_A^{\mathrm{R}}(t)\}\right) \\
&\quad + \gamma_{1,2}^{\mathrm{R}}(2p)\left(\hat{A}_2^{\mathrm{R}}(2p)\hat{\rho}_A^{\mathrm{R}}(t)\hat{A}_1^{\mathrm{R}\dagger}(2p) - \frac{1}{2}\{\hat{A}_1^{\mathrm{R}\dagger}(2p)\hat{A}_2^{\mathrm{R}}(2p), \hat{\rho}_A^{\mathrm{R}}(t)\}\right) \\
&\quad + \gamma_{2,1}^{\mathrm{R}}(2p)\left(\hat{A}_1^{\mathrm{R}}(2p)\hat{\rho}_A^{\mathrm{R}}(t)\hat{A}_2^{\mathrm{R}\dagger}(2p) - \frac{1}{2}\{\hat{A}_2^{\mathrm{R}\dagger}(2p)\hat{A}_1^{\mathrm{R}}(2p), \hat{\rho}_A^{\mathrm{R}}(t)\}\right) \\
&\quad + \gamma_{2,2}^{\mathrm{R}}(2p)\left(\hat{A}_2^{\mathrm{R}}(2p)\hat{\rho}_A^{\mathrm{R}}(t)\hat{A}_2^{\mathrm{R}\dagger}(2p) - \frac{1}{2}\{\hat{A}_2^{\mathrm{R}\dagger}(2p)\hat{A}_2^{\mathrm{R}}(2p), \hat{\rho}_A^{\mathrm{R}}(t)\}\right) \\
&\quad + \gamma_{1,1}^{\mathrm{R}}(-2p)\left(\hat{A}_1^{\mathrm{R}}(-2p)\hat{\rho}_A^{\mathrm{R}}(t)\hat{A}_1^{\mathrm{R}\dagger}(-2p) - \frac{1}{2}\{\hat{A}_1^{\mathrm{R}\dagger}(-2p)\hat{A}_1^{\mathrm{R}}(-2p), \hat{\rho}_A^{\mathrm{R}}(t)\}\right) \\
&\quad + \gamma_{1,2}^{\mathrm{R}}(-2p)\left(\hat{A}_2^{\mathrm{R}}(-2p)\hat{\rho}_A^{\mathrm{R}}(t)\hat{A}_1^{\mathrm{R}\dagger}(-2p) - \frac{1}{2}\{\hat{A}_1^{\mathrm{R}\dagger}(-2p)\hat{A}_2^{\mathrm{R}}(-2p), \hat{\rho}_A^{\mathrm{R}}(t)\}\right) \\
&\quad + \gamma_{2,1}^{\mathrm{R}}(-2p)\left(\hat{A}_1^{\mathrm{R}}(-2p)\hat{\rho}_A^{\mathrm{R}}(t)\hat{A}_2^{\mathrm{R}\dagger}(-2p) - \frac{1}{2}\{\hat{A}_2^{\mathrm{R}\dagger}(-2p)\hat{A}_1^{\mathrm{R}}(-2p), \hat{\rho}_A^{\mathrm{R}}(t)\}\right) \\
&\quad + \gamma_{2,2}^{\mathrm{R}}(-2p)\left(\hat{A}_2^{\mathrm{R}}(-2p)\hat{\rho}_A^{\mathrm{R}}(t)\hat{A}_2^{\mathrm{R}\dagger}(-2p) - \frac{1}{2}\{\hat{A}_2^{\mathrm{R}\dagger}(-2p)\hat{A}_2^{\mathrm{R}}(-2p), \hat{\rho}_A^{\mathrm{R}}(t)\}\right) \\
&= \gamma_{1,1}^{\mathrm{R}}(0)\left(\hat{A}_1^{\mathrm{R}}(0)\hat{\rho}_A^{\mathrm{R}}(t)\hat{A}_1^{\mathrm{R}\dagger}(0) - \frac{1}{2}\{(\hat{A}_1^{\mathrm{R}\dagger}(0)\hat{A}_1^{\mathrm{R}}(0), \hat{\rho}_A^{\mathrm{R}}(t)\}\right) \\
&\quad + [\gamma_{1,1}^{\mathrm{R}}(2p) + \mathrm{i}\gamma_{1,2}^{\mathrm{R}}(2p) - \mathrm{i}\gamma_{2,1}^{\mathrm{R}}(2p) + \gamma_{2,2}^{\mathrm{R}}(2p)] \\
&\quad \times \left(\hat{A}_1^{\mathrm{R}}(2p)\hat{\rho}_A^{\mathrm{R}}(t)\hat{A}_1^{\mathrm{R}\dagger}(2p) - \frac{1}{2}\{\hat{A}_1^{\mathrm{R}\dagger}(2p)\hat{A}_1^{\mathrm{R}}(2p), \hat{\rho}_A^{\mathrm{R}}(t)\}\right) \\
&\quad + [\gamma_{1,1}^{\mathrm{R}}(-2p) - \mathrm{i}\gamma_{1,2}^{\mathrm{R}}(-2p) + \mathrm{i}\gamma_{2,1}^{\mathrm{R}}(-2p) + \gamma_{2,2}^{\mathrm{R}}(-2p)] \\
&\quad \times \left(\hat{A}_1^{\mathrm{R}}(-2p)\hat{\rho}_A^{\mathrm{R}}(t)\hat{A}_1^{\mathrm{R}\dagger}(-2p) - \frac{1}{2}\{\hat{A}_1^{\mathrm{R}\dagger}(-2p)\hat{A}_1^{\mathrm{R}}(-2p), \hat{\rho}_A^{\mathrm{R}}(t)\}\right) \\
&= \gamma_{1,1}^{\mathrm{R}}(0)\left(\hat{A}_1^{\mathrm{R}}(0)\hat{\rho}_A^{\mathrm{R}}(t)\hat{A}_1^{\mathrm{R}\dagger}(0) - \frac{1}{2}\{(\hat{A}_1^{\mathrm{R}\dagger}(0)\hat{A}_1^{\mathrm{R}}(0), \hat{\rho}_A^{\mathrm{R}}(t)\}\right)
\end{aligned}$$

$$
\begin{aligned}
&+ 2[\gamma^{\mathrm{R}}_{1,1}(2p) + \mathrm{i}\gamma^{\mathrm{R}}_{1,2}(2p)] \\
&\times \left(\hat{A}^{\mathrm{R}}_1(2p)\hat{\rho}^{\mathrm{R}}_A(t)\hat{A}^{\mathrm{R}\dagger}_1(2p) - \frac{1}{2}\{\hat{A}^{\mathrm{R}\dagger}_1(2p)\hat{A}^{\mathrm{R}}_1(2p), \hat{\rho}^{\mathrm{R}}_A(t)\} \right) \\
&+ 2[\gamma^{\mathrm{R}}_{1,1}(-2p) - \mathrm{i}\gamma^{\mathrm{R}}_{1,2}(-2p)] \\
&\times \left(\hat{A}^{\mathrm{R}}_1(-2p)\hat{\rho}^{\mathrm{R}}_A(t)\hat{A}^{\mathrm{R}\dagger}_1(-2p) - \frac{1}{2}\{\hat{A}^{\mathrm{R}\dagger}_1(-2p)\hat{A}^{\mathrm{R}}_1(-2p), \hat{\rho}^{\mathrm{R}}_A(t)\} \right) \\
= \Gamma &\left(\frac{\omega_p}{2} \right) \left[\bar{n}\left(\frac{\omega_p}{2} \right) + \frac{1}{2} \right] \left(\hat{A}^{\mathrm{R}}_1(0)\hat{\rho}^{\mathrm{R}}_A(t)\hat{A}^{\mathrm{R}\dagger}_1(0) - \frac{1}{2}\{(\hat{A}^{\mathrm{R}\dagger}_1(0)\hat{A}^{\mathrm{R}}_1(0), \hat{\rho}^{\mathrm{R}}_A(t)\} \right) \\
&+ 2\Gamma\left(\frac{\omega_p}{2} - 2p \right) \bar{n}\left(\frac{\omega_p}{2} - 2p \right) \\
&\times \left(\hat{A}^{\mathrm{R}}_1(2p)\hat{\rho}^{\mathrm{R}}_A(t)\hat{A}^{\mathrm{R}\dagger}_1(2p) - \frac{1}{2}\{\hat{A}^{\mathrm{R}\dagger}_1(2p)\hat{A}^{\mathrm{R}}_1(2p), \hat{\rho}^{\mathrm{R}}_A(t)\} \right) \\
&+ 2\Gamma\left(\frac{\omega_p}{2} - 2p \right) \left[\bar{n}\left(\frac{\omega_p}{2} - 2p \right) + 1 \right] \\
&\times \left(\hat{A}^{\mathrm{R}}_1(-2p)\hat{\rho}^{\mathrm{R}}_A(t)\hat{A}^{\mathrm{R}\dagger}_1(-2p) - \frac{1}{2}\{\hat{A}^{\mathrm{R}\dagger}_1(-2p)\hat{A}^{\mathrm{R}}_1(-2p), \hat{\rho}^{\mathrm{R}}_A(t)\} \right). \qquad \text{(B.31)}
\end{aligned}
$$

Appendix C

Calculations of Z_A in Eq. (5.25) and $\sigma_{1,1}(0)$ in Eq. (5.34)

We calculate Z_A in Eq. (5.25) as in

$$\begin{aligned} Z_A &= \mathrm{Tr}\left[\mathrm{e}^{-\beta_A^0 \hat{H}_A}\right] \\ &= \mathrm{Tr}\left[\exp\left[-\beta_A^0 \hbar\omega_1 \left(\hat{a}_1^\dagger \hat{a}_1 + \frac{1}{2}\right)\right]\right] \\ &= \sum_{n=0}^{\infty} \exp\left[-\beta_A^0 \hbar\omega_1 \left(n + \frac{1}{2}\right)\right] \\ &= \frac{\mathrm{e}^{-\beta_A^0 \hbar\omega_1/2}}{1 - \mathrm{e}^{-\beta_A^0 \hbar\omega_1}} \\ &= \frac{1}{2\sinh(\beta_A^0 \hbar\omega_1/2)}. \end{aligned} \tag{C.1}$$

We calculate $\sigma_{1,1}(0)$ in Eq. (5.34) as in

$$\begin{aligned} \sigma_{1,1}(0) &= \mathrm{Tr}\left[\hat{\rho}(0)\{\hat{r}_1, \hat{r}_1\}\right] \\ &= \mathrm{Tr}\left[2\hat{\rho}_A(0)\hat{r}_1^2\right] \\ &= \mathrm{Tr}\left[\frac{\exp\left[-\beta_A^0 \hbar\omega_1 \left(\hat{a}_1^\dagger \hat{a}_1 + \frac{1}{2}\right)\right]}{Z_A}(2\hat{a}_1^\dagger \hat{a}_1 + 1 + \hat{a}_1^{\dagger 2} + \hat{a}_1^2)\right] \\ &= \frac{2}{Z_A}\sum_{n=0}^{\infty}\left(n + \frac{1}{2}\right)\exp\left[-\beta_A^0 \hbar\omega_1 \left(n + \frac{1}{2}\right)\right] \\ &= -\frac{2}{Z_A}\sum_{n=0}^{\infty}\frac{\partial}{\partial x}\exp\left[-x\left(n + \frac{1}{2}\right)\right]\Big|_{x=\beta_A^0\hbar\omega_1} \\ &= -2\,\frac{\partial}{\partial x}\log\left[\sum_{n=0}^{\infty}\exp\left[-x\left(n + \frac{1}{2}\right)\right]\right]\Big|_{x=\beta_A^0\hbar\omega_1} \\ &= 2\,\frac{\partial}{\partial x}\log\left[2\sinh(x/2)\right]\Big|_{x=\beta_A^0\hbar\omega_1} \\ &= \coth\left(\frac{\hbar\omega_1}{2k_B T_A^0}\right). \end{aligned} \tag{C.2}$$

Appendix D

Derivation of Eq. (5.30)

In this Appendix, we derive Eq. (5.30) [16, Sec. 5.1.2]. The modified position and momentum operators introduced in Eq. (5.21) satisfy the canonical commutation relations:

$$[\hat{r}_j, \hat{r}_k] = \mathrm{i}\Omega_{j,k} \quad \text{for} \quad j,k = 1,\dots,2(N+1), \tag{D.1}$$

where Ω is given by Eq. (5.31). The total Hamiltonian in the Heisenberg picture is

$$\begin{aligned}\hat{H}^H(t) &= \sum_{j=1}^{N+1} \frac{\hbar\omega_j}{2}\left(\hat{r}^H_{2j-1}(t)^2 + \hat{r}^H_{2j}(t)^2\right) + \sum_{j=2}^{N+1} \hbar g_j \left(\hat{r}^H_1(t)\hat{r}^H_{2j-1}(t) + \hat{r}^H_2(t)\hat{r}^H_{2j}(t)\right) \\ &= \frac{\hbar}{2}\left(\hat{\mathbf{r}}^H(t)\right)^{\mathrm{T}} H \hat{\mathbf{r}}^H(t),\end{aligned} \tag{D.2}$$

where $\hat{r}^H_k(t) = \hat{U}^\dagger(t)\hat{r}_k\hat{U}(t)$ for $k = 1,\dots,N+1$ and

$$\hat{\mathbf{r}}^H(t) = \left(\hat{r}^H_1(t), \hat{r}^H_2(t), \dots, \hat{r}^H_{2N+1}(t), \hat{r}^H_{2N+2}(t)\right)^{\mathrm{T}}. \tag{D.3}$$

Then, the canonical commutation relations in the Heisenberg picture are written as

$$\left[\hat{r}^H_j(t), \hat{r}^H_k(t)\right] = \mathrm{i}\Omega_{j,k} \quad \text{for} \quad j,k = 1,\dots,2(N+1), \tag{D.4}$$

The Heisenberg equation of motion reads

$$\begin{aligned}\frac{\mathrm{d}}{\mathrm{d}t}\hat{r}^H_j(t) &= \frac{\mathrm{i}}{\hbar}\left[\hat{H}^H(t), \hat{r}^H_j(t)\right] = \frac{\mathrm{i}}{2}\sum_{k,l}\left[\hat{r}^H_k(t) H_{k,l} \hat{r}^H_l(t), \hat{r}^H_j(t)\right] \\ &= \frac{\mathrm{i}}{2}\sum_{k,l} H_{k,l}\left(\left[\hat{r}^H_k(t), \hat{r}^H_j(t)\right]\hat{r}^H_l(t) + \hat{r}^H_k(t)\left[\hat{r}^H_l(t), \hat{r}^H_j(t)\right]\right) \\ &= \frac{\mathrm{i}}{2}\sum_{k,l} H_{k,l}\left(\mathrm{i}\Omega_{k,j}\hat{r}^H_l(t) + \mathrm{i}\Omega_{l,j}\hat{r}^H_k(t)\right) \\ &= \frac{1}{2}\sum_{k,l}\left(\Omega_{j,k}H_{k,l}\hat{r}^H_l(t) + \Omega_{j,l}H_{l,k}\hat{r}^H_k(t)\right) \\ &= \sum_{k,l}\Omega_{j,k}H_{k,l}\hat{r}^H_l(t),\end{aligned} \tag{D.5}$$

where the fourth line follows from the symmetry of H and the anti-symmetry of Ω. We recast Eq. (D.5) in the vector form

$$\frac{\mathrm{d}}{\mathrm{d}t}\hat{\mathbf{r}}^H(t) = \Omega H \hat{\mathbf{r}}^H(t), \tag{D.6}$$

whose solution is

$$\hat{\mathbf{r}}^H(t) = V(t)\hat{\mathbf{r}} \quad \text{with} \quad V(t) = \mathrm{e}^{\Omega H t}. \tag{D.7}$$

We finally arrive at Eq. (5.30):

$$\sigma(t) = \mathrm{Tr}\left[\hat{\rho}(t)\left\{\hat{\mathbf{r}}, \hat{\mathbf{r}}^{\mathrm{T}}\right\}\right] = \mathrm{Tr}\left[\hat{\rho}(0)\left\{\hat{\mathbf{r}}^H(t), \left(\hat{\mathbf{r}}^H(t)\right)^{\mathrm{T}}\right\}\right] = V(t)\sigma(0)V(t)^{\mathrm{T}}. \tag{D.8}$$

Appendix E

Derivation of Eq. (5.36)

In this Appendix, we derive Eq. (5.36). The components of $\sigma_A(t)$ are written as

$$\sigma_{1,1}(t) = \mathrm{Tr}\left[2\hat{r}_1^2\hat{\rho}(t)\right], \tag{E.1}$$
$$\sigma_{2,2}(t) = \mathrm{Tr}\left[2\hat{r}_2^2\hat{\rho}(t)\right], \tag{E.2}$$
$$\sigma_{1,2}(t) = \sigma_{2,1}(t) = \mathrm{Tr}\left[(\hat{r}_1\hat{r}_2 + \hat{r}_2\hat{r}_1)\hat{\rho}(t)\right] \tag{E.3}$$

with

$$2\hat{r}_1^2 = 2\hat{a}_1^\dagger\hat{a}_1 + 1 + \hat{a}_1^{\dagger 2} + \hat{a}_1^2, \tag{E.4}$$
$$2\hat{r}_2^2 = 2\hat{a}_1^\dagger\hat{a}_1 + 1 - \hat{a}_1^{\dagger 2} - \hat{a}_1^2, \tag{E.5}$$
$$\hat{r}_1\hat{r}_2 + \hat{r}_2\hat{r}_1 = 2\mathrm{i}(\hat{a}_1^{\dagger 2} - \hat{a}_1^2). \tag{E.6}$$

Using the commutation relations

$$[\hat{a}_1, \hat{a}_1^\dagger] = 1, \tag{E.7}$$
$$[\hat{a}_1, \hat{a}_1] = [\hat{a}_1^\dagger, \hat{a}_1^\dagger] = 0, \tag{E.8}$$

we obtain

$$[\hat{a}_1^\dagger, 2\hat{r}_1^2] = -2\hat{a}_1^\dagger - 2\hat{a}_1, \tag{E.9}$$
$$[\hat{a}_1, 2\hat{r}_1^2] = 2\hat{a}_1^\dagger + 2\hat{a}_1, \tag{E.10}$$
$$[\hat{a}_1^\dagger\hat{a}_1, 2\hat{r}_1^2] = [\hat{a}_1\hat{a}_1^\dagger, 2\hat{r}_1^2] = 2\hat{a}_1^{\dagger 2} - 2\hat{a}_1^2, \tag{E.11}$$
$$[\hat{a}_1^\dagger, 2\hat{r}_2^2] = -2\hat{a}_1^\dagger + 2\hat{a}_1, \tag{E.12}$$
$$[\hat{a}_1, 2\hat{r}_2^2] = -2\hat{a}_1^\dagger + 2\hat{a}_1, \tag{E.13}$$
$$[\hat{a}_1^\dagger\hat{a}_1, 2\hat{r}_2^2] = [\hat{a}_1\hat{a}_1^\dagger, 2\hat{r}_2^2] = -2\hat{a}_1^{\dagger 2} + 2\hat{a}_1^2, \tag{E.14}$$
$$[\hat{a}_1^\dagger, \hat{r}_1\hat{r}_2 + \hat{r}_2\hat{r}_1] = 4\mathrm{i}\hat{a}_1, \tag{E.15}$$
$$[\hat{a}_1, \hat{r}_1\hat{r}_2 + \hat{r}_2\hat{r}_1] = 4\mathrm{i}\hat{a}_1^\dagger, \tag{E.16}$$
$$[\hat{a}_1^\dagger\hat{a}_1, \hat{r}_1\hat{r}_2 + \hat{r}_2\hat{r}_1] = [\hat{a}_1\hat{a}_1^\dagger, \hat{r}_1\hat{r}_2 + \hat{r}_2\hat{r}_1] = 4\mathrm{i}(\hat{a}_1^{\dagger 2} + \hat{a}_1^2). \tag{E.17}$$

Under the GKSL equation

$$\begin{aligned}\frac{\mathrm{d}}{\mathrm{d}t}\hat{\rho}_A(t) = {} & \Gamma(\bar{n}(\omega_1) + 1)\left(2\hat{a}_1\hat{\rho}_A(t)\hat{a}_1^\dagger - \left\{\hat{a}_1^\dagger\hat{a}_1, \hat{\rho}_A(t)\right\}\right) \\ & + \Gamma\bar{n}(\omega_1)\left(2\hat{a}_1^\dagger\hat{\rho}_A(t)\hat{a}_1 - \left\{\hat{a}_1\hat{a}_1^\dagger, \hat{\rho}_A(t)\right\}\right),\end{aligned} \tag{E.18}$$

the time derivative of $\sigma_{1,1}(t)$ is calculated as in

$$\begin{aligned}
\frac{\mathrm{d}}{\mathrm{d}t}\sigma_{1,1}(t) &= \mathrm{Tr}\left[2\hat{r}_1^2\frac{\mathrm{d}}{\mathrm{d}t}\hat{\rho}(t)\right] \\
&= \Gamma(\bar{n}(\omega_1)+1)\mathrm{Tr}\left[2\hat{r}_1^2\left(2\hat{a}_1\hat{\rho}_A(t)\hat{a}_1^\dagger - \left\{\hat{a}_1^\dagger\hat{a}_1, \hat{\rho}_A(t)\right\}\right)\right] \\
&\quad + \Gamma\bar{n}(\omega_1)\mathrm{Tr}\left[2\hat{r}_1^2\left(2\hat{a}_1^\dagger\hat{\rho}_A(t)\hat{a}_1 - \left\{\hat{a}_1\hat{a}_1^\dagger, \hat{\rho}_A(t)\right\}\right)\right] \\
&= \Gamma(\bar{n}(\omega_1)+1)\mathrm{Tr}\left[(-2\hat{a}_1^\dagger - 2\hat{a}_1)2\hat{a}_1\hat{\rho}_A(t) - (2\hat{a}_1^{\dagger 2} - 2\hat{a}_1^2)\hat{\rho}_A(t)\right] \\
&\quad + \Gamma\bar{n}(\omega_1)\mathrm{Tr}\left[(2\hat{a}_1^\dagger + 2\hat{a}_1)2\hat{a}_1^\dagger\hat{\rho}_A(t) - (2\hat{a}_1^{\dagger 2} - 2\hat{a}_1^2)\hat{\rho}_A(t)\right] \\
&= -2\Gamma(\bar{n}(\omega_1)+1)\mathrm{Tr}\left[(2\hat{r}_1^2-1)\hat{\rho}(t)\right] + 2\Gamma\bar{n}(\omega_1)\mathrm{Tr}\left[(2\hat{r}_1^2+1)\hat{\rho}(t)\right] \\
&= -2\Gamma\mathrm{Tr}\left[2\hat{r}_1^2\hat{\rho}(t)\right] + 2\Gamma[2\bar{n}(\omega_1)+1] \\
&= -2\Gamma\left[\sigma_{1,1}(t) - \coth\left(\frac{\hbar\omega_1}{2k_BT_B^0}\right)\right],
\end{aligned} \tag{E.19}$$

whose solution is

$$\begin{aligned}
\sigma_{1,1}(t) &= \coth\left(\frac{\hbar\omega_1}{2k_BT_B^0}\right) + \mathrm{e}^{-2\Gamma t}\left[\sigma_{1,1}(0) - \coth\left(\frac{\hbar\omega_1}{2k_BT_B^0}\right)\right] \\
&= \left[\coth\left(\frac{\hbar\omega_1}{2k_BT_A^0}\right)\mathrm{e}^{-2\Gamma t} + \coth\left(\frac{\hbar\omega_1}{2k_BT_B^0}\right)\left(1-\mathrm{e}^{-2\Gamma t}\right)\right].
\end{aligned} \tag{E.20}$$

Similarly, the time derivative of $\sigma_{2,2}(t)$ is calculated as in

$$\begin{aligned}
\frac{\mathrm{d}}{\mathrm{d}t}\sigma_{2,2}(t) &= \mathrm{Tr}\left[2\hat{r}_2^2\frac{\mathrm{d}}{\mathrm{d}t}\hat{\rho}(t)\right] \\
&= \Gamma(\bar{n}(\omega_1)+1)\mathrm{Tr}\left[2\hat{r}_2^2\left(2\hat{a}_1\hat{\rho}_A(t)\hat{a}_1^\dagger - \left\{\hat{a}_1^\dagger\hat{a}_1, \hat{\rho}_A(t)\right\}\right)\right] \\
&\quad + \Gamma\bar{n}(\omega_1)\mathrm{Tr}\left[2\hat{r}_2^2\left(2\hat{a}_1^\dagger\hat{\rho}_A(t)\hat{a}_1 - \left\{\hat{a}_1\hat{a}_1^\dagger, \hat{\rho}_A(t)\right\}\right)\right] \\
&= \Gamma(\bar{n}(\omega_1)+1)\mathrm{Tr}\left[(-2\hat{a}_1^\dagger + 2\hat{a}_1)2\hat{a}_1\hat{\rho}_A(t) - (-2\hat{a}_1^{\dagger 2} + 2\hat{a}_1^2)\hat{\rho}_A(t)\right] \\
&\quad + \Gamma\bar{n}(\omega_1)\mathrm{Tr}\left[(-2\hat{a}_1^\dagger + 2\hat{a}_1)2\hat{a}_1^\dagger\hat{\rho}_A(t) - (-2\hat{a}_1^{\dagger 2} + 2\hat{a}_1^2)\hat{\rho}_A(t)\right] \\
&= -2\Gamma(\bar{n}(\omega_1)+1)\mathrm{Tr}\left[(2\hat{r}_2^2-1)\hat{\rho}(t)\right] + 2\Gamma\bar{n}(\omega_1)\mathrm{Tr}\left[(2\hat{r}_2^2+1)\hat{\rho}(t)\right] \\
&= -2\Gamma\mathrm{Tr}\left[2\hat{r}_2^2\hat{\rho}(t)\right] + 2\Gamma[2\bar{n}(\omega_1)+1] \\
&= -2\Gamma\left[\sigma_{2,2}(t) - \coth\left(\frac{\hbar\omega_1}{2k_BT_B^0}\right)\right],
\end{aligned} \tag{E.21}$$

whose solution is

$$\begin{aligned}
\sigma_{2,2}(t) &= \coth\left(\frac{\hbar\omega_1}{2k_BT_B^0}\right) + \mathrm{e}^{-2\Gamma t}\left[\sigma_{2,2}(0) - \coth\left(\frac{\hbar\omega_1}{2k_BT_B^0}\right)\right] \\
&= \left[\coth\left(\frac{\hbar\omega_1}{2k_BT_A^0}\right)\mathrm{e}^{-2\Gamma t} + \coth\left(\frac{\hbar\omega_1}{2k_BT_B^0}\right)\left(1-\mathrm{e}^{-2\Gamma t}\right)\right].
\end{aligned} \tag{E.22}$$

Finally, the time derivative of $\sigma_{1,2}(t)$ is calculated as in

$$\begin{aligned}
\frac{\mathrm{d}}{\mathrm{d}t}\sigma_{1,2}(t) &= \mathrm{Tr}\left[(\hat{r}_1\hat{r}_2+\hat{r}_2\hat{r}_1)\frac{\mathrm{d}}{\mathrm{d}t}\hat{\rho}(t)\right] \\
&= \Gamma(\bar{n}(\omega_1)+1)\mathrm{Tr}\left[(\hat{r}_1\hat{r}_2+\hat{r}_2\hat{r}_1)\left(2\hat{a}_1\hat{\rho}_A(t)\hat{a}_1^\dagger-\left\{\hat{a}_1^\dagger\hat{a}_1,\hat{\rho}_A(t)\right\}\right)\right] \\
&\quad+\Gamma\bar{n}(\omega_1)\mathrm{Tr}\left[(\hat{r}_1\hat{r}_2+\hat{r}_2\hat{r}_1)\left(2\hat{a}_1^\dagger\hat{\rho}_A(t)\hat{a}_1-\left\{\hat{a}_1\hat{a}_1^\dagger,\hat{\rho}_A(t)\right\}\right)\right] \\
&= \Gamma(\bar{n}(\omega_1)+1)\mathrm{Tr}\left[4\mathrm{i}\hat{a}_1 2\hat{a}_1\hat{\rho}_A(t)-4\mathrm{i}(\hat{a}_1^{\dagger 2}+\hat{a}_1^2)\hat{\rho}_A(t)\right] \\
&\quad+\Gamma\bar{n}(\omega_1)\mathrm{Tr}\left[4\mathrm{i}\hat{a}_1^\dagger 2\hat{a}_1^\dagger\hat{\rho}_A(t)-4\mathrm{i}(\hat{a}_1^{\dagger 2}+\hat{a}_1^2)\hat{\rho}_A(t)\right] \\
&= -2\Gamma(\bar{n}(\omega_1)+1)\mathrm{Tr}\left[(\hat{r}_1\hat{r}_2+\hat{r}_2\hat{r}_1)\hat{\rho}(t)\right]+2\Gamma\bar{n}(\omega_1)\mathrm{Tr}\left[(\hat{r}_1\hat{r}_2+\hat{r}_2\hat{r}_1)\hat{\rho}(t)\right] \\
&= -2\Gamma\mathrm{Tr}\left[(\hat{r}_1\hat{r}_2+\hat{r}_2\hat{r}_1)\hat{\rho}(t)\right] \\
&= -2\Gamma\sigma_{1,2}(t),
\end{aligned} \tag{E.23}$$

whose solution is

$$\sigma_{1,2}(t) = \mathrm{e}^{-2\Gamma t}\sigma_{1,2}(0) = 0. \tag{E.24}$$

Thus, we arrive at Eq. (5.36).

Appendix F

Every harmonic oscillator is in a Gibbs state with a time-dependent temperature

In this Appendix, we show that every harmonic oscillator is in a Gibbs state all the time. As each harmonic oscillator is in a single-mode Gaussian state with vanishing first moments, its density operator is totally determined by its covariance matrix (5.33). Since the time evolution of the covariance matrix is easier to calculate than that of the density operator, we first calculate the covariance matrix of each harmonic oscillator at time t in the next two paragraphs. Then, in the last paragraph, using the relation between the density operator and the covariance matrix in Eq. (F.14), we show that each harmonic oscillator is in a Gibbs state with a time-dependent temperature $T_j(t)$.

The matrix H in Eq. (5.20) with the elements (5.23) has a form of the following symmetric block matrix:

$$H = \begin{pmatrix} \omega_1 I_2 & g_2 I_2 & g_3 I_2 & \cdots & g_{N+1} I_2 \\ g_2 I_2 & \omega_2 I_2 & 0 & \cdots & 0 \\ g_3 I_2 & 0 & \omega_3 I_2 & \ddots & \vdots \\ \vdots & \vdots & \ddots & \ddots & 0 \\ g_{N+1} I_2 & 0 & \cdots & 0 & \omega_{N+1} I_2 \end{pmatrix}. \tag{F.1}$$

Therefore, the nth power of H has a form of the following symmetric block matrix:

$$H^n = \begin{pmatrix} h_{1,1}(n) I_2 & \cdots & h_{1,N+1}(n) I_2 \\ \vdots & \ddots & \vdots \\ h_{1,N+1}(n) I_2 & \cdots & h_{N+1,N+1}(n) I_2 \end{pmatrix}, \tag{F.2}$$

whose elements satisfy

$$\begin{gathered} (H^n)_{2j-1,2k-1} = (H^n)_{2j,2k}\,, \quad (H^n)_{2j-1,2k} = (H^n)_{2j,2k-1} = 0 \\ \text{for} \quad n \in \mathbb{N}, \quad j,k = 1,\ldots,N+1. \end{gathered} \tag{F.3}$$

The $(2n-1)$th and the $(2n)$th powers of the matrix Ω in Eq. (5.31) are given by

$$\Omega^{2n-1} = (-1)^{n-1}\Omega, \quad \Omega^{2n} = (-1)^n I_{2N+2} \quad \text{for} \quad n \in \mathbb{N}, \tag{F.4}$$

where I_{2N+2} is the $(2N+2)$-dimensional identity matrix. The matrices H and Ω commute with each other:

$$H\Omega = \Omega H. \tag{F.5}$$

Using Eqs. (F.4) and (F.5), we can rewrite $V(t) = \mathrm{e}^{\Omega H t}$ in Eq. (5.30) as

$$\begin{aligned} V(t) &= \mathrm{e}^{\Omega H t} \\ &= \sum_{n=0}^{\infty} \frac{\Omega^{2n} (Ht)^{2n}}{(2n)!} + \sum_{n=1}^{\infty} \frac{\Omega^{2n-1} (Ht)^{2n-1}}{(2n-1)!} \\ &= \sum_{n=0}^{\infty} \frac{(-1)^n (Ht)^{2n}}{(2n)!} + \Omega \sum_{n=1}^{\infty} \frac{(-1)^{n-1} (Ht)^{2n-1}}{(2n-1)!} \\ &= \cos Ht + \Omega \sin Ht, \end{aligned} \tag{F.6}$$

whose transpose is

$$V(t)^{\mathrm{T}} = \cos Ht - [\sin Ht]\Omega \tag{F.7}$$

because $\Omega^{\mathrm{T}} = -\Omega$. From Eq. (F.3), we find

$$\begin{gathered} (\cos Ht)_{2j-1,2k-1} = (\cos Ht)_{2j,2k}\,, \quad (\cos Ht)_{2j-1,2k} = (\cos Ht)_{2j,2k-1} = 0, \\ (\sin Ht)_{2j-1,2k-1} = (\sin Ht)_{2j,2k}\,, \quad (\sin Ht)_{2j-1,2k} = (\sin Ht)_{2j,2k-1} = 0 \\ \text{for} \quad j,k = 1,\ldots,N+1. \end{gathered} \tag{F.8}$$

As the initial covariance matrix (5.34) is diagonal, each element of $\sigma(t) = V(t)\sigma(0)V(t)^{\mathrm{T}}$ is written as

$$\begin{gathered} \sigma_{j,k}(t) = \sum_{l=1}^{2N+2} (\cos Ht + \Omega \sin Ht)_{j,l}\, \sigma_{l,l}(0)\, (\cos Ht - [\sin Ht]\Omega)_{l,k} \\ \text{for} \quad j,k = 1,\ldots,2N+2. \end{gathered} \tag{F.9}$$

Let us calculate the elements of the covariance matrix of the jth harmonic oscillator (5.33). We first obtain

$$\begin{aligned} \sigma_{2j-1,2j-1}(t) &= \sum_{l=1}^{2N+2} (\cos Ht + \Omega \sin Ht)_{2j-1,l}\, \sigma_{l,l}(0)\, (\cos Ht - [\sin Ht]\Omega)_{l,2j-1} \\ &= \sum_{l=1}^{2N+2} \Big[(\cos Ht)_{2j-1,l} + (\sin Ht)_{2j,l}\Big]\, \sigma_{l,l}(0)\, \Big[(\cos Ht)_{l,2j-1} + (\sin Ht)_{l,2j}\Big] \\ &= \sum_{m=1}^{N+1} \Big[(\cos Ht)_{2j-1,2m-1}\, \sigma_{2m-1,2m-1}(0)\, (\cos Ht)_{2m-1,2j-1} \\ &\quad + (\sin Ht)_{2j,2m}\, \sigma_{2m,2m}(0)\, (\sin Ht)_{2m,2j}\Big] \\ &= \sum_{m=1}^{N+1} \Big[(\cos Ht)_{2j-1,2m-1}\, \sigma_{2m-1,2m-1}(0)\, (\cos Ht)_{2m-1,2j-1} \\ &\quad + (\sin Ht)_{2j-1,2m-1}\, \sigma_{2m-1,2m-1}(0)\, (\sin Ht)_{2m-1,2j-1}\Big]\,, \end{aligned} \tag{F.10}$$

where the second line follows from the form of Ω in Eq. (5.31), the third line follows from Eq. (F.8), and the last line follows from Eq. (F.8) and the form of $\sigma(0)$ in Eq. (5.34). Similarly, we have

$$\begin{aligned}
\sigma_{2j,2j}(t) &= \sum_{l=1}^{2N+2} (\cos Ht + \Omega \sin Ht)_{2j,l}\, \sigma_{l,l}(0)\, (\cos Ht - [\sin Ht]\Omega)_{l,2j} \\
&= \sum_{l=1}^{2N+2} \Big[(\cos Ht)_{2j,l} - (\sin Ht)_{2j-1,l}\Big]\, \sigma_{l,l}(0)\, \Big[(\cos Ht)_{l,2j} - (\sin Ht)_{l,2j-1}\Big] \\
&= \sum_{m=1}^{N+1} \Big[(\cos Ht)_{2j,2m}\, \sigma_{2m,2m}(0)\, (\cos Ht)_{2m,2j} \\
&\quad + (\sin Ht)_{2j-1,2m-1}\, \sigma_{2m-1,2m-1}(0)\, (\sin Ht)_{2m-1,2j-1}\Big] \\
&= \sum_{m=1}^{N+1} \Big[(\cos Ht)_{2j-1,2m-1}\, \sigma_{2m-1,2m-1}(0)\, (\cos Ht)_{2m-1,2j-1} \\
&\quad + (\sin Ht)_{2j-1,2m-1}\, \sigma_{2m-1,2m-1}(0)\, (\sin Ht)_{2m-1,2j-1}\Big] \\
&= \sigma_{2j-1,2j-1}(t),
\end{aligned} \tag{F.11}$$

$$\begin{aligned}
\sigma_{2j-1,2j}(t) &= \sum_{l=1}^{2N+2} (\cos Ht + \Omega \sin Ht)_{2j-1,l}\, \sigma_{l,l}(0)\, (\cos Ht - [\sin Ht]\Omega)_{l,2j} \\
&= \sum_{l=1}^{2N+2} \Big[(\cos Ht)_{2j-1,l} + (\sin Ht)_{2j,l}\Big]\, \sigma_{l,l}(0)\, \Big[(\cos Ht)_{l,2j} - (\sin Ht)_{l,2j-1}\Big] \\
&= \sum_{m=1}^{N+1} \Big[-(\cos Ht)_{2j-1,2m-1}\, \sigma_{2m-1,2m-1}(0)\, (\sin Ht)_{2m-1,2j-1} \\
&\quad + (\sin Ht)_{2j,2m}\, \sigma_{2m,2m}(0)\, (\cos Ht)_{2m,2j}\Big] \\
&= \sum_{m=1}^{N+1} \Big[-(\cos Ht)_{2j-1,2m-1}\, \sigma_{2m-1,2m-1}(0)\, (\sin Ht)_{2m-1,2j-1} \\
&\quad + (\sin Ht)_{2j-1,2m-1}\, \sigma_{2m-1,2m-1}(0)\, (\cos Ht)_{2m-1,2j-1}\Big] \\
&= \sum_{m=1}^{N+1} \Big[-(\cos Ht)_{2j-1,2m-1}\, \sigma_{2m-1,2m-1}(0)\, (\sin Ht)_{2m-1,2j-1} \\
&\quad + (\sin Ht)_{2m-1,2j-1}\, \sigma_{2m-1,2m-1}(0)\, (\cos Ht)_{2j-1,2m-1}\Big] \\
&= 0,
\end{aligned} \tag{F.12}$$

where the fifth line follows from the symmetry of $\cos Ht$ and $\sin Ht$. We thus arrive at

$$\sigma_j(t) = \sigma_{2j-1,2j-1}(t) I_2, \tag{F.13}$$

which appears in Eq. (5.37) in the main text.

As the jth harmonic oscillator is in a single-mode Gaussian state with vanishing first moments, its density operator is completely characterized by the covariance matrix in Eq. (F.13) and has the following form [74]:

$$\hat{\rho}_j(t) = \frac{\exp\left[-\frac{1}{2}\hat{\mathbf{r}}_j^{\mathrm{T}} G_j(t) \hat{\mathbf{r}}_j\right]}{Z_j(t)}, \tag{F.14}$$

where

$$\hat{\mathbf{r}}_j = (\hat{r}_{2j-1}, \hat{r}_{2j})^{\mathrm{T}}, \tag{F.15}$$

$$G_j(t) = 2\mathrm{i}\Omega_1 \coth^{-1}\left[\sigma_j(t)\mathrm{i}\Omega_1\right] = 2\coth^{-1}\left[\sigma_{2j-1,2j-1}(t)\right] I_2 \quad \text{with} \quad \Omega_1 = \begin{pmatrix} 0 & 1 \\ -1 & 0 \end{pmatrix}, \tag{F.16}$$

$$Z_j(t) = \frac{1}{2}\sqrt{\det\left(\sigma_j(t) + \mathrm{i}\Omega_1\right)} = \frac{1}{2}\sqrt{\sigma_{2j-1,2j-1}(t)^2 - 1}. \tag{F.17}$$

Let us show that $\hat{\rho}_j(t)$ in Eq. (F.14) is a Gibbs state below. The numerator of Eq. (F.14) is transformed using Eqs. (F.15) and (F.16) as

$$\exp\left[-\frac{1}{2}\hat{\mathbf{r}}_j^{\mathrm{T}} G_j(t)\hat{\mathbf{r}}_j\right] = \exp\left[-\frac{2}{\hbar\omega_j}\coth^{-1}\left[\sigma_{2j-1,2j-1}(t)\right]\frac{\hbar\omega_j}{2}\left(\hat{r}_{2j-1}^2 + \hat{r}_{2j}^2\right)\right] = \exp\left[-\beta_j(t)\hat{H}_j\right], \tag{F.18}$$

where

$$\beta_j(t) = \frac{1}{k_B T_j(t)} = \frac{2}{\hbar\omega_j}\coth^{-1}\left[\sigma_{2j-1,2j-1}(t)\right] = \frac{1}{\hbar\omega_j}\ln\left(\frac{\sigma_{2j-1,2j-1}(t)+1}{\sigma_{2j-1,2j-1}(t)-1}\right). \tag{F.19}$$

The trace of the numerator of Eq. (F.14) is equal to the denominator:

$$\begin{aligned}
\mathrm{Tr}\left[\exp\left[-\frac{1}{2}\hat{\mathbf{r}}_j^{\mathrm{T}} G_j(t)\hat{\mathbf{r}}_j\right]\right] &= \mathrm{Tr}\left[\exp\left[-\beta_j(t)\hat{H}_j\right]\right] \\
&= \mathrm{Tr}\left[\exp\left[-\beta_j(t)\hbar\omega_j\left(\hat{a}_j^\dagger\hat{a}_j + \frac{1}{2}\right)\right]\right] \\
&= \sum_{n=0}^{\infty}\exp\left[-\beta_j(t)\hbar\omega_j\left(n+\frac{1}{2}\right)\right] \\
&= \frac{\exp\left[-\beta_j(t)\hbar\omega_j/2\right]}{1-\exp\left[-\beta_j(t)\hbar\omega_j\right]} \\
&= \frac{1}{\exp\left[\beta_j(t)\hbar\omega_j/2\right] - \exp\left[-\beta_j(t)\hbar\omega_j/2\right]} \\
&= \frac{1}{\sqrt{\frac{\sigma_{2j-1,2j-1}(t)+1}{\sigma_{2j-1,2j-1}(t)-1}} - \sqrt{\frac{\sigma_{2j-1,2j-1}(t)-1}{\sigma_{2j-1,2j-1}(t)+1}}} \\
&= \frac{1}{2}\sqrt{\sigma_{2j-1,2j-1}(t)^2 - 1} \\
&= Z_j(t),
\end{aligned} \tag{F.20}$$

where in the sixth line, we have used Eq. (F.19). Therefore, we have derived Eqs. (5.38) and (5.39):

$$\hat{\rho}_j(t) = \frac{\mathrm{e}^{-\beta_j(t)\hat{H}_j}}{Z_j(t)}, \quad Z_j(t) = \mathrm{Tr}\left[\mathrm{e}^{-\beta_j(t)\hat{H}_j}\right] = \frac{1}{2}\sqrt{\sigma_{2j-1,2j-1}(t)^2 - 1}, \tag{F.21}$$

which shows that the jth harmonic oscillator is in the Gibbs state with the time-dependent inverse temperature $\beta_j(t)$.

Appendix G

The time derivative of the mean energy of each harmonic oscillator, the bath, and the interaction

In this Appendix we calculate the time derivative of the mean energy of each harmonic oscillator so that we can transform the thermodynamic entropy production rate (5.56) to the more easily calculable form (5.57). We also calculate the time derivative of the mean energy of the bath and the interaction in order to show in Fig. 5.2 that the interaction energy is negligibly small.

The Heisenberg equations of motions read

$$\frac{\mathrm{d}}{\mathrm{d}t}\hat{r}_1^H(t) = \frac{\mathrm{i}}{\hbar}\left[\hat{H}^H(t), \hat{r}_1^H(t)\right] = \omega_1 \hat{r}_2^H(t) + \sum_{j=2}^{N+1} g_j \hat{r}_{2j}^H(t), \tag{G.1}$$

$$\frac{\mathrm{d}}{\mathrm{d}t}\hat{r}_2^H(t) = \frac{\mathrm{i}}{\hbar}\left[\hat{H}^H(t), \hat{r}_2^H(t)\right] = -\omega_1 \hat{r}_1^H(t) - \sum_{j=2}^{N+1} g_j \hat{r}_{2j-1}^H(t), \tag{G.2}$$

$$\frac{\mathrm{d}}{\mathrm{d}t}\hat{r}_{2j-1}^H(t) = \frac{\mathrm{i}}{\hbar}\left[\hat{H}^H(t), \hat{r}_{2j-1}^H(t)\right] = \omega_j \hat{r}_{2j}^H(t) + g_j \hat{r}_2^H(t) \quad \text{for} \quad j = 2, \ldots, N+1, \tag{G.3}$$

$$\frac{\mathrm{d}}{\mathrm{d}t}\hat{r}_{2j}^H(t) = \frac{\mathrm{i}}{\hbar}\left[\hat{H}^H(t), \hat{r}_{2j}^H(t)\right] = -\omega_j \hat{r}_{2j-1}^H(t) - g_j \hat{r}_1^H(t) \quad \text{for} \quad j = 2, \ldots, N+1. \tag{G.4}$$

Then, the time derivative of the mean energy of each harmonic oscillator is calculated as

$$\begin{aligned}
\frac{\mathrm{d}}{\mathrm{d}t}E_A(t) &= \frac{\mathrm{d}}{\mathrm{d}t}E_1(t) \\
&= \frac{\hbar\omega_1}{2}\frac{\mathrm{d}}{\mathrm{d}t}\sigma_{1,1}(t) \\
&= \frac{\hbar\omega_1}{2}\frac{\mathrm{d}}{\mathrm{d}t}\mathrm{Tr}\left[\hat{\rho}(0)\left\{\hat{r}_1^H(t), \hat{r}_1^H(t)\right\}\right] \\
&= \frac{\hbar\omega_1}{2}\mathrm{Tr}\left[\hat{\rho}(0)\left\{\frac{\mathrm{d}}{\mathrm{d}t}\hat{r}_1^H(t), \hat{r}_1^H(t)\right\}\right] + \frac{\hbar\omega_1}{2}\mathrm{Tr}\left[\hat{\rho}(0)\left\{\hat{r}_1^H(t), \frac{\mathrm{d}}{\mathrm{d}t}\hat{r}_1^H(t)\right\}\right] \\
&= \frac{\hbar\omega_1}{2}\mathrm{Tr}\left[\hat{\rho}(0)\left\{\left(\omega_1\hat{r}_2^H(t) + \sum_{j=2}^{N+1} g_j \hat{r}_{2j}^H(t)\right), \hat{r}_1^H(t)\right\}\right] \\
&\quad + \frac{\hbar\omega_1}{2}\mathrm{Tr}\left[\hat{\rho}(0)\left\{\hat{r}_1^H(t), \left(\omega_1\hat{r}_2^H(t) + \sum_{j=2}^{N+1} g_j \hat{r}_{2j}^H(t)\right)\right\}\right]
\end{aligned}$$

$$
\begin{aligned}
&= \frac{\hbar\omega_1}{2}\left[\omega_1\sigma_{2,1}(t) + \sum_{j=2}^{N+1} g_j\sigma_{2j,1}(t)\right] + \frac{\hbar\omega_1}{2}\left[\omega_1\sigma_{1,2}(t) + \sum_{j=2}^{N+1} g_j\sigma_{1,2j}(t)\right] \\
&= \hbar\omega_1\left[\omega_1\sigma_{1,2}(t) + \sum_{j=2}^{N+1} g_j\sigma_{1,2j}(t)\right] \\
&= \hbar\omega_1 \sum_{j=2}^{N+1} g_j\sigma_{1,2j}(t), \qquad \text{(G.5)}
\end{aligned}
$$

$$
\begin{aligned}
\frac{\mathrm{d}}{\mathrm{d}t}E_j(t) &= \frac{\hbar\omega_j}{2}\frac{\mathrm{d}}{\mathrm{d}t}\sigma_{2j-1,2j-1}(t) \\
&= \frac{\hbar\omega_j}{2}\frac{\mathrm{d}}{\mathrm{d}t}\mathrm{Tr}\left[\hat{\rho}(0)\left\{\hat{r}^H_{2j-1}(t), \hat{r}^H_{2j-1}(t)\right\}\right] \\
&= \frac{\hbar\omega_j}{2}\mathrm{Tr}\left[\hat{\rho}(0)\left\{\frac{\mathrm{d}}{\mathrm{d}t}\hat{r}^H_{2j-1}(t), \hat{r}^H_{2j-1}(t)\right\}\right] + \frac{\hbar\omega_j}{2}\mathrm{Tr}\left[\hat{\rho}(0)\left\{\hat{r}^H_{2j-1}(t), \frac{\mathrm{d}}{\mathrm{d}t}\hat{r}^H_{2j-1}(t)\right\}\right] \\
&= \frac{\hbar\omega_j}{2}\mathrm{Tr}\left[\hat{\rho}(0)\left\{\left(\omega_j\hat{r}^H_{2j}(t) + g_j\hat{r}^H_2(t)\right), \hat{r}^H_{2j-1}(t)\right\}\right] \\
&\quad + \frac{\hbar\omega_j}{2}\mathrm{Tr}\left[\hat{\rho}(0)\left\{\hat{r}^H_{2j-1}(t), \left(\omega_j\hat{r}^H_{2j}(t) + g_j\hat{r}^H_2(t)\right)\right\}\right] \\
&= \frac{\hbar\omega_j}{2}\left[\omega_j\sigma_{2j,2j-1}(t) + g_j\sigma_{2,2j-1}(t)\right] + \frac{\hbar\omega_j}{2}\left[\omega_j\sigma_{2j-1,2j}(t) + g_j\sigma_{2j-1,2}(t)\right] \\
&= \hbar\omega_j\left[\omega_j\sigma_{2j-1,2j}(t) + g_j\sigma_{2,2j-1}(t)\right] \\
&= \hbar\omega_j g_j\sigma_{2,2j-1}(t) \\
&= -\hbar\omega_j g_j\sigma_{1,2j}(t) \quad \text{for} \quad j = 2, \ldots, N+1, \qquad \text{(G.6)}
\end{aligned}
$$

where the last line follows from

$$
\begin{aligned}
\sigma_{1,2j}(t) &= \sum_{l=1}^{2N+2} \left(\cos Ht + \Omega\sin Ht\right)_{1,l}\sigma_{l,l}(0)\left(\cos Ht - [\sin Ht]\Omega\right)_{l,2j} \\
&= \sum_{l=1}^{2N+2}\left[(\cos Ht)_{1,l} + (\sin Ht)_{2,l}\right]\sigma_{l,l}(0)\left[(\cos Ht)_{l,2j} - (\sin Ht)_{l,2j-1}\right] \\
&= \sum_{m=1}^{N+1}\Big[-(\cos Ht)_{1,2m-1}\,\sigma_{2m-1,2m-1}(0)\,(\sin Ht)_{2m-1,2j-1} \\
&\quad + (\sin Ht)_{2,2m}\,\sigma_{2m,2m}(0)\,(\cos Ht)_{2m,2j}\Big] \\
&= \sum_{m=1}^{N+1}\Big[-(\cos Ht)_{1,2m-1}\,\sigma_{2m-1,2m-1}(0)\,(\sin Ht)_{2m-1,2j-1} \\
&\quad + (\sin Ht)_{1,2m-1}\,\sigma_{2m-1,2m-1}(0)\,(\cos Ht)_{2m-1,2j-1}\Big], \qquad \text{(G.7)}
\end{aligned}
$$

$$
\begin{aligned}
\sigma_{2,2j-1}(t) &= \sum_{l=1}^{2N+2}\left(\cos Ht + \Omega\sin Ht\right)_{2,l}\sigma_{l,l}(0)\left(\cos Ht - [\sin Ht]\Omega\right)_{l,2j-1} \\
&= \sum_{l=1}^{2N+2}\left[(\cos Ht)_{2,l} - (\sin Ht)_{1,l}\right]\sigma_{l,l}(0)\left[(\cos Ht)_{l,2j-1} + (\sin Ht)_{l,2j}\right] \\
&= \sum_{m=1}^{N+1}\Big[(\cos Ht)_{2,2m}\,\sigma_{2m,2m}(0)\,(\sin Ht)_{2m,2j}
\end{aligned}
$$

$$
\begin{aligned}
&\quad - (\sin Ht)_{1,2m-1}\, \sigma_{2m-1,2m-1}(0)\, (\cos Ht)_{2m-1,2j-1}\Big] \\
&= \sum_{m=1}^{N+1} \Big[(\cos Ht)_{1,2m-1}\, \sigma_{2m-1,2m-1}(0)\, (\sin Ht)_{2m-1,2j-1} \\
&\quad - (\sin Ht)_{1,2m-1}\, \sigma_{2m-1,2m-1}(0)\, (\cos Ht)_{2m-1,2j-1}\Big] \\
&= -\sigma_{1,2j}(t). \qquad \text{(G.8)}
\end{aligned}
$$

Inserting Eqs. (G.5) and (G.6) into Eq. (5.56), we obtain Eq. (5.57), which we can calculate from the covariance matrix $\sigma(t)$.

The time derivative of the mean energy of the bath is calculated as

$$
\frac{\mathrm{d}}{\mathrm{d}t} E_B(t) = \sum_{j=2}^{N+1} \frac{\mathrm{d}}{\mathrm{d}t} E_j(t) = -\sum_{j=2}^{N+1} \hbar\omega_j g_j \sigma_{1,2j}(t). \qquad \text{(G.9)}
$$

From the conservation of the total energy, the time derivative of the interaction energy is calculated as

$$
\frac{\mathrm{d}}{\mathrm{d}t} E_I(t) = -\frac{\mathrm{d}}{\mathrm{d}t} E_A(t) - \frac{\mathrm{d}}{\mathrm{d}t} E_B(t) = \sum_{j=2}^{N+1} \hbar(\omega_j - \omega_1) g_j \sigma_{1,2j}(t). \qquad \text{(G.10)}
$$

In Fig. 5.2, we compare $\mathrm{d}E_A(t)/\mathrm{d}t$ in Eq. (G.5), $\mathrm{d}E_B(t)/\mathrm{d}t$ in Eq. (G.9), and $\mathrm{d}E_I(t)/\mathrm{d}t$ in Eq. (G.10).

Bibliography

[1] Maximilian Schlosshauer. Quantum decoherence. *Physics Reports*, 831:1–57, 2019. Quantum decoherence.

[2] Maximilian A Schlosshauer. *Decoherence and the Quantum-To-Classical Transition*. Springer, Berlin, Heidelberg, 2007.

[3] Heinz-Peter Breuer and Francesco Petruccione. *The Theory of Open Quantum Systems*. Oxford University Press, Oxford, England, 2002.

[4] Angel Rivas and Susana F Huelga. *Open Quantum Systems*, volume 13 of *SpringerBriefs in Physics*. Springer, Berlin, 2012.

[5] I Rotter and J P Bird. A review of progress in the physics of open quantum systems: theory and experiment. *Reports on Progress in Physics*, 78(11):114001, oct 2015.

[6] Ángel Rivas, A Douglas K Plato, Susana F Huelga, and Martin B Plenio. Markovian master equations: a critical study. *New Journal of Physics*, 12(11):113032, nov 2010.

[7] Vittorio Gorini, Andrzej Kossakowski, and E. C. G. Sudarshan. Completely positive dynamical semigroups of n - level systems. *Journal of Mathematical Physics*, 17(5):821–825, 1976.

[8] G. Lindblad. On the generators of quantum dynamical semigroups. *Communications in Mathematical Physics*, 48(2):119–130, 1976.

[9] Howard J Carmichael. *Statistical Methods in Quantum Optics 1: Master Equations and Fokker-Planck Equations*, volume 1. Springer, Berlin, Heidelberg, 1999.

[10] Hayato Goto. Quantum computation based on quantum adiabatic bifurcations of kerr-nonlinear parametric oscillators. *Journal of the Physical Society of Japan*, 88(6):061015, 2019.

[11] Shruti Puri, Samuel Boutin, and Alexandre Blais. Engineering the quantum states of light in a kerr-nonlinear resonator by two-photon driving. *npj Quantum Information*, 3(1):18, Apr 2017.

[12] Shruti Puri, Alexander Grimm, Philippe Campagne-Ibarcq, Alec Eickbusch, Kyungjoo Noh, Gabrielle Roberts, Liang Jiang, Mazyar Mirrahimi, Michel H. Devoret, and S. M. Girvin. Stabilized cat in a driven nonlinear cavity: A fault-tolerant error syndrome detector. *Phys. Rev. X*, 9:041009, Oct 2019.

[13] A. Grimm, N. E. Frattini, S. Puri, S. O. Mundhada, S. Touzard, M. Mirrahimi, S. M. Girvin, S. Shankar, and M. H. Devoret. Stabilization and operation of a kerr-cat qubit. *Nature*, 584(7820):205–209, Aug 2020.

[14] P. T. Cochrane, G. J. Milburn, and W. J. Munro. Macroscopically distinct quantum-superposition states as a bosonic code for amplitude damping. *Phys. Rev. A*, 59:2631–2634, Apr 1999.

[15] Hayato Goto. Bifurcation-based adiabatic quantum computation with a nonlinear oscillator network. *Scientific Reports*, 6(1):21686, Feb 2016.

[16] Alessio Serafini. *Quantum Continuous Variables: A Primer of Theoretical Methods*. CRC Press, Boca Raton, FL, 2017.

[17] Gerardo Adesso, Sammy Ragy, and Antony R. Lee. Continuous variable quantum information: Gaussian states and beyond. *Open Systems & Information Dynamics*, 21(01n02):1440001, 2014.

[18] Christian Weedbrook, Stefano Pirandola, Raúl García-Patrón, Nicolas J. Cerf, Timothy C. Ralph, Jeffrey H. Shapiro, and Seth Lloyd. Gaussian quantum information. *Rev. Mod. Phys.*, 84:621–669, May 2012.

[19] Xiang-Bin Wang, Tohya Hiroshima, Akihisa Tomita, and Masahito Hayashi. Quantum information with gaussian states. *Physics Reports*, 448(1):1–111, 2007.

[20] Alessandro Ferraro, Stefano Olivares, and Matteo GA Paris. *Gaussian States in Quantum Information*. Biliopolis, Napoli, 2005.

[21] Felix Binder, Luis A Correa, Christian Gogolin, Janet Anders, and Gerardo Adesso. *Thermodynamics in the quantum regime*, volume 195 of *Fundamental Theories of Physics*. Springer, Cham, 2018.

[22] Sai Vinjanampathy and Janet Anders. Quantum thermodynamics. *Contemporary Physics*, 57(4):545–579, 2016.

[23] Ronnie Kosloff. Quantum thermodynamics: A dynamical viewpoint. *Entropy*, 15(6):2100–2128, 2013.

[24] Philipp Strasberg and Andreas Winter. First and second law of quantum thermodynamics: A consistent derivation based on a microscopic definition of entropy. *PRX Quantum*, 2:030202, Aug 2021.

[25] Dominik Šafránek, J. M. Deutsch, and Anthony Aguirre. Quantum coarse-grained entropy and thermalization in closed systems. *Phys. Rev. A*, 99:012103, Jan 2019.

[26] Sheldon Goldstein, Joel L Lebowitz, Roderich Tumulka, and Nino Zanghì. *Gibbs and Boltzmann Entropy in Classical and Quantum Mechanics*, chapter 14, pages 519–581. World Scientific, Singapore, 2020.

[27] Gabriel T. Landi and Mauro Paternostro. Irreversible entropy production: From classical to quantum. *Rev. Mod. Phys.*, 93:035008, Sep 2021.

[28] S. Marcantoni, S. Alipour, F. Benatti, R. Floreanini, and A. T. Rezakhani. Entropy production and non-markovian dynamical maps. *Scientific Reports*, 7(1):12447, 2017.

[29] Samyadeb Bhattacharya, Avijit Misra, Chiranjib Mukhopadhyay, and Arun Kumar Pati. Exact master equation for a spin interacting with a spin bath: Non-markovianity and negative entropy production rate. *Phys. Rev. A*, 95:012122, Jan 2017.

[30] Maria Popovic, Bassano Vacchini, and Steve Campbell. Entropy production and correlations in a controlled non-markovian setting. *Phys. Rev. A*, 98:012130, Jul 2018.

[31] Y. Y. Xu, J. Liu, and M. Feng. Positive entropy production rate induced by non-markovianity. *Phys. Rev. E*, 98:032102, Sep 2018.

[32] Philipp Strasberg and Massimiliano Esposito. Non-markovianity and negative entropy production rates. *Phys. Rev. E*, 99:012120, Jan 2019.

[33] Ángel Rivas. Strong coupling thermodynamics of open quantum systems. *Phys. Rev. Lett.*, 124:160601, Apr 2020.

[34] Inés de Vega and Daniel Alonso. Dynamics of non-markovian open quantum systems. *Rev. Mod. Phys.*, 89:015001, Jan 2017.

[35] Herbert Spohn. Entropy production for quantum dynamical semigroups. *Journal of Mathematical Physics*, 19(5):1227–1230, 1978.

[36] Mark M Wilde. *Quantum information theory*. Cambridge University Press, Cambridge, England, 2013.

[37] Yvonne Y. Gao, M. Adriaan Rol, Steven Touzard, and Chen Wang. Practical guide for building superconducting quantum devices. *PRX Quantum*, 2:040202, Nov 2021.

[38] P. Gaspard and M. Nagaoka. Non-markovian stochastic schrödinger equation. *The Journal of Chemical Physics*, 111(13):5676–5690, 1999.

[39] A. G. Redfield. On the theory of relaxation processes. *IBM Journal of Research and Development*, 1(1):19–31, 1957.

[40] A. G. Redfield. The theory of relaxation processes. In John S. Waugh, editor, *Advances in Magnetic Resonance*, volume 1 of *Advances in Magnetic and Optical Resonance*, pages 1–32. Academic Press, 1965.

[41] F. Benatti and R. Floreanini. Open quantum dynamics: Complete positivity and entanglement. *International Journal of Modern Physics B*, 19(19):3063–3139, 2005.

[42] Klaus Hornberger. *Introduction to decoherence theory*, chapter 5.

[43] Ryogo Kubo. Statistical-mechanical theory of irreversible processes. i. general theory and simple applications to magnetic and conduction problems. *Journal of the Physical Society of Japan*, 12(6):570–586, 1957.

[44] Paul C. Martin and Julian Schwinger. Theory of many-particle systems. i. *Phys. Rev.*, 115:1342–1373, Sep 1959.

[45] Takaaki Aoki, Yuichiro Matsuzaki, and Hideaki Hakoshima. Possibility of the total thermodynamic entropy production rate of a finite-sized isolated quantum system to be negative for the gorini-kossakowski-sudarshan-lindblad-type markovian dynamics of its subsystem. *Phys. Rev. A*, 103:052208, May 2021.

[46] P. W. Anderson. Absence of diffusion in certain random lattices. *Phys. Rev.*, 109:1492–1505, Mar 1958.

[47] P. W. Anderson. Localized magnetic states in metals. *Phys. Rev.*, 124:41–53, Oct 1961.

[48] U. Fano. Effects of configuration interaction on intensities and phase shifts. *Phys. Rev.*, 124:1866–1878, Dec 1961.

[49] K. O. Friedrichs. On the perturbation of continuous spectra. *Communications on Pure and Applied Mathematics*, 1(4):361–406, 1948.

[50] T. D. Lee. Some special examples in renormalizable field theory. *Phys. Rev.*, 95:1329–1334, Sep 1954.

[51] Wei-Min Zhang, Ping-Yuan Lo, Heng-Na Xiong, Matisse Wei-Yuan Tu, and Franco Nori. Zhang et al. reply:. *Phys. Rev. Lett.*, 115:168902, Oct 2015.

[52] A.O. Caldeira and A.J. Leggett. Path integral approach to quantum brownian motion. *Physica A: Statistical Mechanics and its Applications*, 121(3):587–616, 1983.

[53] Inés de Vega, Ulrich Schollwöck, and F. Alexander Wolf. How to discretize a quantum bath for real-time evolution. *Phys. Rev. B*, 92:155126, Oct 2015.

[54] Nathan K. Langford. Circuit QED - Lecture Notes. *arXiv e-prints*, page arXiv:1310.1897, October 2013.

[55] G Wendin. Quantum information processing with superconducting circuits: a review. *Reports on Progress in Physics*, 80(10):106001, Sep 2017.

[56] Jens Koch, Terri M. Yu, Jay Gambetta, A. A. Houck, D. I. Schuster, J. Majer, Alexandre Blais, M. H. Devoret, S. M. Girvin, and R. J. Schoelkopf. Charge-insensitive qubit design derived from the cooper pair box. *Phys. Rev. A*, 76:042319, Oct 2007.

[57] Michael Tinkham. *Introduction to superconductivity*. Dover, Mineola, New York, 2004.

[58] Zhaoyou Wang, Marek Pechal, E. Alex Wollack, Patricio Arrangoiz-Arriola, Maodong Gao, Nathan R. Lee, and Amir H. Safavi-Naeini. Quantum dynamics of a few-photon parametric oscillator. *Phys. Rev. X*, 9:021049, Jun 2019.

[59] Shumpei Masuda, Toyofumi Ishikawa, Yuichiro Matsuzaki, and Shiro Kawabata. Controls of a superconducting quantum parametron under a strong pump field. *Scientific Reports*, 11(1):11459, Jun 2021.

[60] B. Yurke and D. Stoler. Generating quantum mechanical superpositions of macroscopically distinguishable states via amplitude dispersion. *Phys. Rev. Lett.*, 57:13–16, Jul 1986.

[61] Michael A. Nielsen and Isaac L. Chuang. *Quantum Computation and Quantum Information: 10th Anniversary Edition*. Cambridge University Press, 2010.

[62] Christopher Chamberland, Kyungjoo Noh, Patricio Arrangoiz-Arriola, Earl T. Campbell, Connor T. Hann, Joseph Iverson, Harald Putterman, Thomas C. Bohdanowicz, Steven T. Flammia, Andrew Keller, Gil Refael, John Preskill, Liang Jiang, Amir H. Safavi-Naeini, Oskar Painter, and Fernando G. S. L. Brandão. Building a fault-tolerant quantum computer using concatenated cat codes. *arXiv e-prints*, page arXiv:2012.04108, December 2020.

[63] J.R. Johansson, P.D. Nation, and Franco Nori. Qutip: An open-source python framework for the dynamics of open quantum systems. *Computer Physics Communications*, 183(8):1760 – 1772, Aug 2012.

[64] J.R. Johansson, P.D. Nation, and Franco Nori. Qutip 2: A python framework for the dynamics of open quantum systems. *Computer Physics Communications*, 184(4):1234 – 1240, Apr 2013.

[65] Yoshitsugu Oono. *Perspectives on Statistical Thermodynamics*. Cambridge University Press, Cambridge, England, 2017.

[66] Herbert B Callen. *Thermodynamics and an Introduction to Thermostatistics*. Wiley, New York, 1985.

[67] John Von Neumann. *Mathematical foundations of quantum mechanics: New edition*. Princeton university press, Princeton, NJ, 2018.

[68] Alfréd Rényi. *On measures of entropy and information*, page 547 – 561. University of California Press, Berkeley, California, 1961.

[69] Anatoli Polkovnikov. Microscopic diagonal entropy and its connection to basic thermodynamic relations. *Annals of Physics*, 326(2):486–499, 2011.

[70] Georgy Lebon, David Jou, and José Casas-Vázquez. *Understanding Non-equilibrium Thermodynamics*. Springer-Verlag, Berlin, 2008.

[71] Luca D'Alessio, Yariv Kafri, Anatoli Polkovnikov, and Marcos Rigol. From quantum chaos and eigenstate thermalization to statistical mechanics and thermodynamics. *Advances in Physics*, 65(3):239–362, 2016.

[72] Ralf Bulla, Hyun-Jung Lee, Ning-Hua Tong, and Matthias Vojta. Numerical renormalization group for quantum impurities in a bosonic bath. *Phys. Rev. B*, 71:045122, Jan 2005.

[73] Taro Kanao, Shumpei Masuda, Shiro Kawabata, and Hayato Goto. Quantum Gate for Kerr-Nonlinear Parametric Oscillator Using Effective Excited States. *arXiv e-prints*, page arXiv:2108.03091, August 2021.

[74] Leonardo Banchi, Samuel L. Braunstein, and Stefano Pirandola. Quantum fidelity for arbitrary gaussian states. *Phys. Rev. Lett.*, 115:260501, Dec 2015.